ABSTRACT

Title of dissertation: NEW INSIGHTS INTO THE SIGN PROBLEM OF QCD AND HEAVY TETRAQUARKS

Yiming Cai
Doctor of Philosophy, 2020

Dissertation directed by: Thomas Cohen
Department of Physics

Quantum Chromodynamics (QCD) describes strong interactions among the fundamental particles known as quarks and gluons. In principle, QCD can be used to explain complicated phenomena in the strong sector. However, at the energy scale of hadronic physics, the strong coupling constant is so large that the traditional perturbative method is not applicable. There are two powerful alternative approaches utilized in the non-pertubative regime: (1) lattice QCD, which discretizes space-time and utilizes Monte Carlo computer simulations, and (2) finding new systematic expansion regimes to obtain physical insights in certain limits.

In this dissertation, three problems are studied in the context of these two approaches. In Chapter 2, a notorious numeric problem in lattice QCD known as the sign problem is explored. A subtle phenomenon caused by the interplay between the sign problem and the infinite volume limit is discussed and explained using the saddle point approximation. This work provides insight into the sign problem and the physics of the QCD θ-vacuum.

Chapter 3 and Chapter 4 focus on tetraquarks, which are unconventional hadrons containing four valence quarks. Despite numerous tetraquark candidates seen in experiments, there is no unified and well-accepted theoretical descriptions of the tetraquark state yet. This dissertation examines the existence of tetraquarks in the heavy quark mass limit. A powerful systematic expansion regime can be built when the heavy quark mass is extremely large.

In Chapter 3, a framework is established to analyze tetraquarks in the heavy quark mass limit. It is shown in a model-independent way that multiple parametrically narrow $\bar{q}\bar{q}'QQ$ tetraquarks must exist in this limit. Many of these states will be parametrically close to the threshold of decaying into two heavy mesons.

In Chapter 4, based on a modification of the framework in Chapter 3, it is shown that $q\bar{q}'Q\bar{Q}$ tetraquarks with appropriate large angular momentum must exist in the heavy quark mass limit. This may provide insights into the experimentally-observed narrow near-threshold tetraquarks which contain a heavy quark and a heavy antiquark.

NEW INSIGHTS INTO THE SIGN PROBLEM OF QCD AND HEAVY TETRAQUARKS

by

Yiming Cai

Dissertation submitted to the Faculty of the Graduate School of the
University of Maryland, College Park in partial fulfillment
of the requirements for the degree of
Doctor of Philosophy
2020

Advisory Committee:
Professor Thomas Cohen, Chair/Advisor
Professor Paulo Bedaque
Professor Zackaria Chacko
Professor Sarah Eno
Professor Alice Mignerey

Dedication

To my wife Huijing Gong,

and my parents Dengping Zuo and Zhichun Cai.

Acknowledgments

First and foremost, I would like to express my gratitude to my advisor, Tom Cohen, for his continuous support during my time in graduate school. I enjoyed numerous helpful conversations with him, and the discussions cleared up tons of my confusion. His guidance, encouragement and patient mentorship made this dissertation possible.

I also want to thank all other members of the Maryland Center for Fundamental Physics. I learned a lot from the courses taught by the professors here, and I enjoyed the friendship with many graduate students in this group. In particular, I want to thank Paulo Bedaque for his kindly help along these years. I got lots of training in his reading group, which lasting several years. I also want to especially thank Zohreh Davoudi. I have been fortunate to work with her and learn a lot of physics and research skills through the collaboration.

I want to thank my parents for their love and supports. The books they bought during my childhood introduced me to the fantastic world of physics.

The best thing happened during my graduate program is that I met my wife, Huijing Gong. I want to thank her for the love, companionship, and support. I cherish the time we spent here in Maryland.

Table of Contents

List of Figures

Chapter 1: Introduction

1.1 Overview

Quantum Chromodynamics (QCD) is the quantum field theory of the strong interaction, one of the four fundamental interactions of nature. QCD describes the interactions of quarks and gluons. In principle, it can be used to explain rich and complicated hadronic phenomena, which is an important task of QCD physics. However, due to the non-perturbative nature of QCD in strong coupling regimes, it is extremely challenging to study hadronic physics and other strong interaction related phenomena using first principle derivation based on traditional perturbative Feynman diagram approach.

There are alternative methods to study QCD. The first is lattice QCD, which utilizes numerical brute force with the help of advancement in high-performance computing. The second is the development of a systematic expansion with appropriate approximations, such as various Effective Field Theories (EFT) and Large N QCD, under which QCD physics becomes more tractable. This dissertation will cover aspects of both methods to gain insights on problems that are currently hard to handle with perturbative QCD.

1.2 QCD: underlying theory of the strong interacion

The QCD Lagrangian for N_F quark flavors is written as[3]:

$$\mathcal{L} = \sum_{k=1}^{N_F} \bar{q}_k (i\gamma^\mu D_\mu - m_k) q_k - \frac{1}{4} G^a_{\mu\nu} G^{a\mu\nu}, \tag{1.1}$$

where q_k is quark Dirac field with mass parameter m_k. $D_\mu = (\partial_\mu - i g_s A_\mu)$ is the gauge covariant derivative. $A_\mu = A^a_\mu t^a$ is the gluon field, where t^a with $a = 1, 2, ..., 8$ are 3×3 matrices and are generators of $SU(3)$ color group. $G^a_{\mu\nu}$ is the field strength of gluon field given by:

$$G^a_{\mu\nu} = \partial_\mu A^a_\nu - \partial_\nu A^a_\mu - g_s f_{abc} A^b_\mu A^c_\nu \tag{1.2}$$

$$[t^a, t^b] = i f_{abc} t^c,$$

where the f_{abc} are completely anti-symmetric structure constants of the $SU(3)$ group with $f_{abc} = f_{cba} = -f_{acb}$.

Conventionally, t^as take the form of Gell-Mann matrices as in Eq. (1.3), which are similar to the role of the Pauli spin matrices of $SU(2)$ physics.

$$\lambda^1 = \begin{pmatrix} 0 & 1 & 0 \\ 1 & 0 & 0 \\ 0 & 0 & 0 \end{pmatrix} \quad \lambda^2 = \begin{pmatrix} 0 & -i & 0 \\ i & 0 & 0 \\ 0 & 0 & 0 \end{pmatrix} \quad \lambda^3 = \begin{pmatrix} 1 & 0 & 0 \\ 0 & -1 & 0 \\ 0 & 0 & 0 \end{pmatrix}$$
$$\lambda^4 = \begin{pmatrix} 0 & 0 & 1 \\ 0 & 0 & 0 \\ 1 & 0 & 0 \end{pmatrix} \quad \lambda^5 = \begin{pmatrix} 0 & 0 & -1 \\ 0 & 0 & 0 \\ -i & 0 & 0 \end{pmatrix} \quad \lambda^6 = \begin{pmatrix} 0 & 0 & 0 \\ 0 & 0 & 1 \\ 0 & 1 & 0 \end{pmatrix}$$
$$\lambda^7 = \begin{pmatrix} 0 & 0 & 0 \\ 0 & 0 & -i \\ 0 & i & 0 \end{pmatrix} \quad \lambda^8 = \frac{1}{\sqrt{3}} \begin{pmatrix} 1 & 0 & 0 \\ 0 & 1 & 0 \\ 0 & 0 & -2 \end{pmatrix} \tag{1.3}$$

The structure constants f_{abc} can be obtained using these matrices. Most of the structure constants are 0, while all non-zero ones can be obtained by completely anti-symmetric relation from the following values:

$$\begin{aligned} & f_{123} = 1 \\ & f_{147} = f_{165} = f_{246} = f_{257} = f_{345} = f_{376} = \frac{1}{2} \\ & f_{485} = f_{678} = \frac{\sqrt{3}}{2}. \end{aligned} \tag{1.4}$$

The current experimentally known quarks imply $N_f = 6$ flavors, named as the up quark, down quark, strange quark, charm quark, bottom quark (also referred to as the beauty quark), and top quark (also referred to as the truth quark). These

six quarks have different quantum numbers and masses. The mass parameters m_k in Eq. (1.1) depend on renormalization scheme and renormalization scale. Under $\overline{\text{MS}}$ scheme, the current-quark masses are reported as[3]: $m_u = 2.16\,\text{MeV}$, $m_d = 4.67\,\text{MeV}$, $m_s = 93\,\text{MeV}$, $m_c = 1.27\,\text{GeV}$, $m_b = 4.18\,\text{GeV}$, and $m_t = 172\,\text{GeV}$. These quark masses have apparent different energy scales, and result in different physic behaviors.

An important symmetry of QCD is called the chiral symmetry, which happens in the limit that quark masses are taken to be 0. This symmetry is spontaneously broken by dynamic chiral symmetry breaking, which happens at scale $\Lambda_\chi \sim 1\text{GeV}$, and is explicitly broken by the non-zero quark masses in reality. Conventionally, a quark is considered to be heavy if its mass $m_k > \Lambda_\chi$, and light if $m_k < \Lambda_\chi$[3]. Thus, charm quark, bottom quark, and top quark are called heavy quarks, which will play important roles in the work presented later in this dissertation.

Another important symmetry of QCD is the $SU(3)$ color symmetry. In the above Lagrangian Eq. (1.1), each quark is assigned to the fundamental representations of the non-abelian local gauge group $SU(3)$. The gauge quantum number is named "color", and the corresponding symmetry is $SU(3)$ color symmetry. There are three different color charges. Conventionally, they are named red, green, and blue. Quarks carry one of these three colors; while anti-quark carries one of the anti-red, anti-green and anti-blue color charges.

The gauge boson of QCD is called the gluon. Gluons transform under the adjoint representation of $SU(3)$ group. The dimension of the adjoint representation is $N_c^2 - 1 = 8$, so there are 8 kinds of gluons, which are known as a "color octet".

The eight kinds of gluons are commonly written as the following linear independent basis:[4]:

$$
\begin{aligned}
&(r\bar{b}+b\bar{r})/\sqrt{2}, \quad -i(r\bar{b}-b\bar{r})/\sqrt{2}, \\
&(r\bar{g}+g\bar{r})/\sqrt{2}, \quad -i(r\bar{g}-g\bar{r})/\sqrt{2}, \\
&(b\bar{g}+g\bar{b})/\sqrt{2}, \quad -i(b\bar{g}-g\bar{b})/\sqrt{2}, \\
&(r\bar{r}-b\bar{b})/\sqrt{2}, \quad (r\bar{r}+b\bar{b}-2g\bar{g})/\sqrt{6}
\end{aligned}
\tag{1.5}
$$

where r, g, and b are red, green, and blue; $\bar{r}$, $\bar{g}$, and $\bar{b}$ are anti-red, anti-green, and anti-blue.

There is no color singlet gluon as $(r\bar{r}+g\bar{g}+b\bar{b})/\sqrt{3}$, otherwise it can be exchanged between two color singlets such as proton and neutron, which contradicts with the experimental fact that there is no long-range force with strong coupling[4]. Another way to interpret this fact is that the existence of a color singlet gluon requires QCD to be in $U(3)$ symmetry, which has 9 degree-of-freedom, rather than $SU(3)$ symmetry with octet representation in the real world. Even if the world was created with "$U(3)$ symmetry QCD", the $U(3)$ would decouple into $U(1)$ symmetry plus $SU(3)$ symmetry with different renormalization scheme. Thus, they would have different coupling constants and representations, and it effectively still looks like our world.

As is the case with photons, gluons are formally massless particles of spin 1. However, the gluon itself carries color charges, which is different from QED where the gauge boson photon does not carry an electro-weak charge. As a result, the

gluon not only interacts with quarks but also interacts with each other. Triple-gluon vertex of order g_s and four-gluon vertex of order g_s^2 can be read from the Lagrangian Eq. (1.1), and are shown in Fig. 1.1.

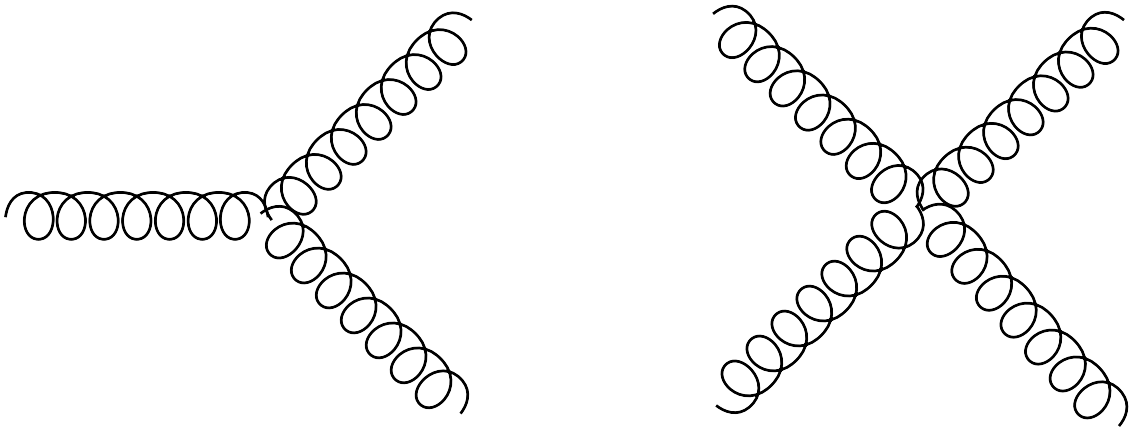

Figure 1.1: Gluon vertexes.

Neither quark nor gluon is observed as a free particle, while a hadron, which is color-singlet combination of (anti)quarks and gluons, and therefore color-neutral, can be observed as a free particle. The fact that color-charged particles cannot be experimentally isolated is called "color confinement". The color confinement is not yet formally proved, and it belongs to one of the seven Millennium Prize Problems: Yang-Mills Existence and Mass Gap Problem[5].

The quantity g_s (or $\alpha_s = \frac{g_s^2}{4\pi}$) appears in the covariant derivative D_μ and field strength $G_{\mu\nu}$ is the QCD coupling constant, which may be thought of as the fundamental unit of color[4]. It is the only fundamental parameter of QCD besides quark masses. The renormalized coupling $\alpha_s(\mu_R^2 \sim Q^2)$ indicates the strength of strong interaction depends on the momentum transfer Q. The renormalization group equation (RGE) of this coupling is[3]:

$$\mu_R^2 \frac{d\alpha_s}{d\mu_R^2} = \beta(\alpha_s) = -(b_0\alpha_s^2 + b_1\alpha_s^3 + b_2\alpha_s^4 + ...). \tag{1.6}$$

The minus sign in Eq. (1.6) indicates that the strong coupling becomes weaker for processes with larger momentum transfer. The strong coupling approaches 0 logarithmically when momentum transfer $Q \to \infty$[6], which can be seen from[4]:

$$\alpha_s(|Q^2|) = \frac{\alpha_s(\mu^2)}{1 + \frac{\alpha_s(\mu^2)}{12\pi}(11N_c - 2N_f)\ln(\frac{|Q^2|}{\mu^2})} \quad , \quad (|Q^2| \gg \mu^2) \tag{1.7}$$

This is the so-called "asymptotic freedom". Under this regime, such as high-momentum-transfer scattering processes, because the coupling is weak, QCD can be studied perturbatively in expansion of the coupling constant, in a similar methodology used in study of QED.

However, when the energy is around or below a scale called Λ_{QCD} (around $89 \sim 332$ MeV under $\overline{MS}$[3]), the coupling gets large, and QCD becomes strongly coupled. In this case, the theory is highly non-perturbative, so that perturbative calculation of Feynman diagrams is no longer reliable as in the weak coupling regime. This makes it difficult to study. Thus, alternative methods are required to analyze enormous phenomena in this regime.

1.3 Lattice QCD

As an important non-perturbative approach to study QCD, Lattice Quantum Chromodynamics (LQCD), proposed by K. Wilson in 1974[7], has been successfully used in research with the help of high-performance computing. It has been used to calculate properties of hadrons, determine fundamental parameters of the standard model, such as strong coupling constants, quark masses, and many other important research topics.

1.3.1 Methodology of lattice QCD

Lattice QCD is defined on a discretized hypercubic lattice with Euclidean space-time with appropriate boundary conditions. The finite lattice spacing a imposes an ultraviolet cut-off, so the theory is ultraviolet regulated. The continuum limit is recovered by taking $a \to 0$.

Lattice formulation of QCD preserves gauge symmetry. The gauge transformations of quark field $q(x)$ and gluon field $U_\mu(x)$ are:

$$q(x) \to V(x)q(x) \tag{1.8}$$

$$\bar{q}(x) \to \bar{q}(x)V^\dagger(x) \tag{1.9}$$

$$U_\mu(x) \to V(x)U_\mu(x)V^\dagger(x + a\hat{\mu}), \tag{1.10}$$

both $V(x)$ and $U_\mu(x)$ are elements of SU(3) group, and $\hat{\mu}$ is the unit vector in direction μ. Gluon field $U_\mu(x)$ is also called gauge link, because it connects quark

field on lattice site x to another lattice site $x + a\hat{\mu}$.

A simplest gauge-invariant action for gluon field called Wilson gauge action is given by[3]:

$$S_g = \beta \sum_{x,\mu,\nu} [1 - \frac{1}{3} \mathrm{ReTr}[\mathrm{U}_\mu(\mathrm{x})\mathrm{U}_\nu(\mathrm{x} + \mathrm{a}\hat{\mu})]\mathrm{U}^\dagger(\mathrm{x} + \mathrm{a}\hat{\nu})\mathrm{U}_\nu^\dagger(\mathrm{x})] \tag{1.11}$$

It involves a trace along a simplest closed loop on the lattice as shown in Fig (1.2)

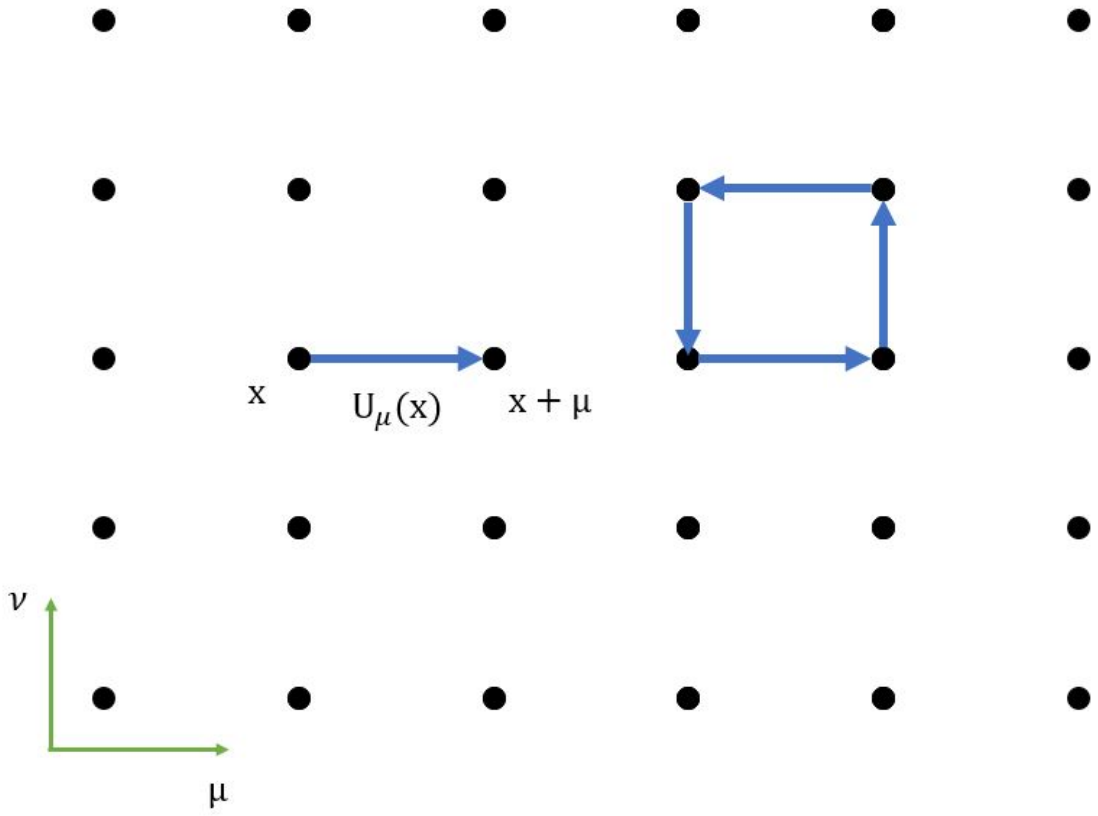

Figure 1.2: The sketch of a lattice.

One can obtain the continuum limit of this simple action and verify if it

matches Eq. (1.1). To do so, notice that $U(x)$ joins quark fields on adjacent lattice points along direction μ. Thus classically, $U(x)$ is determined by integral of quark field A_μ along the link as[8]:

$$U_\mu(x) = \mathcal{P} \exp(-i \int_x^{x+a\hat{\mu}} A \cdot dy) \tag{1.12}$$

Under the continuum limit, a is small, so that $U_\mu(x) \sim e^{-iaA_\mu(x)}$, and can be expressed in powers of a. Then the leading order Wilson action becomes:

$$S_g \to \int d^4x \frac{1}{4g^2_{\text{lattice}}} \text{Tr}[\text{G}_{\mu\nu}\text{G}^{\mu\nu}], \tag{1.13}$$

which matches the continuum form of gluon action in Eq. (1.1).

The lattice version of fermion action is much more non-trivial than the gluon action. Naive implementation of fermion action has the fermion doubling problem, which means the appearance of extra unphysical "doubler" fermions. Nielsen and Ninomiya [9] have proved a no-go theorem states that there is no discretization form of local fermion action that i) is local, ii) has correct continuum limit, iii) preserves chiral symmetry, and iv) have no fermion doublers.

Several strategies have been proposed to deal with the fermion doubling problem, with the price of violating other conditions in the Nielsen-Ninomiya no-go theorem. The Wilson fermion action [7] violates chiral symmetry, and introduce extra error linear in a. The Twisted mass fermion action [10] modifies the Wilson fermion action to remove the error linear in a, but results in an isospin breaking effects. The

Staggered fermion action [11] preserves certain chiral symmetry but not completely removes all the doublers. The Ginsparg-Wilson fermion action [12, 13, 14] has no doublers and preserves a modified version of chiral symmetry. One commonly used type of the Ginsparg-Wilson fermion action in lattice QCD simulation is called the Domain wall fermion action[15, 16, 17], which introduces a fictitious fifth dimension space.

After the action is chosen, Monte Carlo simulation method is used to create gauge configurations with probability measure $[dU]e^{-S_g[U]}\prod_f \det(D[U]+m_f)$[3]. For example, a simple Monte Carlo method to generate a Markov chain of configurations is the Metropolis-Hastings algorithm[18, 19], and an example is given in Ref. [8]. The basic idea is that every-time a new random change in configuration is made, one needs to calculate the difference in action ΔS caused by this change. The new configuration is only accepted when the action is decreased or $\exp(-\Delta S) > \eta$, where η is a uniform random variable between 0 and 1.

A large number of configuration should be generated, in order to calculate the average of certain correlation functions. There are two subtleties when select proper configurations. Firstly, a number of configurations should be discarded before the lattice is well thermalized. After that, since the successive configurations generated by this way are quite correlated to each other, there should be a sufficient number of configurations that are not selected between configurations that are actually selected to carry on numerical evaluation.

Next, in order to extract desired physical information, one should measure the expectation of correlation functions among these selected configurations. Take

lattice study of hadron spectroscopy as an example, hadron interpolators O and $\bar{O}$ with certain quantum numbers are at first constructed, which can annihilate and create certain hadron state on the lattice. For simplicity, we will take these operators to be integrated over space and thus carry zero momentum. These interpolators are used to construct correlator as:

$$C_{n_t} = \big\langle O(n_t)\bar{O}(0)\big\rangle = \sum_k \big\langle 0|O(n_t)|k\big\rangle\big\langle k|\bar{O}(0)|0\big\rangle e^{-n_k E_k}, \tag{1.14}$$

where E_k is the energy of different states with the same quantum numbers as the interpolator. When n_t is large, the exponential term of the ground state energy dominate $C_{n_t} \sim Z_0 e^{-n_k E_0}$, and excited states terms can be neglected. Thus, physical information such as mass of the lowest energy state can be extracted out from the fitting of the results.

There are two important facts. Firstly, the interpolators not only create the state we want but also create other states with the same quantum numbers. These states can be higher excited states, and may even be states with different hadron species. Secondly, for any set of quantum numbers, there is an infinite number of ways to construct different interpolators. These interpolators all create the same set of states with the same quantum numbers, but different interpolators may have different overlapping with different states, which means the coefficient before the exponential would be different. Thus, usually, we want to construct better interpolators that have a larger overlap with the state we want, to decrease the contamination from other states.

Besides hadron spectroscopy, Lattice QCD has been successfully used in many other physical problems. A review can be found in Ref. [3]. However, there are still some limitations of the lattice QCD method.

For example, the well-known signal-to-noise problem[20, 21, 22] states that correlation functions describing one or more baryons have signal-to-noise ratios that are exponentially bad at late Euclidean times. For instance, when evaluating a single nucleon correlation function projected to 0 momentum, the desired signal is the expectation of correlation function:

$$\left\langle OO^{\dagger}\right\rangle \sim e^{-M_N t}, \tag{1.15}$$

where O is the nucleon interpolator. However, at large times, the variance of this signal is

$$\left\langle (OO^{\dagger})^{\dagger} OO^{\dagger}\right\rangle \sim e^{-3m_{\pi} t}, \tag{1.16}$$

because three pions system can have the same quantum numbers as two nucleons system. Thus $(OO^{\dagger})^{\dagger}OO^{\dagger}$ have overlapping with both two nucleons system and three pions system, while the latter have lower mass thus dominants the behavior in Eq. (1.16). As a result, the signal-to-noise ratio is $e^{-(M_N-\frac{3}{2}m_{\pi})t}$, which decreases exponentially at large times.

There is another well-known numerical problem encountered in Lattice QCD simulation called the sign problem. In regime such as QCD with finite chemical

potential and QCD with a θ-term, which will be introduced later in Eq. (2.3), the standard Monte Carlo method cannot be directly used because the probability measure used in generating configurations become negative or complex. This issue will be explained in further detail in the discussions of Chapter 2.

1.4 Systematic expansions

An alternative method to study complex phenomena of QCD is to find a good expansion parameter other than the strong coupling constant in QCD Lagrangian. As mentioned before, the strong coupling constant is not small in the hadronic energy regime, so a perturbative expansion cannot be constructed. If we can instead find a new expansion parameter that is small, then we may be able to capture non-perturbative features of QCD in a systematic expansion of this new parameter.

Moreover, approximations can be made once we have written down the power counting rule of this expansion regime, since we can truncate the expansion to any desired order, and the error caused by this truncation is controlled by the expansion parameter. Under a proper approximation, the complicated theory becomes much easier to handle, while still provides insight into the physical reality.

One successful example is Large N_c QCD, which was at first proposed by Gerard't Hooft[23, 24] for meson physics and then extended to baryon sector by Edward Witten[25]. In this theory, the QCD $SU(3)$ color gauge group is replaced by $SU(N_c)$. By allowing the number of colors N_c to be large, $1/N_c$ will become a small expansion parameter. One can systematically include polynomial correction

of $1/N_c$ order by order. Besides meson and baryon phenomenology, Large N_c QCD has been used to study the U(1) problem and QCD θ-vacuum[26, 27, 28], exotic hadrons[29, 30, 31, 32, 33, 34] and many other questions. In some situations, the quantities in the large N_c limit are not far away from the real world, while in other cases the physics may even be qualitatively different since $N_c = 3$ may not be large enough. Detailed reviews of Large N_c QCD method and its applications can be found in Ref. [35, 36, 37, 38].

Another prominent application of this idea is effective field theory (EFT), such as chiral perturbation theory. Reviews on various of effective field theories can be seen in Ref. [39, 40, 41, 42, 43]. By taking advantage of the separation of different energy scales in the physical world, one can make precise calculations on a lower energy scale without knowing the detail of the underlying ultraviolet (UV) theory on the higher energy scale. This provides enormous simplifications because it is often unnecessary to take into account the details of the short-distance physics. There are also cases that exact full theory is even unknown, so one has to use effective field theory as a practical approximation. In this sense, effective field theory is the low-energy limit of a more fundamental theory. The current Standard Model of particle physics is also viewed as an effective field theory since the underlying UV theory is still unknown.

Effective field theory has one or more small expansion parameters with specific power counting rules. Calculations are done in systematic expansion to a certain order of expansion parameters, with errors controlled to be one order higher.

Since the high energy scale and short distance physical details are wrapped

in this manner, effectively the heavy particles, which require large energy to create and only propagate short distance, are eliminated from the theory. The effective field theory is thus only valid up to energy scale below the masses of these heavy particles.

The short distance physics is encoded in the coefficients of the effective theory's Lagrangian. The numerical values of these parameters can be obtained by experiment measurements, lattice QCD simulation, or matching to the underlying short-distance physics. Once the finite number of coefficients are fixed, one can conduct predictions for all other relevant quantities.

An example is the chiral perturbation theory (χPT), which describes the low-energy dynamics of QCD. The underlying full theory QCD is non-perturbative in the hadronic scale, and QCD Lagrangian is written in terms of quarks fields and gluons fields. In contrast, the degree-of-freedoms in chiral perturbation theory are meson fields and baryon fields. The expansion parameter in QCD is p/Λ_χ or m/Λ_χ, where p is the momentum transfer during the process, and $\Lambda_\chi \sim 1$ GeV is the scale of chiral symmetry breaking. Below Λ_χ, chiral symmetry is preserved given that the light quarks are considered as massless. Chiral perturbation theory is widely used in the study of interactions among hadrons, and reviews can be found in Ref. [44, 45, 46, 47].

1.4.1 Heavy quark effective theory and non-relativistic QCD

Two chapters of this dissertation will be devoted to analysis related to heavy quarks and heavy mesons, so it is important to have a short introduction on two commonly used effective field theories about the heavy quarks system. One of them is called heavy quark effective theory (HQET), and the other is called non-relativisitic QCD (NRQCD).

HQET[48, 49, 50, 51, 52, 53] describes low-energy interactions of a single heavy quark with light particles. The expansion parameter is Λ_{QCD}/m_Q. Λ_{QCD} is the confinement scale where perturbative-defined coupling would diverge, and non-perturbative dynamics dominates. Λ_{QCD} is around $89 \sim 332$ MeV under $\overline{MS}$[3]. m_Q is the heavy quark mass. Recall that heavy quark masses $m_c = 1.27\,\text{GeV}$, $m_b = 4.18\,\text{GeV}$ and $m_t = 172\,\text{GeV}$. Thus heavy quark mass m_Q is considered to be much larger than Λ_{QCD}.

In this theory, the heavy quark is viewed as nearly on-shell, so its 4-momentum p_Q can be decomposed as:

$$p_Q^\mu = m_Q v^\mu + k^\mu, \tag{1.17}$$

where v^μ is the velocity, and the residue momentum k^μ is of order Λ_{QCD}.

The leading order Lagrangian of HQET is written as[3]:

$$\mathcal{L}^{(0)}_{\text{HQET}} = \bar{h}_\nu i v \cdot D_s h_\nu, \tag{1.18}$$

where h_ν is the field that destroys the heavy quark with velocity v. The covariant derivative $D_s^\mu = \partial^\mu - igA_s^\mu$ only contains soft gluon field.

Notice that, this leading order Lagrangian does not depend on the spin of the heavy quark, which suggests there is an emergent $SU(2)$ spin symmetry[54, 55]. This in turns implies the degeneracy of hadronic states with quantum numbers that only differ in the heavy quark spin, such as D meson and D^* meson, in the heavy quark mass limit.

Another important physical phenomenon in the heavy quark mass limit is that the creation and annihilation of heavy quark and heavy anti-quark is suppressed, so the number of heavy quarks and heavy anti-quarks is conserved.

The next-to-leading order HQET Lagrangian contains two terms[3]:

$$\mathcal{L}^{(1)}_{\text{HQET}} = \frac{1}{2m_Q}\bar{h}_v(iD_s)^2 h_v + \frac{1}{2m_Q}C_{\text{mag}}(\nu)\frac{g}{2}\bar{h}_\nu \sigma_{\mu\nu}G_s^{\mu\nu}h_\nu. \tag{1.19}$$

The first term is the kinetic energy term, corresponding to the first order correction in Taylor expansion of the energy. The second term is the chromo-magnetic interaction term.

HQET has also been extended to describe hadronic degree-of-freedom by combining with chiral perturbation theory. The resulting heavy hadron chiral perturbation theory (HHχ PT)[56, 57, 58, 59, 60, 61] describes the interaction of heavy hadron containing one heavy quark with light mesons. The chiral symmetry is assumed for the light mesons so that one can treat them as pseudo-Goldstone bosons.

A lot of properties of hadron systems containing a single heavy quark have

been studied using HQET. However, HQET is not the appropriate effective field theory for hadrons containing two or more heavy quarks (or heavy anti-quarks). The correct effective theory for this kind of system is the Nonrelativistic Quantum Chromodynamics (NRQCD)[62, 63]. Detailed introductions can be found in Ref.[64, 65, 66].

NRQCD has the same Lagrangian as HQET, but is formulated with a different expansion parameter[67]: the velocity of heavy quarks $v \sim \alpha_s(m_Q)$. With different power counting rules, the relative scalings of terms in Lagrangian are also quite different.

For a bound state containing two or more heavy quarks, the typical momentum scale of the heavy quarks is $m_Q v$, and the typical kinetic energy of the heavy quarks is $m_Q v^2$. Since v is small, we have $m_Q \gg m_Q v \gg m_Q v^2$. The energy and momentum of light degree-of-freedom are both of the scale Λ_{QCD}. At the extreme heavy quark mass limit, $m_Q v^2 \gg \Lambda$, while in reality for charm quark system $m_Q v^2 \sim \Lambda_{QCD} \sim$ 400MeV[67].

Chapter 2: Sign problems and the infinite volume limit

2.1 Sign problems in Monte Carlo simulations

As introduced in the previous chapter, lattice QCD relies on the Monte Carlo method. Monte Carlo method is a powerful and widely-used numerical method for understanding the physics of many-body systems and strongly correlated theories, for which analytical methods are intractable. Thus, it is not only used in lattice QCD but also used in condensed matter physics to study interesting properties of many-body systems. However, there are circumstances where the Monte Caro method faces a great challenge, which is known as the sign problem. In particle and nuclear physics, the sign problem prevents QCD at finite chemical potential[68, 69, 70], QCD with a θ-term[71] and real-time quantum field theories[72] from being explored by lattice simulation. In condensed matter physics, the sign problem also causes trouble in simulation of many-body fermionic systems or frustrative models, such as the repulsive Hubbard model[73, 74, 75], electron structure calculations[76, 77, 78], polymer theory[79], and so on.

The physical quantity one normally computes using a Monte Carlo method is

the phase space average of an observable as in Eq. (2.1).

$$\langle \mathcal{O} \rangle = \frac{\sum_c \mathcal{O}(c) p(c)}{\sum_c p(c)} \tag{2.1}$$

The quantity $\mathcal{O}$ is summed over every possible configuration c with corresponding weight $p(c)$. In field theories, like lattice QCD, the $p(c)$ here is usually the Boltzmann factor e^{-S}, where S is the Euclidean-space action; while in a general case, $p(c)$ may be more complicated form associated with the Hamiltonian or Lagrangian of the system, which depends on the specific scheme and basis one works with. For example, in Handscomb's simulation scheme using Suzuki-Trotter approach[80, 81, 82], which is widely used in Quantum Monte Carlo simulating of spin system, $e^{-\beta H}$ is expanded in a Taylor series, and the weight $p(c)$ turns out to be $\frac{(-\beta)^n}{n!}\mathrm{Tr}(\prod_{\mathrm{j}=1}^{\mathrm{n}} \mathrm{H_j})$, where β is inverse temperature and the original Hamiltonian is divided into n separated pieces H_j. It is important to notice that the usage of Monte Carlo method relies on considering these weights as the probabilities to generate configurations.

The sign problem arises when the weights $p(c)$s are not positive definite. For example, in fermionic many-body systems, weights with a negative sign appear due to the Pauli exclusion principle when two fermions are changed. What's more, in gauge field theories, the weights are generally complex numbers with phase factors like $e^{i\phi}$. Then the standard Monte Carlo regime is not directly applicable to these problems, because only non-negative real numbers can be viewed as probabilities. One may formally eliminate the negative sign or phase factor $e^{i\phi}$ of the weights $p(c)$s by absorbing the sign or phase factor into observable $\mathcal{O}$, and define $\tilde{\mathcal{O}} = \mathcal{O}e^{i\phi}$. Then

the new weight $\tilde{p}(c) = p(c)/e^{i\phi}$ becomes positive and can be used as the probability of generating certain configurations in Monte Carlo simulation. However, it usually turns out this gives extremely large cancellations due to the oscillating signs of the $\tilde{\mathcal{O}}$. Accordingly, the computational cost to obtain $\langle \mathcal{O} \rangle$ is usually scaling exponentially with the size of the system and the inverse temperature.

For QCD, there are well-known cases where sign problems exist. One is QCD at non-zero chemical potential μ, in which case the fermion determinant has a complex phase because the Dirac operator is non-hermitian for non-zero μ:

$$\det(\mathrm{D} + \mu\gamma_0 + \mathrm{m}) = \mathrm{e}^{\mathrm{i}\theta} |\det(\mathrm{D} + \mu\gamma_0 + \mathrm{m})|. \tag{2.2}$$

This renders the standard Monte Carlo method inapplicable. It has been pointed out that, the actual problem is that the phase of the fermion determinant fluctuates wildly for $\mu > m_\pi/2$, so that the average phase factor is exponentially small in volume[83, 84]. It is also pointed out that the origin of non-positive weights in QCD-like theories is different from the fermionic problem in Monte Carlo simulation of condensed matter physics. Rather, it is related to the existence of a tightly bound state of valence fermions, which is accompanied by dynamical chiral symmetry breaking[85].

Another example of the sign problem is QCD with a θ-term, which will be the main focus of this chapter. The QCD Lagrangian density with a θ-term has the form:

$$\mathcal{L} = \sum_{k=1}^{N_F} \bar{q}_k (i\gamma^\mu D_\mu - m_k) q_k - \frac{1}{4} G^a_{\mu\nu} G^{a\mu\nu} - \frac{g_s^2}{32\pi^2} \theta \epsilon^{\alpha\beta\mu\nu} G_{\alpha\beta} G^{\mu\nu}, \tag{2.3}$$

where the last term is often omitted as in Eq. (1.1). Then the Euclidean space QCD partition function has a factor $\exp(-\mathrm{S_{YM}} + \mathrm{i}\theta\mathrm{Q})$, where S_{YM} and Q are functionals of the gluon field configurations on a space-time region of volume V. The factor is not positive definite because of the existence of the θ-term. The severity of the sign problem in this regime will be explained further in following sections.

Since the form of Monte Carlo weights $p(c)$ in Eq. (2.1) depends on the particular scheme and basis used, it is noticed that, by choosing a different scheme or basis, the sign problem may be eliminated. This is true for specific cases. However, it is often difficult to find such kind of transformation, and the difficulty of solving the numerical sign problem may change to the difficulty of solving other hard problems. For example, it is shown that a sign problem in double-spin-chain system disappears by switching to a special basis[86], but it is nearly impossible to find that kind of basis to eliminate the sign problem for a generic complicated system. For another example, a QCD-like theory Nambu-Jona-Lasinio (NJL) model is shown to have a sign problem in one formulation but not have a sign problem in another formulation. However, the formulation without sign problem has a new problem, called "overlap problem", which is also hard to solve[85].

Over the past two decades, many algorithms and methods have been proposed to evade the sign problem. These techniques includes Taylor expansion[87,

88, 89, 90, 91, 92] , analytic continuation[93, 94, 95, 96, 97, 98, 99], imaginary chemical potential[69, 93, 95, 96, 100], reweighting[101, 102, 103, 104, 105], the density of states method[106, 107, 108], the complex Langevin method[109, 110, 111], the Lefschetz-thimble path-integral method[112, 113, 114], the generalized thimble method[115], the sign optimized manifolds method [115, 116, 117], the meron-cluster method[118, 119], the worm algorithms[120], the canonical ensemble approach[121, 122, 123, 124, 125], and so on. A good but not complete review can be found in Ref.[126].

Due to these progress in the past years, it is now possible to perform reliable calculations in some systems where sign problems are not extremely severe, such as the region near the finite temperature phase transition with a non-zero but small chemical potential μ.

However, most of the methods are currently only reliable on simple systems, and it is still not clear whether it can be successfully extended to complicated problems such as the high-density regime of QCD. Some of these methods depend significantly on the specific physics details of the system and uses the special property of the system to eliminate the random signs, which makes it not applicable to different systems.

Currently, none of these methods is accepted by the community as a generic solution to the sign problem. This is not surprising since there is a no-go theorem by Troyer and Wiese[127] that precludes the existence of a generic solution to the sign problem. The argument of Troyer and Wiese is that a generic solution to the sign problem means one can solve all the NP-hard problems in the sense of complexity

theory in theoretical computer science.

2.2 Motivations

As mentioned in the previous section, QCD with a θ-term has a sign problem. This chapter focuses on a specific phenomenon related to it, which may shed some light on how to avoid the sign problem.

The other motivation of this chapter is related to the so-called strong CP problem. The resolution[128, 129] of the axial U(1) problem[130] requires a nontrivial topological effect. This topological effect implies the existence of CP-violating term in the QCD Lagrangian: the so-called θ-term as in Eq. (2.3). In principle, the coefficient θ can take any value between $-\pi$ and π. (There is no need to consider other values of θ because of the periodicity of 2π.) However, the extracted value in the neutron electric dipole experiments leads to the bound $|\theta| < 10^{-9}$[131, 132]. This extraordinary small value apparently violates Gell-Mann's famous statement about particle physics: "what is not forbidden is mandatory"[133]. The puzzle why θ, the coefficient marks the strength of CP violation in the strong sector, is so close to zero is called the strong CP problem. One famous theoretical attempt to solve this problem was proposed by Peccei and Quinn (PQ) in 1977[134, 135]. They introduced an auxiliary chiral $U(1)_{\rm PQ}$ symmetry, which is spontaneously broken. The PQ solution implies the existence of a pseudo-Goldstone boson, the axion[136, 137]. The properties of axion makes it becomes a popular candidate of dark matter[138, 139]. However, up to now, the existence of axion in the real world is still neither confirmed

nor excluded by experiments[138, 139], thus PQ solution to strong CP problem is not experimentally verified yet.

The subtlety here is that, in the real world, the possibility that $\theta \approx \pi$ rather than $\theta \approx 0$ is not rigorously ruled out. The neutron electric dipole moment experiments only tell us that the CP-violation in the strong sector is too tiny to be observed. Since we know the value of θ is proportional to CP violation, and the lattice calculations are done with $\theta = 0$ appear to matches the real world well, people imply the missing of CP violation as $|\theta| < 10^{-9}$. However, theoretically, $|\theta - \pi| < 10^{-9}$ is also not conflict with neutron electric dipole moment experiments, since $\theta = \pi$ is also CP invariant.

It is thus of theoretical interest if one can rule out the case that $\theta = \pi$, which will enhance our understanding of QCD θ-vacuum. Fortunately, it has been pointed out that this case can be easily falsified if CP is spontaneously broken around $\theta = \pi$[140]. If CP symmetry is indeed spontaneously broken at $\theta = \pi$, then the energy density with respect to θ, $\varepsilon(\theta)$ will have a cusp at $\theta = \pi$ (in the infinite volume limit). In other words, the slope of $\varepsilon(\theta)$ will have discontinuity at $\theta = \pi$, which is clearly different from $\theta = 0$ where the slope is 0. The appearance of cusp in $\varepsilon(\theta)$'s curve at $\theta = \pi$ is named Dashen's phenomenon[140].

There are certain theoretical regimes where Dashen's phenomenon occurs at $\theta = \pi$. For example, in the large N_c limit, high order terms in $\varepsilon(\theta)$ are suppressed by $1/N_c$, and thus the even function $\varepsilon(\theta)$ is approximated as only having a quadratic term. Then given the periodicity of 2π, $\varepsilon(\theta)$ must be a piece-wise function proportional to $\min \sum_k (\theta - 2\pi k)^2$ [141, 142]. It is easy to see that this form leads to a

cusp at $\theta = \pi$. For another example, it has been shown that near the chiral limit with isospin symmetry, $\varepsilon(\theta)$ is proportional to $(1-\cos\frac{\theta}{N_f})$ in region $\theta \in [-\pi, \pi]$ with higher-order terms neglected, where N_f is the number of degenerate quarks which are massless in the chiral limit[143]. This regime also leads to Dashen's phenomenon for $N_f \geq 2$. The illustration of these two regimes are shown in Fig.2.1, where the curves of $\varepsilon(\theta)$ are plotted in units of the topological susceptibility and with $\varepsilon(0)$ subtracted off. The dashed line is at the large N_c limit and solid line is at leading nontrivial order in a chiral expansion for two degenerate light flavors.

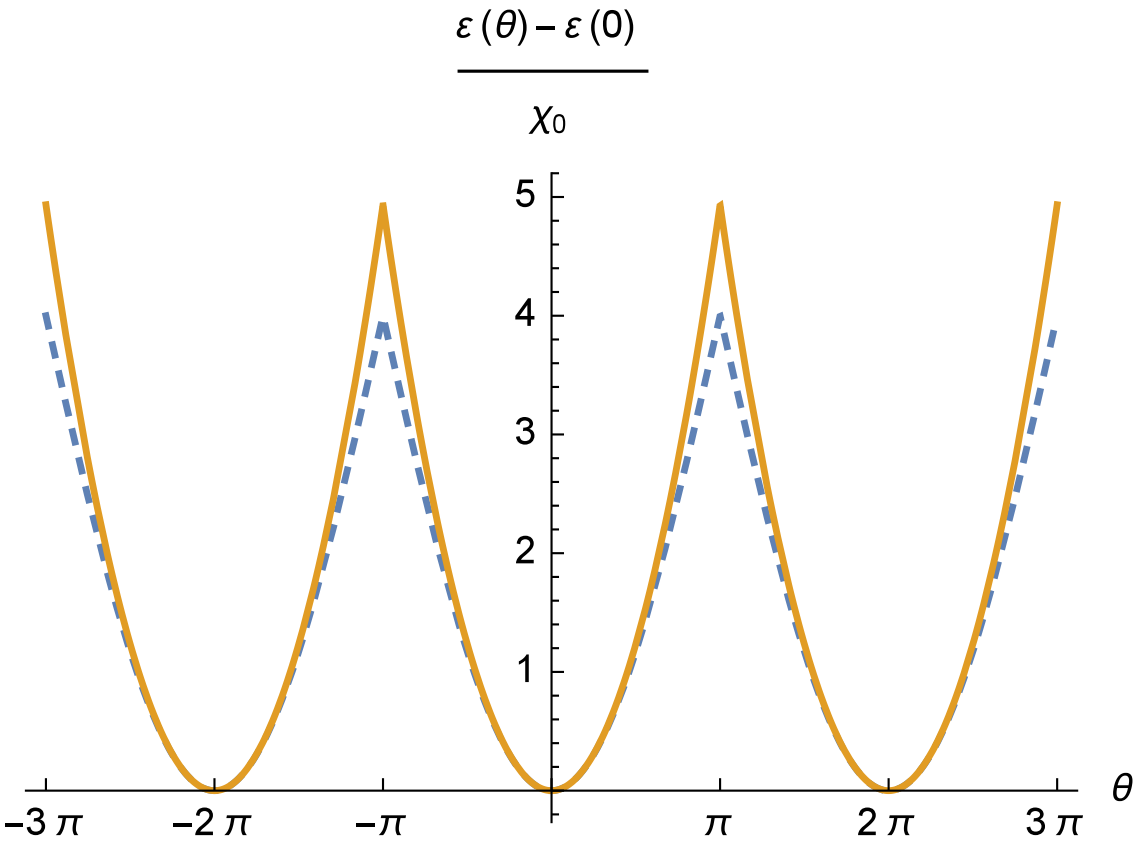

Figure 2.1: Dashen's phenonena occur at $\varepsilon(\theta)$ in the large N_c limit (dashed line) and $\varepsilon(\theta)$ in a chiral expansion for two degenerate light flavors (solid line). χ_0 is the topological susceptibility.

However, the occurrence of Dashen's phenomenon does not guarantee that the

same thing happens in the real world. It is possible that, though CP is spontaneous broken at $\theta = \pi$ in regime with $N_c = \infty$, CP may be unbroken in the real world with $N_c = 3$. Similarly, though there is a discontinuity at $\theta = \pi$ in the massless limit of light quarks, the light quarks have small and different masses in the real world, which may render $\varepsilon(\theta)$ smooth at $\theta = \pi$.

In the absence of lattice studies near $\theta = \pi$, one cannot say for sure whether Dashen's phenomenon happens in the real world. In order to obtain a deeper understanding of QCD vacuum, it is important to have direct lattice calculations in this region. However, as mentioned before, this is difficult because of the sign problem, especially when θ approaches π.

In this chapter, we will study an interesting phenomenon related to the sign problem and Dashen's phenomenon, with the interplay of the infinite volume limit. The hope is that this may help to improve our understanding of the sign problem and the strong CP problem in the future.

2.3 Formalism

To show the main observation of this chapter, it is necessary to first define the key quantities. As the related measurement of energy density can be done in lattice studies, here we define these quantities in Euclidean space within a four-dimensional space-time box with volume $V = L_x L_y L_z L_t$. Periodic and anti-periodic boundary conditions are imposed at the edge of this box for bosons and fermions respectively. Practically, V is finite rather than infinity, however, it should be large enough to

reduce the finite volume corrections. For simplicity, we consider the continuum limit of the discrete lattice setting. There are some subtleties related to topological charge in discrete lattice[144, 145, 146, 147], but it is irrelevant to the discussion of this chapter.

The QCD partition function on a space-time region volume V is given by path integral:

$$\mathcal{Z}(\theta, V) = \int [dA] \, \det[iD[A] - M] \, \exp(-S_{YM} + i\theta Q),, \tag{2.4}$$

where θ is the vacuum angle, and integer Q is the topological charge dependent on the gluon field configuration. It is well-known that $\mathcal{Z}(\theta, V)$ is an even function and is periodic in θ[148].

According to Atiyah-Singer index theorem[149], the winding number Q equals the difference between the number of right-handed modes and the number of left-handed modes of the Dirac operator. Q is given by:

$$Q = \int_V \frac{g^2}{32\pi^2} \epsilon^{\alpha\beta\mu\nu} G_{\alpha\beta} G_{\mu\nu}. \tag{2.5}$$

The energy density with respect to vacuum angle θ, which is the most important quantity of this chapter, is given by the QCD partition function $\mathcal{Z}(\theta, V)$ as:

$$\varepsilon(\theta) = -\lim_{V\to\infty} \frac{1}{V} \log \mathcal{Z}(\theta, V), \tag{2.6}$$

$\mathcal{Z}(\theta, V)$ can be written as a Fourier sum over partition function $\mathcal{Z}_Q(V)$ with fixed topological charge Q as:

$$\begin{aligned} \mathcal{Z}(\theta, V) &= \sum_{Q\in\mathbb{Z}} \mathcal{Z}_Q(V)\ e^{i\theta Q} \\ &= \sum_{Q\in\mathbb{Z}} \mathcal{Z}_Q(V)\ \cos(\theta Q), \end{aligned} \tag{2.7}$$

where we have used the feature of even function. The corresponding inverse transformation is

$$\begin{aligned} \mathcal{Z}_Q(V) &= \frac{1}{\pi} \int_0^\pi \mathcal{Z}(\theta)\, e^{-i\theta Q}\, \mathrm{d}\theta \\ &= \frac{1}{\pi} \int_0^\pi \mathcal{Z}(\theta)\ \cos(\theta Q)\, \mathrm{d}\theta, \end{aligned} \tag{2.8}$$

One can further define energy density with respect to topological charge density $q \equiv \frac{Q}{V}$ as:

$$\tilde{\varepsilon}(q, V) = -\frac{1}{V} \log(\mathcal{Z}_{(qV)}(V)), \tag{2.9}$$

where $Q \equiv qV$ can only be integer.

Then, the relation between the two kinds of energy density functions are:

$$\varepsilon(\theta) = -\lim_{V\to\infty} \frac{1}{V} \log\left(\sum_{Q=-\infty}^{\infty} e^{-\tilde{\varepsilon}(\frac{Q}{V},V)V}\, e^{i\theta Q}\right). \tag{2.10}$$

Since one expects that $\tilde{\varepsilon}(q,V)$, the energy density function with respect to q, is well-defined in the infinite volume limit, it is natural to define its infinite volume limit as:

$$\begin{aligned}\tilde{\varepsilon}(q) &\equiv \lim_{V\to\infty} \tilde{\varepsilon}(q,V) \ \text{ with } qV \text{ a positive integer} \\ &= -\lim_{V\to\infty} \frac{1}{V} \log\left(\frac{1}{\pi}\int_0^{\pi} e^{-\varepsilon(\theta)V}\, e^{-i\theta qV}\, \mathrm{d}\theta\right).\end{aligned} \tag{2.11}$$

It would be helpful if one could directly compute the energy density near $\theta = \pi$ through lattice simulations, then one can tell whether there is spontaneous CP broken at $\theta = \pi$. However, the well-known sign problem prevents it from being done as mentioned in previous sections. To see exactly how sign problem looks in this problem, we consider the difference between $\varepsilon(\pi)$ and $\varepsilon(0)$, which can be written as:

$$\begin{aligned}\varepsilon(\pi) - \varepsilon(0) &= -\lim_{V\to\infty} \frac{1}{V} \log\left(\frac{A(V) - B(V)}{A(V)}\right) \\ \text{with } \ A(V) &\equiv \frac{\mathcal{Z}_{Q=0}(V)}{\mathcal{Z}(\theta=0,V)} \\ \text{and } \ B(V) &\equiv -\frac{2\sum_{Q=1}^{\infty}(-1)^Q \mathcal{Z}_Q(V)}{\mathcal{Z}(\theta=0,V)},\end{aligned} \tag{2.12}$$

where we have used the fact that $\tilde{\varepsilon}\left(\frac{-Q}{V}, V\right) = \tilde{\varepsilon}\left(\frac{Q}{V}, V\right)$ because of CP invariance.

Notice that [150],

$$\lim_{V\to\infty} \mathcal{Z}_{Q=0}(V) = \lim_{V\to\infty} \mathcal{Z}(\theta = 0, V)\,, \tag{2.13}$$

which implies that $A(V)$ is a sub-exponential function of V.

Thus, if one assumes that the difference $\varepsilon(\pi) - \varepsilon(0)$ is of order unity, then one must compute the difference between $A(V)$ and $B(V)$ with an accuracy of the same level as $\exp\left(-V\left(\varepsilon(\theta) - \varepsilon(0)\right)\right)$, which is exponentially small in V, in order to get a sensible result of $\varepsilon(\pi) - \varepsilon(0)$ through Fourier sum. Lattice simulation can be used to obtain the result in each topological sector with specific Q, however, the time complexity of the Monte Carlo algorithm is polynomial in accuracy. This in turns means, one need to spend computational resource exponentially large in V to compute each part of $A(V)$ and $B(V)$ exponentially accurate in V. This difficulty is caused by the oscillating sign of the summation over different topology sectors in Eq. (2.7), so it is a sign problem.

This sign problem is tractable when θ is small but becomes severe near $\theta = \pi$ where the cancellation caused by oscillating sign is the most serious. Since there is no sign problem when θ is purely imaginary, one may analytically continue the calculation result from the imaginary θ region to real θ. This strategy has been used to calculate deconfinement temperature, electric dipole moment and so on[151, 152, 153, 154, 155, 156] for small real θ near 0. The validity of this method is because that when θ is small, one can use the lowest order terms in Taylor expansion to

approximate the behavior of the exact form of $\varepsilon(\theta)$. However, when θ is away from 0, this method is no longer valid if we lack knowledge of the exact form of $\varepsilon(\theta)$. This is because the higher-order terms in θ is not negligible for not small θ, and there might exist non-analytic discontinuities.

The main purpose of this section is not solving this sign problem associated with θ-term. The actual focus is on a theoretical issue related to the subtle interplay of this sign problem and the infinite volume limit. The issue is as following: suppose one could calculate $\tilde{\varepsilon}(q)$, which is the infinite volume limit of $\tilde{\varepsilon}(\frac{Q}{\tilde{V}}, \tilde{V})$, to arbitrary accuracy, could we use this information to re-obtain full information of $\varepsilon(\theta)$? Naively, the answer seems to be yes, since both quantities are well-defined intensive quantities in the infinite volume limit, and are independent of finite volume corrections. However, the true answer is subtle. To show this subtlety, let us define a new quantity:

$$\begin{aligned} \underline{\varepsilon}(\theta) &= -\lim_{V\to\infty} \frac{1}{V} \log\left(\sum_Q \; e^{-\tilde{\varepsilon}(\frac{Q}{V})V} \, e^{i\theta Q}\right) \\ &= -\lim_{V\to\infty} \lim_{\tilde{V}\to\infty} \frac{1}{V} \log\left(\sum_Q \; e^{-\tilde{\varepsilon}(\frac{Q}{\tilde{V}},\tilde{V})V} \, e^{i\theta Q}\right). \end{aligned} \tag{2.14}$$

The only difference between $\underline{\varepsilon}(\theta)$ and $\varepsilon(\theta)$ is the order of taking limits. In obtaining $\underline{\varepsilon}(\theta)$, the limit $\tilde{V} \to \infty$ is taking before the limit $V \to \infty$, which means $\underline{\varepsilon}(\theta)$ is constructed from $\tilde{\varepsilon}(q)$ without the finite volume correction; while in obtaining $\varepsilon(\theta)$ in Eq. (2.10), these two limits are taken at the same time, so the finite volume correction in $\tilde{\varepsilon}(\frac{Q}{\tilde{V}}, \tilde{V})$ is taken into account. Thus, the previous question is equivalent

to ask: whether $\underline{\varepsilon}(\theta) = \varepsilon(\theta)$.

The answer turns out to be tricky. It seems plausible that $\underline{\varepsilon}(\theta) = \varepsilon(\theta)$ since both of them are intensive quantities. It turns out that, it is true if $\varepsilon(\theta)$ curves upward (*i.e.* $\varepsilon''(\theta) > 0$) everywhere in the region $-\pi < \theta < \pi$, one can find $\underline{\varepsilon}(\theta) = \varepsilon(\theta)$. Notice that, in this case, $\varepsilon(\theta)$ has Dashen's phenomenon because $\varepsilon''(\theta) > 0$ in the whole region. However, if there is a region where $\varepsilon''(\theta) < 0$, $\underline{\varepsilon}(\theta)$, obtained by direct summation over topological sectors, would be different from $\varepsilon(\theta)$. This seems to imply that the sign problem is so severe that, even perfect knowledge of $\tilde{\varepsilon}(q)$ is insufficient to reconstruct the original $\varepsilon(\theta)$ in this regime.

In the following section, at first, a toy model will be used as a demonstration of this phenomenon. The analysis and generalization will be given in subsequent sections.

2.4 A toy problem: dilute instanton gas

For illustrative purposes, we are going to consider a toy problem: the dilute instanton gas. Though it is known that QCD is not well approximated by dilute instanton gas [157], this toy model has two virtues: it has a θ term with a sign problem, which is similar to QCD, and its $\varepsilon(\theta)$ has a known analytical form, which simplifies the relevant discussion.

2.4.1 $\varepsilon(\theta)$ versus $\underline{\varepsilon}(\theta)$

Instantons in quantum field theories are solutions of the classical field equations in Euclidean space with finite action. It describes tunneling processes in Minkowski space-time from one vacuum at one time to another vacuum at another time[158]. They are thus often used to study the tunneling behavior among vacuums of quantum field theory. Historically, instantons were involved in the discussion of the chiral $U(1)$ anomaly problem[128, 129, 159], and was closely related to the introduction of θ-term[160, 161, 162]. Detailed reviews of the dilute instanton gas model can be found in Ref. [157, 158, 163].

The partition function of the dilute instanton gas model is obtained by summing over all instantons and anti-instantons as:

$$\mathcal{Z}_Q(V) = \mathcal{Z}_0 \sum_{n=0}^{\infty} \frac{\left(\frac{1}{2}\, c\, e^{-S_0} V\right)^{|Q|+2n}}{n!\,(n+|Q|)!} = \mathcal{Z}_0 I_Q(c e^{-S_0} V), \tag{2.15}$$

where $\mathcal{Z}_0$ is a real prefactor that sums up effects other than instantons, S_0 is the action of a single instanton, V is the space time volume, and c is a constant with dimension 4 that includes the effects of fluctuations. The sum yields a modified Bessel function of the first kind $I_Q(ce^{-S_0}V)$.

With Eq. (2.7) and taking into account the fact that

$$I_Q(z) = \frac{1}{2\pi} \int_{-\pi}^{\pi} e^{z\cos\theta} \cos(Q\theta) d\theta, \tag{2.16}$$

for integer Q, it is easy to derive the partition function with respect to θ:

$$\mathcal{Z}(\theta) = \mathcal{Z}_0 \exp\left(ce^{-S_0} V \cos(\theta)\right). \tag{2.17}$$

Then it is straight forward to obtain the energy density function with respect to θ as:

$$\begin{aligned} \varepsilon(\theta) &= \varepsilon_0 + \chi_0(1 - \cos(\theta)) \\ \text{with } \chi_0 &\equiv ce^{-S_0}, \text{and } \varepsilon_0 \equiv \frac{-\log(\mathcal{Z}_0)}{V} - ce^{-S_0}, \end{aligned} \tag{2.18}$$

which is well known in the literature[163] .

In order to obtain the energy density function with respect to topological charge, we need to use the series expansion of the modified Bessel function of the first kind $I_\nu(\nu z)$ in the uniform limit $\nu \to \infty$ for positive real values,

$$\begin{aligned} I_\nu(\nu z) &\sim \frac{e^{\nu\eta}}{(2\pi\nu)^{\frac{1}{2}}(1+z^2)^{\frac{1}{4}}} \sum_{k=0}^{\infty} \frac{U_k(p)}{\nu^k}, \\ \text{with } \eta &= (1+z^2)^{\frac{1}{2}} + \log\left(\frac{z}{1+(1+z^2)^{\frac{1}{2}}}\right), \text{ and } p = (1+z^2)^{-\frac{1}{2}}, \end{aligned} \tag{2.19}$$

where $U_k(p)$s are polynomials in p of degree $3k$ with $U_0(p)$ equal to unity[164].

Then,

$$\begin{aligned} \tilde{\varepsilon}(q, V) = \varepsilon_0 + \chi_0 + q\log\left(\frac{q+\sqrt{\chi_0^2+q^2}}{\chi_0}\right) - \sqrt{\chi_0^2+q^2} \\ + \frac{\log\left((2\pi)^2 V^2 (q^2+\chi_0^2)\right) - 4\log\left(\sum_k \frac{U_k\left(\frac{q}{\sqrt{q^2+\chi_0^2}}\right)}{(qV)^k}\right)}{4V}. \end{aligned} \tag{2.20}$$

After taking the infinite volume limit, one can get rid of the tedious finite volume correction and obtain a clean analytic form:

$$\begin{aligned}\tilde{\varepsilon}(q) &= \lim_{V\to\infty} \tilde{\varepsilon}(q,V) \\ &= \varepsilon_0 + \chi_0 + q\log\left(\frac{q+\sqrt{\chi_0^2+q^2}}{\chi_0}\right) - \sqrt{\chi_0^2+q^2} \\ &= \varepsilon_0 + \chi_0 + q\,\sinh^{-1}\left(\frac{q}{\chi_0}\right) - \sqrt{\chi_0^2+q^2}\,. \end{aligned} \tag{2.21}$$

The plot of $\tilde{\varepsilon}(q)$ is shown in Fig. 2.2.

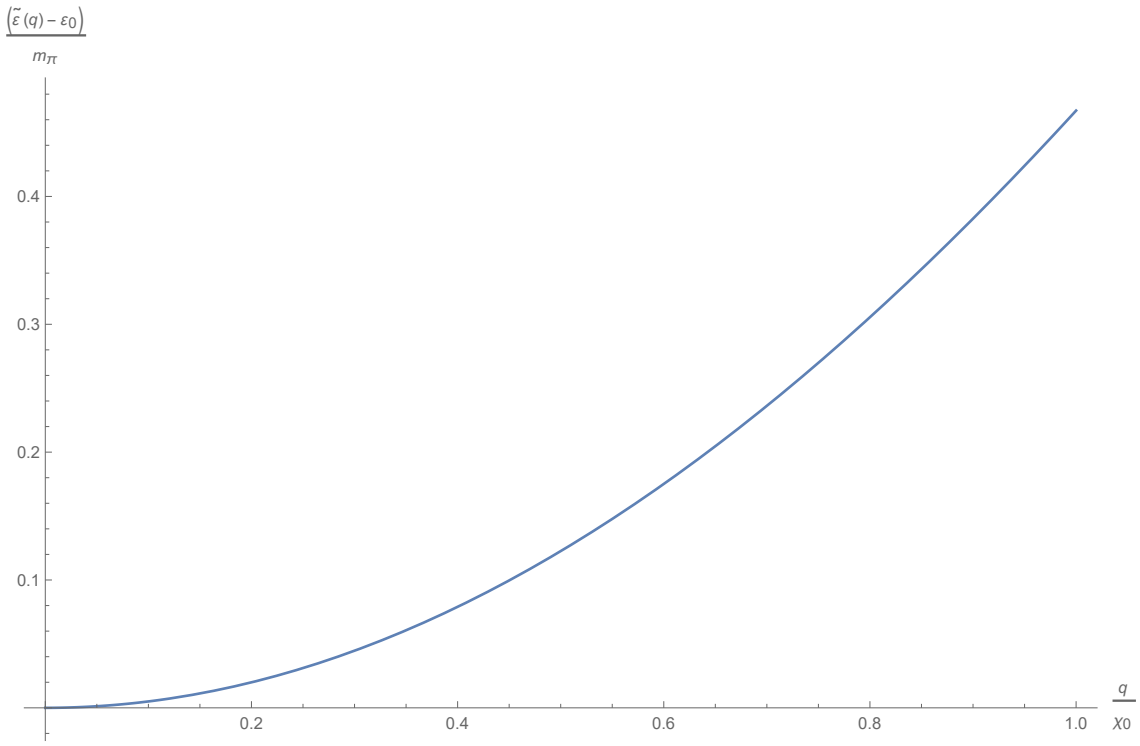

Figure 2.2: The plot of $\tilde{\varepsilon}(q)$.

The topological charge density q is a real number, however, if we analytically continuate it to complex q plane, the function $\tilde{\varepsilon}(q)$ is multi-branched with branch

cuts starting from branch points at $\pm i\chi_0$ and extending to infinity along the imaginary axis. This is an important feature that will be used later.

We can use this expression of $\tilde{\varepsilon}(q)$ to calculate $\underline{\varepsilon}(\theta)$ though Eq. (2.14) , and verify whether $\underline{\varepsilon}(\theta) = \varepsilon(\theta)$ is true. However, there is no analytic closed form expression for $\underline{\varepsilon}(\theta)$ in this case, so we can only conduct the calculation numerically with large but finite V.

The numerical evaluation of $\underline{\varepsilon}(\theta)$ was done in finite four dimensional volume. Define dimensionless quantity $v = V\chi_0$, where constant $\chi_0 = \frac{\partial^2 \varepsilon(\theta)}{\partial \theta^2}|_{\theta=0}$ is the topological susceptibility. The tendency of increasing volume is shown in Fig. 2.3, where v is between 5 and 50. One can see that, as v increases, $\underline{\varepsilon}(\theta)$ appears to become more and more cuspy at $\theta = \pi$, which seems to imply the Dashen's phenomenon is going to happen for $\underline{\varepsilon}(\theta)$ at the infinite volume limit.

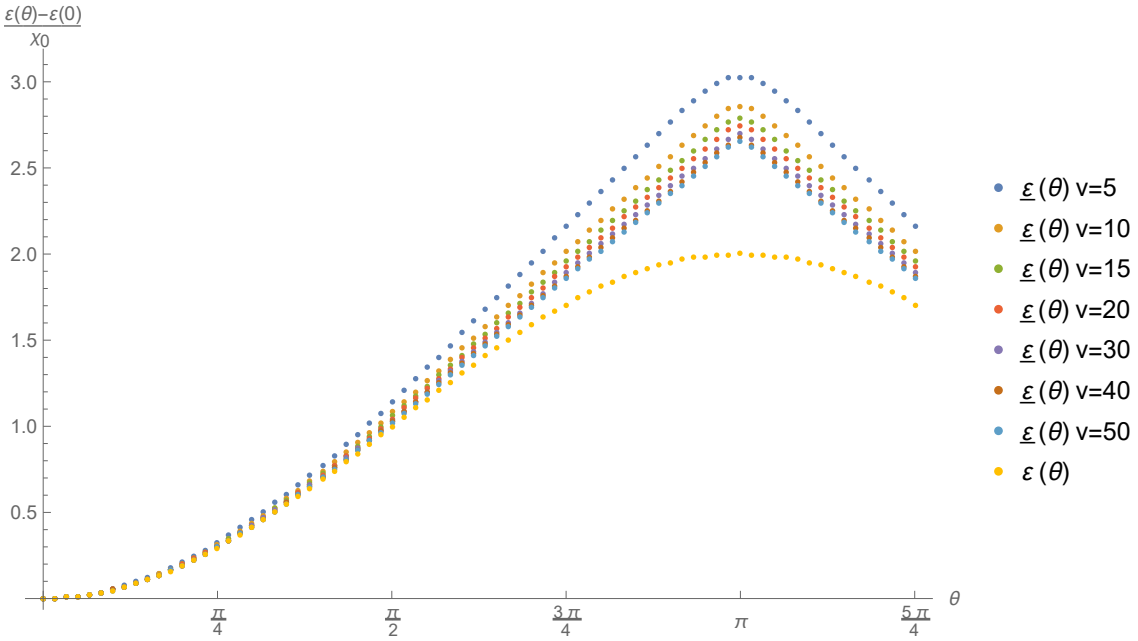

Figure 2.3: The cusp behavior when v increases.

For very large $v = V\chi_0 = 350$, the result is already quite stable, and shown in

Fig. 2.4. In the plot, $\varepsilon(\theta)$ and $\underline{\varepsilon}(\theta)$, in units of χ_0, for a dilute instanton gas model are compared. There are two important things to notice in this plot. The first is that, the curve of $\underline{\varepsilon}(\theta)$ matches the curve of $\varepsilon(\theta)$ very well for $0 < \theta < \frac{\pi}{2}$. However, for $\frac{\pi}{2} < \theta < \pi$, $\underline{\varepsilon}(\theta)$ looks linear, which is very different from $\varepsilon(\theta)$. This difference indicates that in this region, knowledge of $\tilde{\varepsilon}(q)$ is insufficient to reproduce $\varepsilon(\theta)$ by direct summation, even though they are both intensive quantities. For $\theta > \pi$, the result is symmetric to $\theta < \pi$ because of the function is even and periodic in θ. Thus, as mentioned before, the answer to whether $\underline{\varepsilon}(\theta) = \varepsilon(\theta)$ is "it depends". $\underline{\varepsilon}(\theta) = \varepsilon(\theta)$ when $\varepsilon(\theta)$ curves upward; while $\underline{\varepsilon}(\theta) \neq \varepsilon(\theta)$ when $\varepsilon(\theta)$ curves downward. The reason of this phenomena will be discussed later.

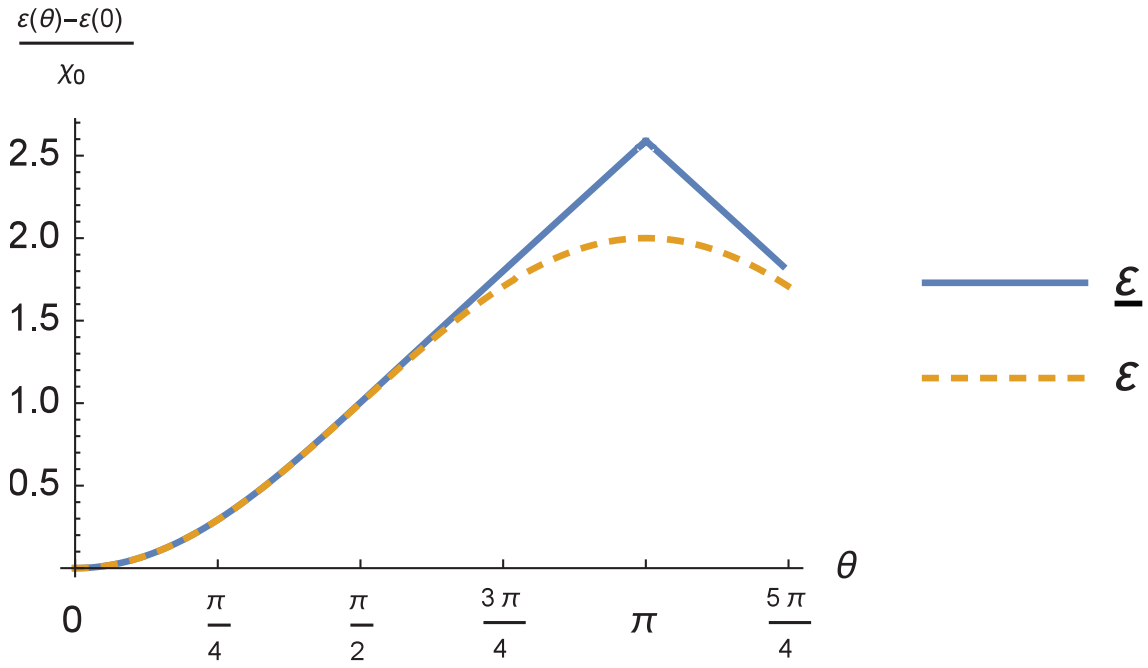

Figure 2.4: For a dilute instanton gas model with $v = V\chi_0 = 350$, compare $\varepsilon(\theta)$ with $\underline{\varepsilon}(\theta)$

2.4.2 The severity of the sign problem

The difference between $\underline{\varepsilon}(\theta)$ and $\varepsilon(\theta)$ for $\frac{\pi}{2} < \theta < \pi$ shows clearly the severity of the sign problem in this region. Even though the difference between $\tilde{\varepsilon}(q)$ and $\tilde{\varepsilon}(q, V)$ is tiny and vanishes in the infinite volume limit, the associated energy density function of θ, $\underline{\varepsilon}(\theta)$ and $\varepsilon(\theta)$, becomes very different for $\theta > \frac{\pi}{2}$.

Before proceeding, it is useful to examine this example in more detail. Notice that in the summation with oscillating sign Eq. (2.7), the key quantity being summed is $\mathcal{Z}_Q(V)$ rather than $\tilde{\varepsilon}(q, V)$. An order $\frac{1}{V}$ difference between $\tilde{\varepsilon}(q)$ and $\tilde{\varepsilon}(q, V)$ will result in an order unity difference in $\mathcal{Z}_Q(V)$. Naively, one may think this is what causes the order unity difference between $\underline{\varepsilon}(\theta)$ and $\varepsilon(\theta)$. However, this naive reasoning is not correct.

To see this, it is useful to define a new quantity $\tilde{\varepsilon}_n(q, V)$, which is an approximation to $\tilde{\varepsilon}(q, V)$ that includes all terms up to $\mathcal{O}(V^{-n})$ but truncates higher order corrections.

$$
\begin{aligned}
\tilde{\varepsilon}_0(q, V) &= \tilde{\varepsilon}(q) \\
\tilde{\varepsilon}_1(q, V) &= \tilde{\varepsilon}(q) + \frac{\log\left((2\pi)^2 V^2 (q^2 + \chi_0^2)\right)}{4V} \\
\tilde{\varepsilon}_2(q, V) &= \tilde{\varepsilon}_1(q, V) - \frac{U_1\left(\frac{q}{\sqrt{q^2+\chi_0^2}}\right)}{qV^2} \\
&\ldots \ .
\end{aligned}
\tag{2.22}
$$

Then the corresponding energy density function with respect to θ can be defined as:

$$\varepsilon_n(\theta) = -\lim_{V\to\infty} \frac{1}{V} \log\left(\sum_{Q=-\infty}^{\infty} e^{-\tilde{\varepsilon}_n(\frac{Q}{V},V)V}\, e^{i\theta Q}\right), \tag{2.23}$$

which is just Eq. (2.10) with the original $\tilde{\varepsilon}(q,V)$ replaced by $\tilde{\varepsilon}_n(q,V)$.

Then $\varepsilon_n(\theta)$ can be numerically computed following the same procedure as $\underline{\varepsilon}(\theta)$ for large but finite volume. If the order unity difference between $\underline{\varepsilon}(\theta)$ and $\varepsilon(\theta)$ is really caused by $\mathcal{O}(1/V)$ term in $\tilde{\varepsilon}_1(q,V)$, then $\varepsilon_n(\theta)$ with $n \geq 1$ should matches $\varepsilon(\theta)$ for very large volume, since correction term of this order is already included. However, this is not the case.

The comparison of $\underline{\varepsilon}(\theta)$, $\varepsilon_2(\theta)$ and $\varepsilon(\theta)$ is shown in Fig. 2.5, where the numerical computation of $\underline{\varepsilon}(\theta)$ and $\varepsilon_2(\theta)$ are both done in $v = V\chi_0 = 350$. It is clear that $\varepsilon_2(\theta)$ is indistinguishable from $\underline{\varepsilon}(\theta)$, rather than $\varepsilon(\theta)$. This indicates that, the order unity difference between $\underline{\varepsilon}(\theta)$ and $\varepsilon(\theta)$ for $\theta > \frac{\pi}{2}$ is not caused by the order $\mathcal{O}(1/V)$ and order $\mathcal{O}(1/V^2)$ term in $\tilde{\varepsilon}(q,V)$.

The reason is that, an accurate calculation of $\varepsilon(\theta)$ requires cancellations of $\mathcal{Z}_Q(V)$ that are exponentially accurate in terms of volume, so it is not surprising that the inclusion of any power law correction term is not sufficient for a full reconstruction. Then, the actual surprising thing is not $\underline{\varepsilon}(\theta) \neq \varepsilon(\theta)$ for $\frac{\pi}{2} < \theta < \pi$, but $\underline{\varepsilon}(\theta) = \varepsilon(\theta)$ for $0 < \theta < \frac{\pi}{2}$. The question of why $\underline{\varepsilon}(\theta)$ matches $\varepsilon(\theta)$ for $0 < \theta < \frac{\pi}{2}$ even though there is an order $\mathcal{O}(1/V)$ difference between $\tilde{\varepsilon}(q,V)$ and $\tilde{\varepsilon}(q)$ will be answered in the next several sections.

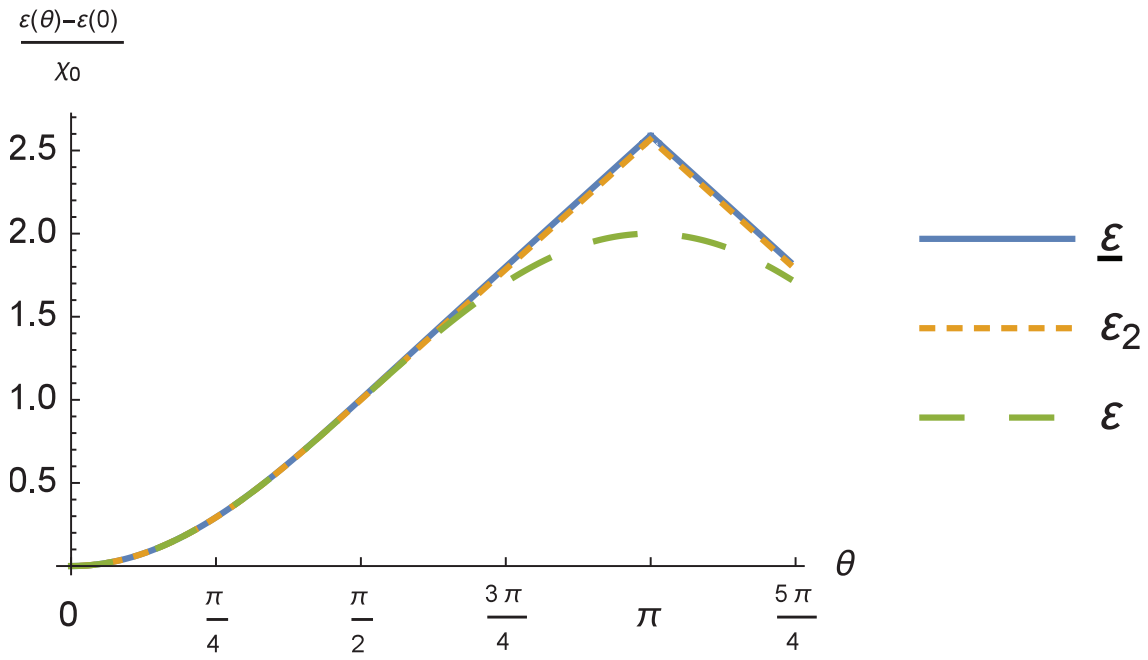

Figure 2.5: A comparison of $\varepsilon(\theta)$, $\varepsilon_2(\theta)$ and $\underline{\varepsilon}(\theta)$

2.5 Saddle point approximation for the instanton gas model

2.5.1 An identity relating sum and integral

Before go into details of the explanation of the phenomena found in previous section, it is useful to at first introduce an important identity that relates sum and integral under the limit of parameter λ approaches infinity:

$$\lim_{\lambda\to 0}\frac{\int_{-\infty}^{\infty} dx \exp\left(-\lambda f\left(\frac{x}{\lambda}\right)\right)\exp(i\theta\, x)}{\sum_{n=-\infty}^{\infty}\exp\left(-\lambda f\left(\frac{n}{\lambda}\right)\right)\exp(i\theta\, n)}=1, \tag{2.24}$$

where $f(x)$ can be any well-behaved function that goes positive infinity as $x\to\pm\infty$ along the real axis. Using this identity, one can replace the sum of $e^{-\tilde{\varepsilon}(\frac{Q}{V})V}\, e^{i\theta Q}$ in Eq. (2.10) by integral, so that it can be studied analytically using techniques of complex analysis.

Notice that, the validity of Eq. (2.24) is not trivial since it is not the case that the limit of the sum converges due to Riemann's construction for integrals. Rather, the derivation of this identity requires some complicated manipulations.

The proof of this identity is as following. At first, use the property of Dirac delta function $\sum_{n=-\infty}^{\infty}\delta(x-n) = \sum_{k=-\infty}^{\infty}\exp(i2\pi kx)$ to rewrite the integral in Eq. (2.24) as:

$$\begin{aligned}
&\sum_{n=-\infty}^{\infty}\exp\left(-\lambda f\left(\frac{n}{\lambda}\right)\right)\exp(i\theta\, n) = \\
&\sum_{k=-\infty}^{\infty}\int_{-\infty}^{\infty}dx\exp\left(-\lambda f\left(\frac{x}{\lambda}\right)\right)\exp(i\theta x)\exp(i2\pi kx) = \\
&\sum_{k=-\infty}^{\infty}\lambda\int_{-\infty}^{\infty}dy\exp\left(-\lambda\left(f(y)-i(\theta+2\pi k)\,y\right)\right),
\end{aligned} \tag{2.25}$$

where function $f(x)$ is assumed to be well behaved so that the sums and integrals are all convergent.

Then, assuming appropriate analytic properties, in the limit of λ approaches infinity, the integrals in the last line of Eq. (2.25) can be approximated using the the function value at saddle point with the help of saddle point approximations[165] as

$$\begin{aligned}
&\int_{-\infty}^{\infty}dy\exp\left(-\lambda\left(f(y)-i(\theta+2\pi k)\,y\right)\right)\sim \max_{\mathrm{k}}\exp(-\lambda \mathrm{g_k}) \\
&\text{where}\ \ \mathrm{g_k}=\min_{\mathrm{j}}(\mathrm{g_k^j})\ \ \text{with}\ \mathrm{g_k^j}=(\mathrm{f(y_k^j)}-\mathrm{i}(\theta+2\pi\mathrm{k})\,\mathrm{y_k^j}),
\end{aligned} \tag{2.26}$$

where we have neglected power law factors in λ. y_k^j is the j^{th} saddle point for the

function $(f(y) - i(\theta + 2\pi k)\, y)$ which satisfies:

$$\left.\frac{d\left(f(y(t)) - i(\theta + 2\pi k)\, y(t)\right)}{dt}\right|_{t=t_k^j} = 0, \tag{2.27}$$

where $y(t)$ is a contour in the the complex plane parametricalized by t, and $y_k^j \equiv y(t_k^j)$.

At the saddle point of the complex plane, the derivative along any direction is exactly zero, so it will be the local minimum point along certain contours and the local maximum point along other contours. A function may have more than one saddle point on the complex plane. When λ is large enough, each integral in Eq. (2.25) is dominated by its minimum saddle point. Furthermore, the sum over an infinite number of integrals labeled with k is dominated by the largest integral which is exponentially larger than all other integrals when λ approaches infinity.

This dominant integral is the one that has the smallest g_k. Typically, this is the $k = 0$ term for $-\pi < \theta < \pi$ for a wide classes of functions. When $\pi < \theta < 3\pi$, the $k = -1$ term will take its turns and become the dominant one, and so forth for other values of θ because of the periodic property. Our discussion will only focus on the region $-\pi < \theta < \pi$ since the behavior in other regions are just the replicas of this region. Thus, we only concentrate on the case that $k = 0$ dominates, which leads to the desired identity Eq. (2.24).

As mentioned before, the saddle point approximation relies on function's appropriate analytic properties in the complex plane, this is because this approximation relies on distorting the integral contour on the analytic region of the complex

plane without crossing any singularity or non-analytic point. If the function is not analytic everywhere on the complex plane, there is another kind of point that can also dominate the integral in a similar manner as the saddle point, so that can be used to approximate the value of the integral. This kind of point is a branch point, which is the endpoint of the branch cut on the complex plane. All the previous derivation with the help of the saddle point also applies to this kind of branch point. Notice that, one function may have multiple saddle points and multiple branch points, the integral will be exponentially dominated by one of them when the parameter λ is large as shown in Eq. (2.26). This kind of saddle point approximation with the possibility of saddle point being replaced by branch point is important to understand the subtle relation between $\underline{\varepsilon}(\theta)$ and $\varepsilon(\theta)$.

Now we can use the identity Eq. (2.24) to analyze the expression of $\underline{\varepsilon}(\theta)$ while the volume V serves as the role of parameter λ.

$$\begin{aligned}
\underline{\varepsilon}(\theta) &= -\lim_{V\to\infty} \frac{1}{V} \log\left(\sum_{Q}\ e^{-\tilde{\varepsilon}(\frac{Q}{V})V}\, e^{i\theta Q}\right) \\
&= -\lim_{V\to\infty} \frac{1}{V} \log\left(\int dQ\ e^{-\tilde{\varepsilon}(\frac{Q}{V})V}\, e^{i\theta Q}\right) \\
&= -\lim_{V\to\infty} \frac{1}{V} \log\left(V\int dq\ e^{-V(\tilde{\varepsilon}(q)-i\theta q)}\right) \\
&= \tilde{\varepsilon}(q_\theta^{\mathrm{sp}}) - i\theta q_\theta^{\mathrm{sp}},
\end{aligned} \tag{2.28}$$

where we have used the saddle point approximation and q_θ^{sp} is the dominant saddle point associated with $\tilde{\varepsilon}(q) - i\theta q$.

Since in Euclidean space, $\frac{1}{V}\frac{\partial \log(\mathcal{Z}(\theta))}{\partial\theta} = iq$, which means real θ corresponds to

imaginary q, one expects the dominant saddle point appears on the imaginary axis of q. Because $\tilde{\varepsilon}(q)$ is even function, $(\tilde{\varepsilon}(q) - i\theta q)$ is real when q is imaginary and $\tilde{\varepsilon}(q)$ is locally analytic. After rewrite $q = iq_0$, the saddle point condition on imaginary axis is:

$$\left.\frac{\partial\left(\tilde{\varepsilon}(ix) - i\theta \cdot ix\right)}{\partial x}\right|_{x=q_0} = 0\ . \tag{2.29}$$

Eq. (2.28) shows that, in the infinite volume limit $V \to \infty$, the relation between $\underline{\varepsilon}(\theta)$ and $\tilde{\varepsilon}(q)$ is similar to a Legendre transformation but with an extra i:

$$\begin{aligned} \tilde{\varepsilon}(q(\theta)) &= \underline{\varepsilon}(\theta) + i\,\theta\,q(\theta) \quad \text{with} \quad q(\theta) = i\frac{\partial \underline{\varepsilon}(\theta)}{\partial \theta} \\ \underline{\varepsilon}(\theta(q)) &= \tilde{\varepsilon}(q) - i\,\theta(q)\,q \quad \text{with} \quad \theta(q) = -i\frac{\partial \tilde{\varepsilon}(q)}{\partial q}\ . \end{aligned} \tag{2.30}$$

This equation is the central equation of the following analysis. It is also important to recall that the pre-required conditions of this equation: i) $\tilde{\varepsilon}(q)$ should be analytic on certain regions so that appropriate distorting of the integral contour can be done; ii) the saddle point approximation is valid and there exists saddle point or branch point that dominates the integral in the infinite volume limit; iii) the sum of integrals over k in Eq. (2.25) is dominated by $k = 0$ term when V is large.

2.5.2 The saddle point approximation for the dilute instanton gas for $|\theta| < \pi/2$

Now let us go back to the toy model dilute instanton gas. We will assume the key equation Eq. (2.30) is valid in this case and combine it with the specific energy density expressions of dilute instanton gas, to see what will happen. We will at first consider the region $0 < \theta < \frac{\pi}{2}$, and test if $\underline{\varepsilon}(\theta) = \varepsilon(\theta)$ in this region.

For dilute instanton gas, the energy density with respect to θ is given by $\varepsilon(\theta) = \varepsilon_0 + \chi_0 (1 - \cos(\theta))$. If $\underline{\varepsilon}(\theta) = \varepsilon(\theta)$ is true, one obtains $\frac{\partial \underline{\varepsilon}}{\partial \theta} = \chi_0 \sin(\theta)$. Then Eq. (2.30) changes into:

$$\tilde{\varepsilon}\left(i\chi_0 \sin(\theta)\right) = \varepsilon_0 + \chi_0 \left(1 - \cos(\theta)\right) - \chi_0 \sin(\theta)\theta. \tag{2.31}$$

Next, using $\tilde{\varepsilon}(q) = \varepsilon_0 + \chi_0 - \sqrt{\chi_0^2 + q^2} + q \sinh^{-1}\left(\frac{q}{\chi_0}\right)$ and $q(\theta) = i\frac{\partial \underline{\varepsilon}}{\partial \theta} = i\chi_0 \sin(\theta)$, the left-hand side of Eq. (2.31) becomes

$$\begin{aligned} &\tilde{\varepsilon}\left(i\chi_0 \sin(\theta)\right) \\ &= \varepsilon_0 + \chi_0(1 - \sqrt{1 - \sin(\theta)^2} - \chi_0 \sin(\theta) \sin^{-1}\left(\sin(\theta)\right) \\ &= \varepsilon_0 + \chi_0 \left(1 - \cos(\theta)\right) - \chi_0 \sin(\theta)\theta, \end{aligned} \tag{2.32}$$

which is equal to the righthand side of Eq. (2.31) because $\sin^{-1}\left(\sin(\theta)\right) = \theta$ and $\sqrt{1 - \sin(\theta)^2} = \cos(\theta)$ when $|\theta| < \pi/2$.

Thus, we shows that the numerically observed $\underline{\varepsilon}(\theta) = \varepsilon(\theta)$ for $|\theta| < \pi/2$ in Fig. 2.4 is consistent given Eq. (2.30) is true.

Let us now check the three conditions of Eq. (2.30). It is easy to see Condition i) is valid. On the complex plain, $\tilde{\varepsilon}(q)$ is analytic except two branch cuts along imaginary axis: one from $i\chi_0$ to ∞ and the other from $-\infty$ to $-i\chi_0$. The function is analytic between two branch points $-i\chi_0$ and $i\chi_0$, so it is appropriate to distorting the integral contour from the real axis to any other contour as long as it does not crosses the two branch cuts.

As there is a solution $q = i\chi_0 \sin(\theta)$ for the saddle point existence condition Eq. (2.29) on the imaginary axis, Condition ii) is also satisfied.

For Condition iii), it is straightforward to show there is no saddle point for $k \neq 0$ terms on the imaginary axis using proof by contradiction. Let us at first assume a saddle point exists for $k \neq 0$, then

$$\theta + 2\pi k = -i \left. \frac{\partial \tilde{\varepsilon}(q)}{\partial q} \right|_{q=q^{\mathrm{sp}}} . \tag{2.33}$$

Combined with $\tilde{\varepsilon}(q) = \varepsilon_0 + \chi_0 - \sqrt{\chi_0^2 + q^2} + q \sinh^{-1}\left(\frac{q}{\chi_0}\right)$, this yields

$$\theta + 2\pi k = -\sin^{-1}\left(i \frac{q^{\mathrm{sp}}}{\chi_0}\right) . \tag{2.34}$$

Notice that q^{sp} is supposed to be imaginary, so $i\frac{q^{sp}}{\chi_0}$ is real. For $\sin^{-1}$, the principle branch is taken, so a real value input corresponding to result between $-\frac{\pi}{2}$ and $\frac{\pi}{2}$. Recall that we are restricting the consideration in $-\pi < \theta < \pi$ because of periodicity, so $k \neq 0$ contradicts with Eq. (2.34).

Thus, there is no saddle point on the imaginary axis. As explained before, physically one expects the dominant saddle point should be on imaginary axis if

it exists. Since there is no such saddle point, the branch point $q^{\rm bp} = \pm\chi_0$ on the imaginary axis may dominate the integral in a similar manner as saddle point:

$$\begin{aligned} \varepsilon_k(\theta) &\equiv -\lim_{V\to\infty} \frac{1}{V} \log\left(V \int dq\; e^{-V(\tilde{\varepsilon}(q) - i(\theta+2\pi k)q)} \right) \\ &= \tilde{\varepsilon}(q^{\rm bp}) - (\theta + 2\pi k)(iq^{\rm bp}), \end{aligned} \tag{2.35}$$

Using $q^{\rm bp} = \pm\chi_0$, we have:

$$\varepsilon_k(\theta) = \varepsilon_0 + \chi_0 + \chi_0(|\theta + 2\pi k| - \frac{\pi}{2})\,. \tag{2.36}$$

Recall that here $k \neq 0$, when $|\theta| < \frac{\pi}{2}$, $\varepsilon_k(\theta)$ is larger than $\underline{\varepsilon}(\theta) = \varepsilon_0 + \chi_0(1 - \cos(\theta)$ which is the $k = 0$ term. Thus, in the sum of exponential with negative factor times ε in Eq. (2.25), $k \neq 0$ terms are exponentially suppressed by the volume, V, compared to $k = 0$ term, which means the Condition iii) is satisfied.

In other words, for $|\theta| < \frac{\pi}{2}$, the saddle point on the imaginary axis dominates the computation and causes $\underline{\varepsilon}(\theta) = \varepsilon(\theta)$, which agrees with the result shown in Fig. 2.4. The existence of this saddle point prevents the sensitive cancellation in the oscillating sum being ruined by the difference between $\tilde{\varepsilon}(q)$ and $\tilde{\varepsilon}(q, V)$, even though the sign problem requires exponentially accuracy in V.

2.5.3 The saddle point approximation for the dilute instanton gas for $\pi/2 < |\theta| < \pi$

Now let us considering the case for $\frac{\pi}{2} < |\theta| < \pi$. It is easy to see that the saddle point in the previous section no longer exists on the imaginary axis.

As in Eq. (2.34), the existence condition of saddle point says:

$$\begin{aligned} \theta + 2\pi k &= -i \left. \frac{\partial \tilde{\varepsilon}(q)}{\partial q} \right|_{q=q^{\mathrm{sp}}} \\ &= -\sin^{-1}\left(i \frac{q^{\mathrm{sp}}}{\chi_0} \right), \end{aligned} \tag{2.37}$$

where q^{sp} is imaginary, so the the equation's right-hand side $-\sin^{-1}\left(i\frac{q^{\mathrm{sp}}}{\chi_0}\right)$ should take the principal branch value between $-\pi/2$ and $\pi/2$. However, the left-hand side of the equation $\theta + 2\pi k$ ranges from $\pi/2 + 2\pi k$ to $\pi + 2\pi k$ for integer k, which has no overlapping range with the right-hand side. Thus, this equation is not consistent with $\frac{\pi}{2} < |\theta| < \pi$, and there is no saddle point on imaginary axis of q for any integer k.

Thus, one cannot arrive at $\underline{\varepsilon}(\theta) = \varepsilon(\theta)$ following the same argument in the previous section when θ takes a different range where sign problem is softer.

The other way to see the break down of $\underline{\varepsilon}(\theta) = \varepsilon(\theta)$ is to at first assume there is a saddle point or branch point that makes Eq. (2.30) true. Notice that, for $\frac{\pi}{2} < |\theta| < \pi$, $\sin^{-1}(\sin(\theta)) = \pm(\pi - \theta)$ (where $\pm$ is the same as the sign of θ) and $\sqrt{1 - \sin(\theta)^2} = -\cos(\theta)$. Then if one assume $\underline{\varepsilon}(\theta) = \varepsilon(\theta)$, Eq. (2.32)'s last step is changed to:

$$\begin{aligned}\tilde{\varepsilon}\left(i\chi_0\sin(\theta)\right) &= \varepsilon_0 + \chi_0\left(1+\cos(\theta)\right) \pm \chi_0\sin(\theta)(\pi-\theta) \\ &\neq \varepsilon_0 + \chi_0\left(1-\cos(\theta)\right) - \chi_0\sin(\theta)\theta,\end{aligned} \tag{2.38}$$

which says, either $\underline{\varepsilon}(\theta) \neq \varepsilon(\theta)$ or that there is no appropriate saddle point or branch point so that Eq. (2.30) is wrong.

When there is no saddle point on the imaginary axis, one expects that the branch point $q^{\text{bp}} = \pm i\chi_0$ dominates the integral. In this case, the result is given by:

$$\varepsilon_k(\theta) = \varepsilon_0 + \chi_0 + \chi_0(|\theta + 2\pi k| - \frac{\pi}{2})\,. \tag{2.39}$$

as derived in Eq. (2.36).

It is obvious that $k = 0$ branch is dominant over $k \neq 0$ branches in the infinite volume limit, so the final result is given by:

$$\underline{\varepsilon}(\theta) = \varepsilon_0 + \chi_0 + \chi_0|\theta| - \frac{\pi}{2}, \tag{2.40}$$

which matches what we have seem in Fig. (2.4): $\underline{\varepsilon}(\theta)$ is a linear function for $\pi/2 < \theta < \pi$.

It is intuitive to understand why $\underline{\varepsilon}(\theta)$ is a linear in this case. The branch point is fixed point and cannot move as the saddle point do when θ changes. Thus, Eq. (2.30), which is similar to Legendre transformation with an extra i, leads to a linear $\underline{\varepsilon}(\theta)$.

To summarize, for $\pi/2 < |\theta| < \pi$, there is no saddle point on the imaginary axis of q so that $\underline{\varepsilon}(\theta) \neq \varepsilon(\theta)$. However, the branch point on the imaginary axis dominates the integral in a similar way, and the fixed position of branch point yields linear behavior of $\underline{\varepsilon}(\theta)$.

2.5.4 Analytic considerations

We have shown that, one cannot reconstruct $\varepsilon(\theta)$ for $\pi/2 < |\theta| < \pi$ via direct summation over topological sectors. However, does that means $\tilde{\varepsilon}(q)$, which is the infinite volume limit of $\tilde{\varepsilon}(q, V)$, does not contain enough information to reconstruct $\varepsilon(\theta)$ for $\pi/2 < |\theta| < \pi$? The answer is subtle.

In principle, one can use $\tilde{\varepsilon}(q)$ to reconstruct $\varepsilon(\theta)$ for $|\theta| < \pi/2$, then analytically continuate from $|\theta| < \pi/2$ to $\pi/2 < |\theta| < \pi$. For a dilute instanton gas, the energy density with respect to θ is known to be analytic, so there is no problem of doing this. In this way, it seems that one can reconstruct $\varepsilon(\theta) = \varepsilon_0 + \chi_0 (1 - \cos(\theta))$ for $\pi/2 < |\theta| < \pi$ from $\tilde{\varepsilon}(q)$, and $\tilde{\varepsilon}(q)$ have the full information needed.

How to reconcile these two views? The key point is to observe that, on the complex plane, $\tilde{\varepsilon}(q)$ has multiple branches. When we use $\tilde{\varepsilon}(q) = \varepsilon_0 + \chi_0 - \sqrt{\chi_0^2 + q^2} + q \sinh^{-1}\left(\frac{q}{\chi_0}\right)$ in previous sections, we are actually using the principal branch. If one circles around the branch point, in other words, crosses the branch cut along the imaginary axis, one can arrive at other branches.

It can be easily verified that if one uses the branch:

$$\tilde{\tilde{\varepsilon}}(q) = \varepsilon_0 + \chi_0 + \sqrt{\chi_0^2 + q^2} + q\left(i\pi - \sinh^{-1}\left(\frac{q}{\chi_0}\right)\right) . \tag{2.41}$$

in the previous section's analysis, one will be able to reconstruct $\varepsilon(\theta) = \varepsilon_0 + \chi_0\left(1 - \cos(\theta)\right)$ for $\pi/2 < |\theta| < \pi$ via direct summation of topological sectors.

However, it is obvious that $\tilde{\tilde{\varepsilon}}(q)$'s value is not real when q is real, so it is impossible to get $\tilde{\tilde{\varepsilon}}(q)$ though directly taking infinite volume limit of $\tilde{\varepsilon}(q, V)$. In practice, the only way to get the value of $\tilde{\tilde{\varepsilon}}(q)$ is though analytical continuating $\tilde{\varepsilon}(q)$ onto another branch in the complex plane, which is numerically non-trivial, and may require knowledge of $\tilde{\varepsilon}(q)$ with extraordinary high accuracy.

2.6 The general case

The previous discussion focuses on a toy model: the dilute instanton gas, because the simple form of the energy density of this model makes it easy to conduct analysis. However, the analysis can be generalized to cases that have no simple closed-form expression.

The original energy density $\varepsilon(\theta)$ and the reconstructed one $\underline{\varepsilon}(\theta)$ in general case are shown as:

$$\varepsilon(\theta) = -\lim_{V\to\infty} \sum_{k=-\infty}^{\infty} \frac{1}{V} \log\left(V \int dq\ e^{-V(\tilde{\varepsilon}(q,V) - i(\theta+2\pi k)q)}\right) . \tag{2.42}$$

$$\underline{\varepsilon}(\theta) = -\lim_{V\to\infty}\sum_{k=-\infty}^{\infty}\frac{1}{V}\log\left(V\int dq\; e^{-V(\tilde{\varepsilon}(q)-i(\theta+2\pi k)q)}\right), \tag{2.43}$$

The key argument is that when there exists a saddle point that dominates the integral for a range of θ, $\underline{\varepsilon}(\theta) = \varepsilon(\theta)$. The proof is straightforward and is as follows. Eq.(2.30) is true as long as there is saddle point. If a saddle point exists for Eq.(2.43), one has $\underline{\varepsilon}(\theta(q^{sp})) = \tilde{\varepsilon}(q^{sp}) - i\theta(q^{sp})q^{sp}$ and $\theta(q^{sp}) = -i\frac{\partial\tilde{\varepsilon}(q^{sp})}{\partial q^{sp}}$. Then $\theta(q^{sp}) = -i\lim_{V\to\infty}\frac{\partial\tilde{\varepsilon}(q^{sp},V)}{\partial q^{sp}}$ is true because $\tilde{\varepsilon}(q) = \lim_{V\to\infty}\tilde{\varepsilon}(q,V)$. Thus, saddle point also exist for Eq.(2.42) in infinite volume limit, and $\varepsilon(\theta(q^{sp})) = \lim_{V\to\infty}\tilde{\varepsilon}(q^{sp},V) - i\theta(q^{sp})q^{sp} = \underline{\varepsilon}(\theta(q^{sp}))$. Thus, $\underline{\varepsilon}(\theta) = \varepsilon(\theta)$ is true as long as saddle point exists for the range of θ considered.

Then the question becomes, what is the range of θ that $\underline{\varepsilon}(\theta) = \varepsilon(\theta)$? In other words, where does $\underline{\varepsilon}(\theta) \neq \varepsilon(\theta)$ happen?

The general answer is that for analytic $\varepsilon(\theta)$ with $|\theta| < \pi$,

$$\underline{\varepsilon}(\theta) = \varepsilon(\theta) \;\text{ if }\; |\theta| < \theta_{\max}, \tag{2.44}$$

where $\theta_{\max}$ is the smallest positive value of θ satisfying either of the following conditions

1. $\left.\frac{d^2\varepsilon(\theta)}{d\theta^2}\right|_{\theta=\theta_{\max}} = 0$.

2. $\theta_{\max} = \pi$.

Condition 2) is just because of the periodicity of 2π. To see the reason of Condition 1), let's start by assuming $\underline{\varepsilon}(\theta) = \varepsilon(\theta)$ is true for small real $|\theta|$ near 0. This is reasonable because at small enough $|\theta|$, any even function of θ is well-approximated by θ^2 because of Taylor expansion. The case of $\varepsilon(\theta) = \theta^2$ can be easily shown to satisfy $\underline{\varepsilon}(\theta) = \varepsilon(\theta)$.

Note that, for small $|\theta|$, if $\underline{\varepsilon}(\theta) = \varepsilon(\theta)$, the integral must be dominated by a saddle point near $q = 0$ on the imaginary axis, rather than a branch point on the imaginary axis. This is because the branch point is a fixed point, which will result in linear $\underline{\varepsilon}(\theta)$, so it contradicts with the assumption that $\varepsilon(\theta)$ is analytic in this small region.

We start from this small $|\theta|$ region, and without loss of generality, we consider positive θ. When increases positive θ's value, the saddle point q^{sp} moves correspondingly along imaginary q axis. The $\underline{\varepsilon}(\theta) = \varepsilon(\theta)$ keeps valid since the saddle point still exists on imaginary q axis. This breaks when the saddle point disappears or when it moves to a non-analytic point such that it cannot exist after this point. Then, the $\underline{\varepsilon}(\theta) = \varepsilon(\theta)$ breaks down.

The argument is that this break down happens when θ is at the inflection point, which means $\frac{d^2\varepsilon(\theta)}{d\theta^2} = 0$, Condition 1). To see why the corresponding saddle point on imaginary q axis no longer exists after θ increases and passes this reflection point, it is useful to notice that, when $\underline{\varepsilon}(\theta) = \varepsilon(\theta)$ is valid before this inflection point, one can use Eq. (2.30) to obtain:

$$\frac{\partial^2 \varepsilon(\theta)}{\partial \theta^2} \left. \frac{\partial^2 \tilde{\varepsilon}(q)}{\partial q^2} \right|_{q_\theta^{\rm sp}} = 1, \tag{2.45}$$

Right at the inflection point, $\frac{d^2\varepsilon(\theta)}{d\theta^2} = 0$, the only way it can be consistent with Eq.(2.45) is that, $\frac{\partial^2 \tilde{\varepsilon}(q)}{\partial q^2}|_{q_\theta^{\rm sp}}$ diverges as θ approaches the inflection point from small positive θ. The divergence of $\frac{\partial^2 \tilde{\varepsilon}(q)}{\partial q^2}|_{q_\theta^{\rm sp}}$ means that saddle point $q^{\rm sp}$ approaches the non-analytic point of $\tilde{\varepsilon}(q)$ on the imaginary axis, so that it cannot proceed beyond this point. In the case of dilute instanton gas, the saddle point disappears after it hits the branch point, which is the starting point of the non-analytic branch cut along the imaginary axis.

The inflection point therefore serves as a signal of where $\underline{\varepsilon}(\theta) = \varepsilon(\theta)$ starts to break down. After this point, in general $\underline{\varepsilon}(\theta) \neq \varepsilon(\theta)$. Since the inflection point, if it exists, is the point where $\frac{d^2\varepsilon(\theta)}{d\theta^2}$ changes from negative to positive, it implies that, for $0 < \theta < \pi$, when increases θ, $\underline{\varepsilon}(\theta) = \varepsilon(\theta)$ remains valid until $\varepsilon(\theta)$ changes from curving up to curving down, as shown clearly in the numerical result Fig. 2.4. More examples are shown in Fig. 2.6 and Fig. 2.7 for $\varepsilon(\theta) = 1 - \cos(2\theta)$ and $\varepsilon(\theta) = 1 - \cos(3\theta)$ with corresponding $\underline{\varepsilon}(\theta)$s.

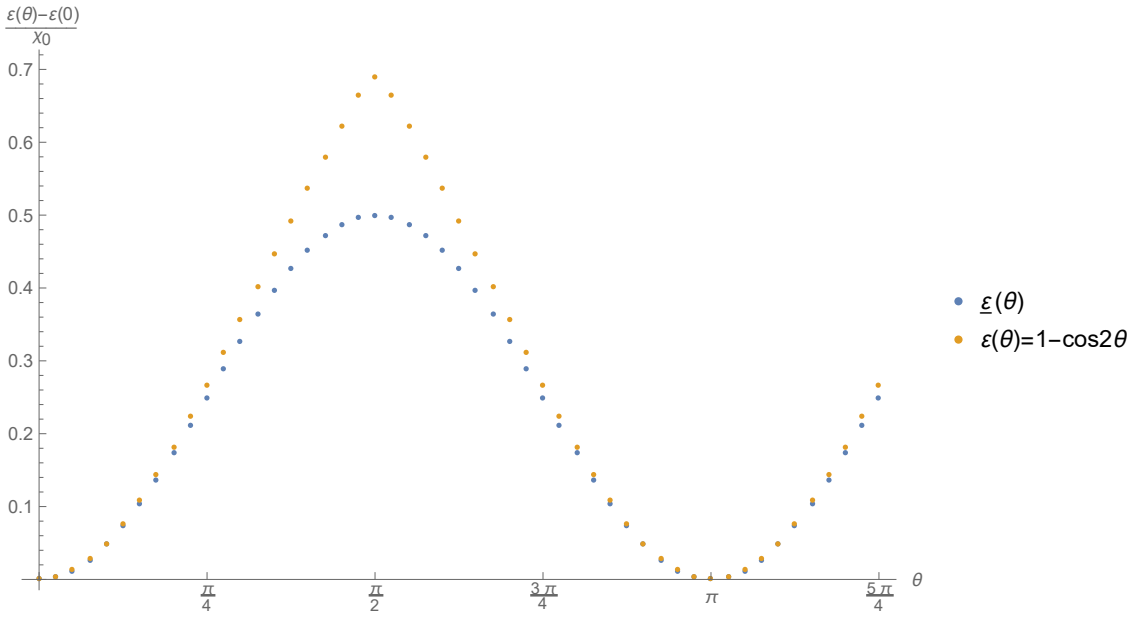

Figure 2.6: $\varepsilon(\theta) = 1 - \cos(2\theta)$ and the corresponding $\underline{\varepsilon}(\theta)$

2.7 Summary

This chapter focused on an interesting phenomenon caused by the interplay of the infinite volume limit and the sign problem in QCD with a θ-term.

As a conclusion, it has been shown that if $\varepsilon(\theta)$ has reflection point in $\theta \in (-\pi, \pi)$, then there exists regions where one can not correctly reconstruct the $\varepsilon(\theta)$ by direction summation over different topological charge Q using $\tilde{\varepsilon}(q)$. The reason is that the sign problem in these regions are so severe that even though $\varepsilon(\theta)$ is intensive quantity in the infinite volume limit, the finite volume difference between $\tilde{\varepsilon}(q)$ and $\tilde{\varepsilon}(q, V)$ can spoil the delicate summation.

However, it is also worth noting that, given the sensitivity of this summation, it is remarkable that one can reconstruct $\varepsilon(\theta)$ using $\tilde{\varepsilon}(q)$ in other regions of θ. Recall that a power-law difference of $1/V$ between $\tilde{\varepsilon}(q)$ and $\tilde{\varepsilon}(q, V)$ will result in order unity

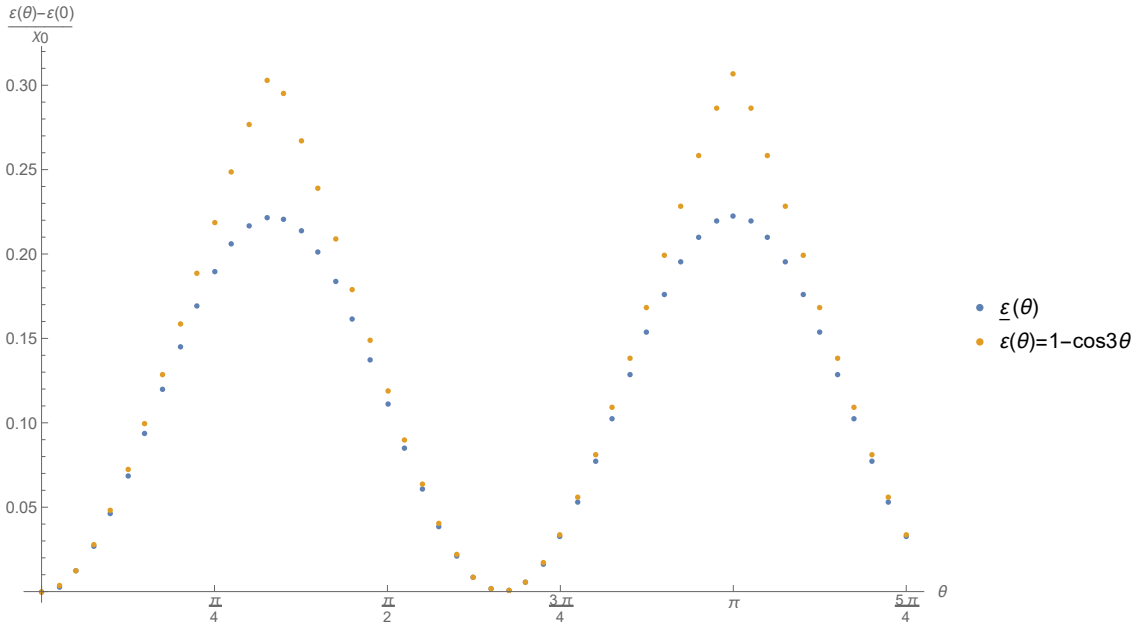

Figure 2.7: $\varepsilon(\theta) = 1 - \cos(3\theta)$ and the corresponding $\underline{\varepsilon}(\theta)$

error in Z_Q. As the summation result of Z_Q is exponentially small in V compared to individual terms of Z_Q, this summation requires exponentially accurate cancellation between terms. The fact that each term has order unity error but still yields to correct $\varepsilon(\theta)$ after cancellation is surprising. The reason behind this phenomenon is that in this region, the sum can be replaced by integral, which is dominated by a saddle point.

One interesting implication of this analysis is that unless both $\varepsilon(\theta)$ and $\tilde{\varepsilon}(q)$ are trivial constant functions, at least one of them cannot be analytic over the whole complex plane. It is because the inflection point of $\varepsilon(\theta)$ corresponding to the branch point of $\tilde{\varepsilon}(q)$, which is the starting point of the non-analytic branch cut in the complex plane of q. While if non-constant $\varepsilon(\theta)$ does not have any inflection point for $\theta \in (-\pi, \pi)$, then $\varepsilon''(\theta)$ is positive over the whole region between $-\pi$ and π. However, if this is true, due to the periodicity of 2π, $\varepsilon(\theta)$ must have Dashen's

phenomenon at $\theta = \pi$, which is non-analytic.

Though the analysis in this section does not solve the sign problem in QCD with a θ-term, it may help to shed light on extracting information of $\varepsilon(\theta)$ near $\theta = \pi$, which is related to the strong CP problem.

Chapter 3: Tetraquarks in the heavy quark mass limit: $\bar{q}\bar{q}'QQ$

3.1 Review of exotic hadrons

When the naive quark model was invented during the 1960s, the phenomenological evidence seems to imply that there are only two kinds of hadrons: mesons as bound states of quark and antiquark $q\bar{q}$ and baryons as bound states of three quarks. However, it was realized that the naive quark model in principle also allows for multiquark states[166]. Ten years later, QCD was formulated. The complicated interaction of gluons and quarks described in QCD Lagrangian allows for a much more complicated structure of hadron. Exotic mesons called glueballs, which are made only by gluons, and hybrids, which are $q\bar{q}$ pairs with an excited gluon, seem possible because of gluons' self-coupling. Moreover, multiquark color singlet exotic states may also exist, such as tetraquark with four valence quarks and pentaquark with five valence quarks.

In the light quark sector, there have been many theoretical predictions and experimental evidence for the existence of exotic hadrons such as glueball and hybrid state. For example, it is suggested that isoscalar resonance $f_0(1500)$ is mainly glue[167, 168]. $\pi_1(1600)$ observed by E852 collaboration is considered to be good candidate of hybrid state[169, 170]. The $a_0(980)$ and $f_0(980)$ are strong candidates

of tetraquark state[171, 172, 173, 174, 175, 176]. However, there is still no universal agreement on the true structure of these states. A detailed review of exotic hadrons in the light quark sector can be found in Ref. [167].

The difficulty of distinguishing exotic states in the light quark sector is that it is very easy to create light quark anti-quark pair from gluons, which makes it hard to tell, for example, whether there were indeed a strange quark and an anti-strange quark in the state we are looking at before decaying into Kaons. The other difficulty comes from the fact that the light quark spectrum is full of broad and overlapping conventional states, so it is difficult to unambiguously identify these multiquark states candidates[177]. The situation changes in the heavy quark sector. The heavy quark is much more non-relativistic than the light quarks, thus it is difficult to have pair creation and pair annihilation of heavy quark and heavy anti-quark. As a result, it is easy to tell whether there were heavy quarks from the decay products, and there are not so many broad and overlapping conventional states because there are fewer decay channels.

In 2003, the surprising discovery of X(3872), which is believed to have $q\bar{q}Q\bar{Q}$ configuration, in decay process $B^0 \to J/\Psi\pi^+\pi^- K$ by Belle[178] opened a new era in hadronic physics. This discovery was latter confirmed by BABAR[179, 180], CDF II[181, 182, 183], D0[184], LHCb[185] and CMS[186]. Since then, more than two dozen of exotic candidates with heavy flavor are found in experiments. These include exotic meson configurations X, Y, Z, and pentaquark P_c, with their masses in MeV added in parentheses, such as i) $Y(4260)$[187], $Z_c(4430)$[178], and $Z_c(3900)$[188] in charmonium sector; ii) $Z_b(10610)$ and $Z_b(10650)$[189] in bottomonium sector; iii)

the hidden-charm pentaquark states $P_c(4380)^+$, $P_c(4450)^+$[190], and the very recent hidden-charm molecular pentaquark $P_c(4312)^+$, $P_c(4440)^+$, $P_c(4457)^+$ announced by LHCb in 2019 with strong evidence[191]. For example, Fig. 3.1 and Fig. 3.2 show the S-wave open charm thresholds and exotic states candidates in the charmonium sector, where Fig. 3.1 is taken from Ref.[1] with data from Ref.[192] and Fig. 3.2 is taken from Ref.[2]. Similarly, Fig. 3.3 from Ref.[2] shows the exotic states candidates in the bottomonium sector. However, no consensus on the interpretation of these states has been achieved, so there is still an ongoing effort to study their properties both theoretically and experimentally. Detailed reviews on these exotic states in heavy quark sector can be found in Ref.[1, 177, 193, 194, 195, 196, 197, 198, 199, 200, 201, 202, 203, 204, 205, 206].

Lattice QCD simulations have found some exotic candidates close to the experimental data for certain configurations. For example, an isosinglet $I = 0$ candidate for $X(3872)$ was found[207, 208, 209] only if both the $c\bar{c}$ and $D\bar{D}^*$ interpolators are included. There is no candidate if use the diquark-antidiquark and $D\bar{D}^*$ interpolators without $c\bar{c}$ interpolator, which suggests the $c\bar{c}$ Fock component is important for $X(3872)$. However, this result was obtained at unphysical pion mass $m_\pi = 266\text{MeV}$, which is larger than the physical pion mass $m_\pi \approx 140\text{MeV}$, and the lattice volume used was also small. If the pion mass in the lattice simulation was smaller, the $D\bar{D}^*$ component may play a more important role, since the one-pion-exchange potential would be exponentially larger with a smaller pion mass in the hadronic molecular picture. In order to explore the structure of these XYZ exotic states, it would be important to have full lattice QCD simulations near the physical point. Reviews of

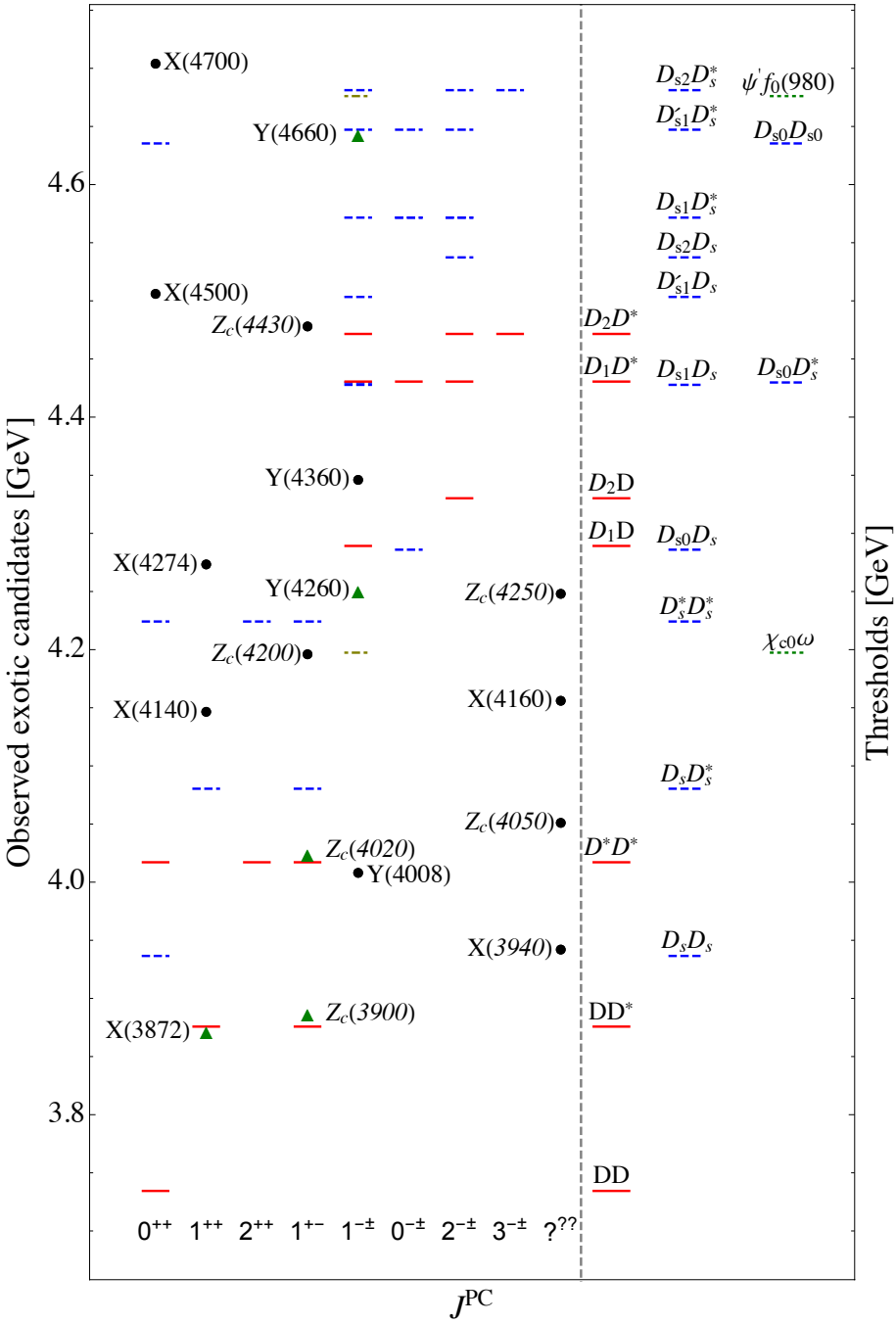

Figure 3.1: Candidates for exotic states in charmonium sector from Ref.[1] .

current lattice investigation on exotic hadrons can be found in Ref. [206].

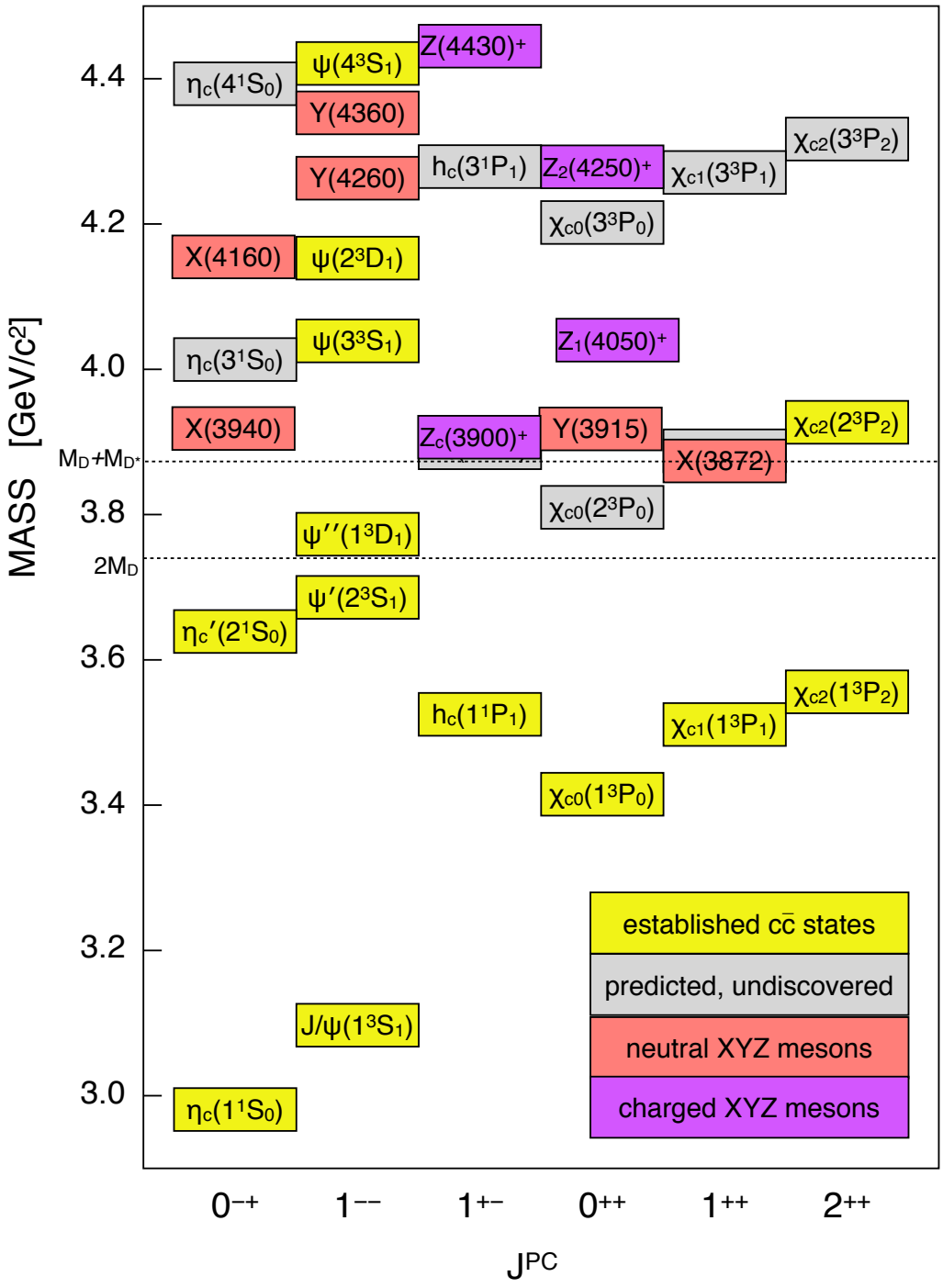

Figure 3.2: Candidates for exotic states in charmonium sector from Ref.[2].

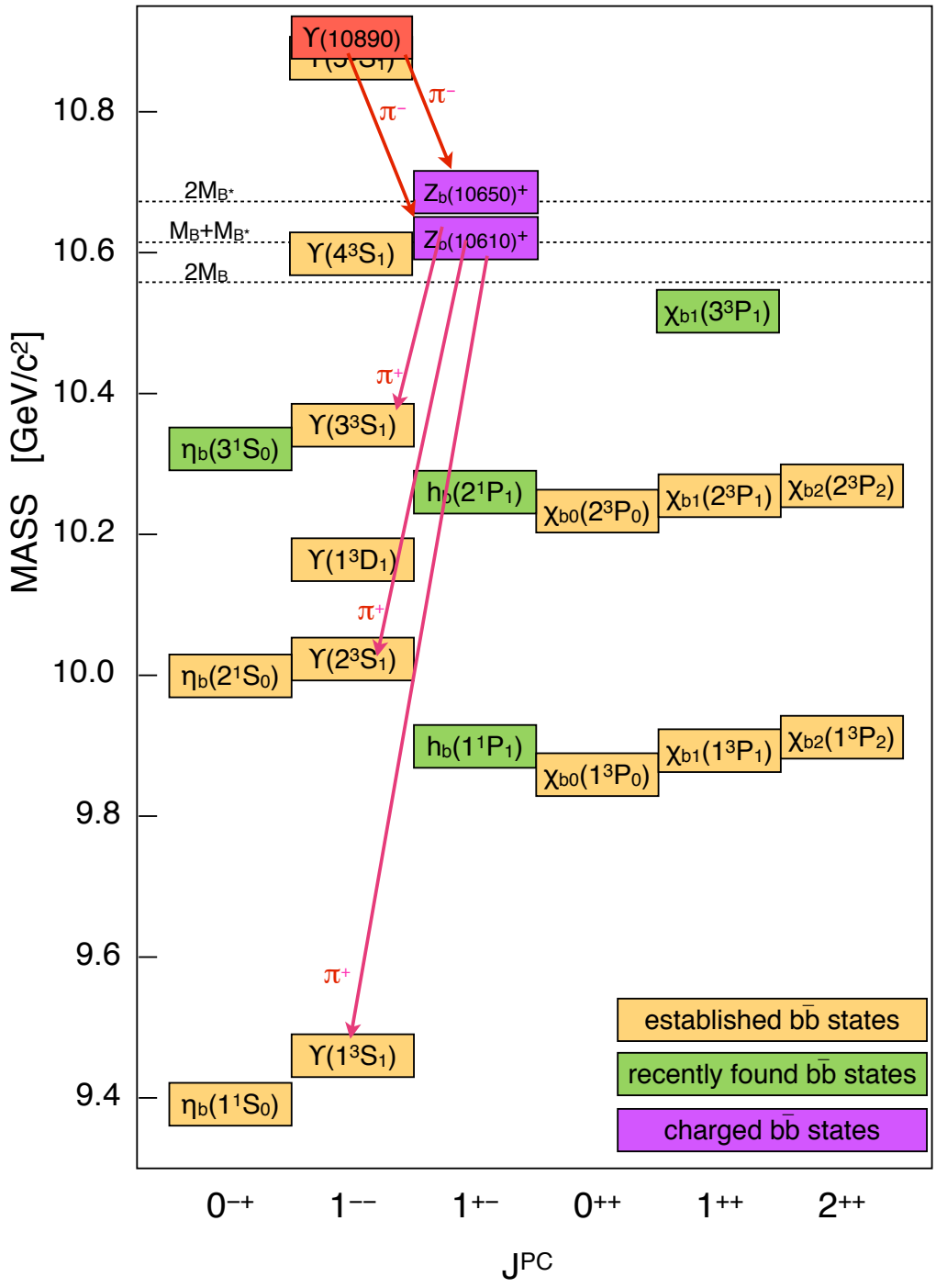

Figure 3.3: Candidates for exotic states in bottomonium sector from Ref.[2].

3.1.1 Tetraquarks with heavy flavor

The main focus of this chapter and the next chapter is on tetraquark with heavy quark flavors.

Despite the numerous exotic tetraquark candidates that have been found in the heavy quarkonium sector since the discovery of $X(3872)$, a unified and well-accepted theoretical description of these tetraquarks candidates has still not appeared. Several theoretical models often used to describe tetraquark states are listed below:

- Hadronic molecules: these models are often used to treat near-threshold tetraquark as a loosely bound state of two mesons[210, 211, 212, 213]. A review of this approach can be found in Ref. [1].

- Hadroquarkonia: these models treat heavy tetraquark as $Q\bar{Q}$ compact core surrounded by the light degrees-of-freedom[214, 215].

- Diquark-antidiquark mesons: this approach use color-nonsinglet diquark as tightly bounding blocks to build tetraquark[195, 196, 197, 216].

A detailed review of these and other models can be found in Ref. [198]. However, even for the most thoroughly studied candidate $X(3872)$, there are still controversies on whether it is primarily a $D^0\bar{D}^{*0}$ molecular because of its exceedingly closeness to threshold, or it has large $c\bar{c}$ component[1, 195].

3.1.2 $\bar{q}\bar{q}'QQ$ Tetraquarks in the heavy quark mass limits

As described in the introduction, systematic expansions in certain physical limits is a good way to study heavy tetraquark systems. The analysis of this chapter and the next chapter will use a systematic expansion around the heavy quark mass limit to show the existence of near-threshold tetraquarks with configuration $\bar{q}\bar{q}'QQ$, and $q\bar{q}'Q\bar{Q}$ tetraquarks with large angular momentum.

For tetraquark with the configuration $\bar{q}\bar{q}'QQ$, there have been two distinct arguments regarding its existence in the heavy quark mass limit. These arguments are valid for deeply bounded tetraquark states, which is different from the focus of this chapter: loosely bounded near-threshold tetraquark. However, it is still worthwhile to briefly review these works.

The first argument relies on the fact that the Coulomb potential of two heavy quarks is attractive in $\bar{3}$ color configuration[217, 218]. This implies that, in the heavy quark mass limit, two heavy quarks can form a deeply bound diquark in $\bar{3}$ configuration with a binding energy of order $\mathcal{O}(\alpha_s^2 M_Q)$ and characteristic size $\mathcal{O}(\alpha_s M_Q)^{-1}$. The binding energy $\mathcal{O}(\alpha_s^2 M_Q)$ is much larger than the hadronic scale $\Lambda_{\rm QCD}$ in the heavy quark mass limit, so this diquark system is tightly bound and has a small size. As a result, it acts as a nearly point-like static source of color Coulomb field, which behaviors dynamically the same way as a heavy antiquark.

This similarity between a heavy diquark and a heavy antiquark is the so-called doubly-heavy-diquark-anti-quark (DHDA) duality. This duality becomes exact when M_Q is infinitely large. The duality states that, as long as the system is well below the excitation energy of heavy diquark, every hadronic state of the system containing two heavy quarks has an analog state for the system with one heavy antiquark. As a result, since an antibaryon with a heavy antiquark is a strong-interaction stable state, the dual state, $\bar{q}\bar{q}'QQ$ tetraquark, must also exist as strong-interaction stable state in the extreme heavy quark mass limit, with corrections that vanishes when $M_Q \to \infty$.

However, it is also known that charm quark mass is too small for DHDA to

apply, and bottom quark mass is at best marginal[217, 218]. Thus, the DHDA duality is not an appropriate approach to treat the heavy tetraquark system in the real world, while it is still of theoretical interest since it shows that the structure of QCD does not exclude the existence of heavy tetraquarks.

The second argument treats $\bar{q}\bar{q}'QQ$ tetraquark system as a bound state of two heavy mesons[217, 218], each containing a heavy quark. The key point is to notice that, if these two heavy mesons remain distinct, are located far away from each other, move non-relativistically, and there are no new particles created, then the system can be described by Schrödinger equation.

Consider a system containing two non-relativistic particles, between which the relative dynamics can be described by Schrödinger equation, and assume there exists a parameter λ which can be used to tune the mass but only weakly affects the potential. For simplicity, if one consider s-wave channel without mixing from other channels, then the Schrödinger equation for the n-th bound state is written as:

$$\left(-\frac{1}{2\mu(\lambda)}\frac{\partial^2}{dr^2}+V(r;\lambda)\right)u_n(r;\lambda)=E_n(\lambda)u(r;\lambda) \tag{3.1}$$

where $\mu \equiv m_1 m_2/(m_1+m_2)$ is the reduced mas. u is normalized so that $\int dr|u(r)|^2 = 1$. The potential goes to zero at infinity.

From the equation, one can see that increasing μ is equivalent to increasing V when solving bound state for this equation, since only the product μV matters. Based on the basic conclusions of quantum mechanics, it is clear that if V is attractive, there will exist bound states if μ is large enough. A similar argument holds for

systems in other channels, or with mixing degrees of freedom.

As for the system consisting of two heavy mesons, each containing one heavy quark, it is known that the long-distance interaction is the one-pion-exchange potential. The precise form of this one-pion-exchange potential depends on the heavy quark symmetry and can be described with HHχPT[56, 218]. For certain channels, this potential can be negative, thus the previous simple quantum mechanics conclusion can be extended to here to show the existence of a bound state of two heavy mesons. Imagine these two heavy mesons are released far away from each other at long distance, with negative potential configuration, they are attracted to each other and are going to form a bound state. After they are trapped together and form a tetraquark, the tetraquark may but is not required to be in a "hadronic molecule" picture since one is unclear about the short distance interaction, which might be outside the regime of validity of the Schrödinger equation. However, one can still deduce a bound state exists since the true ground state energy must be below any trial wave function that is in the region of validity of the Schrödinger equation. Thus, even though at first glance this approach seems to rely on the validity of the "hadronic molecule" picture, it actually holds independent of whether the "hadronic molecule" picture is true.

The previous paragraphs have shown the two arguments regarding the existence of $\bar{q}\bar{q}'QQ$ tetraquark in the heavy quark mass limit. The first argument is for deeply bound tetraquark, while the second argument does not specify the dynamics and energy scales inside the tetraquark. Starting from the next section, the principal result of this chapter will be shown, regarding the existence of parametri-

cally narrow near-threshold $\bar{q}\bar{q}'QQ$ tetraquarks, which was not covered by previous literature. The near-threshold tetraquarks are of theoretical importance because many experimentally detected tetraquarks are close to the threshold, but these are in $q\bar{q}'Q\bar{Q}$ configuration which will be discussed in next chapter.

3.2 On the existence of multiple $\bar{q}\bar{q}'QQ$ tetraquarks with fixed quantum numbers in a toy model description

As mentioned before, this chapter focuses on the near-threshold tetraquark system with two heavy quarks. For the near-threshold system we are focusing on, the two heavy quarks are separating from each other by a long distance. A key point is that, in the heavy quark mass limit, this system with long distances between heavy quarks is well-described by two heavy meson interacting via a Yukawa-type potential.

In this section, we start from a toy model: use the two-body Schrödinger equation description and use semi-classical analysis to show the existence of a large number of bound states of the two heavy mesons in the heavy quark mass limit. We will begin the discussion with a system with a simple quantum number, and then generalize it to other quantum numbers.

However, as will be discussed later, in a more complete description with more degree of freedom, these states are narrow resonances rather than stable bound states. This will be discussed in the next section.

3.2.1 Description based on the two-body Schrödinger equation

For illustrative purposes, initially, we start with $I = 1$, $J = 0$, positive parity states with two heavy mesons. The virtue of this kind of state is that it does not involve coupled channels; it involves only one single degree of freedom, the distance r between the two heavy mesons.

According to standard semi-classical analysis, the number of bound states between energy E_0 and $E_0 + \Delta E$ for this system is approximated by:

$$\begin{aligned} N(E_0, \Delta E) &\approx \frac{\int_{E_0}^{E_0+\Delta E} \mathrm{d}E \int \mathrm{d}p\, \mathrm{d}q\, \delta(E - H(p,q))}{2\pi} \\ &= \frac{\int \mathrm{d}p\, \mathrm{d}q\, \Theta(E_0 + \Delta E - H(p,q))\Theta(H(p,q) - E_0)}{2\pi} \end{aligned} \tag{3.2}$$

where H is the classical Hamiltonian and Θ is a Heaviside step function. The more number of states there are, the more accurate this approximation will be. The number of bound states is around $(2\pi)^{-1}$ times the area of phase space with energies in the appropriate range. Suppose potential $V(q)$ is independent of reduced mass μ in Hamiltonian $H = \frac{p^2}{2\mu} + V(q)$. It is easy to see the phase space area between energy E_0 and $E_0 + \Delta E$ is proportional to $\sqrt{\mu}$, and so is $N(E_0, \Delta E)$, which validates the usage of semi-classical analysis in heavy quark mass limit.

The purpose of this section is to show that, for this toy model, there exists a large number of bound states increasing with heavy quark mass. Since we do not have much knowledge of short-range interaction, we will use the knowledge of long-range interaction to derive a lower bound.

For $S_l = 0$ states, one-pion exchange potential is given by Yukawa form:

$$\tilde{V}_{\text{long}}(r) = -\left(I(I+1) - \frac{3}{4}\right)\frac{g^2 m_\pi^2}{\pi f_\pi^2}\frac{e^{-m_\pi r}}{r} \tag{3.3}$$

where I is the total isospin of the state, g is the coupling constant for $H - H^* - \pi$ coupling (evaluated at $q = 0$) and $f_\pi \approx 93$ MeV is the pion decay constant; the quantities g, f_π and m_π are all understood to be at their heavy-quark limit.

Since we only know the form of interaction at long distance, we will focus on the number of bound states with r large enough to be in the region where the Yukawa potential is valid, which is denoted by $N^{\text{long}}(E_0, \Delta E)$. The logic is, if assume $N^{\text{long}}(E_0, \Delta E)$ is large, we can use semi-classical approximation. Then, $N^{\text{long}}(E_0, \Delta E)$ is proportional to square root of reduced mass $\mu = M_Q/2$. In the heavy quark mass limit, $N^{\text{long}}(E_0, \Delta E)$ diverges as $\sqrt{M_Q}$, so there is a large number of states, which justify the usage of semi-classical approximation.

The total number of two heavy meson bound states n_{tot} is bounded by $N^{\text{long}}(-B, B)$ as

$$n_{\text{tot}} \geq n_B \equiv N^{\text{long}}(-B, B), \tag{3.4}$$

where n_B is the number of bound states with binding energy less than B.

Define r_B through $\tilde{V}_{\text{long}}(r_B) = -B$, and B should be small enough to make r_B large enough, so that the system is in the appropriate regime. According to WKB approximation:

$$N^{\text{long}}(-B, B) \geq \int_{r_B}^{\infty} \mathrm{d}r\, \frac{\sqrt{-M_Q \tilde{V}_{\text{long}}(r)}}{\pi}, \tag{3.5}$$

With explicit quantum number put into Eq. (3.3), one can prove that:

$$n_B > \frac{\sqrt{M_Q B}}{2\sqrt{2}\, m_\pi} \sim \frac{\sqrt{M_Q B}}{\Lambda} \,. \tag{3.6}$$

Recall that the condition of this analysis is that the number of states n_B is large so that semi-classical analysis can be used. When a small B is a fixed value, n_B grows with $\sqrt{M_Q}$, which is large in the heavy quark mass limit. Thus, this analysis is self-consistent.

Suppose one is interested in the states close to threshold. Let us consider the case that B is not held fixed; rather, it is chosen to decrease parametrically with increasing M_Q to ensure that, the states are parametrically close to threshold at large M_Q:

$$B = b^2\, 2\pi^2\, \frac{m_\pi^{2-\epsilon}}{M_Q^{1-\epsilon}} \sim \frac{\Lambda^{2-\epsilon}}{M_Q^{1-\epsilon}}, \tag{3.7}$$

where b is a dimensionless numerical constant of order unity and $0 < \epsilon \leq 1$.

Then Eq. (3.6) yields $n_b > b\,(M_Q/m_\pi)^{\epsilon/2}$, which means n_b is still large in heavy quark mass limit, and grows when M_Q increases. Thus, the system is still in semi-classical limit, and the previous analysis is self-consistent.

This tells us that even if one restricts the consideration to very near threshold states, there are still a large number of them exist in the formal large M_Q limit. The physical scenario is that, as M_Q increases, new bound tetraquark states will continue to emerge at the threshold. After a new state appears, it moves below the threshold with increasing M_Q, eventually leaving the regime that can be identified as being

"near-threshold". However, as the old state leaves the near-threshold regime, there are always new states that enter at threshold, which ensures that there are always a large number of near-threshold states.

To quantify this behavior, it is useful to look at the binding energy of the least bound state $B_{min}(M_Q)$. $B_{min}(M_Q)$ is zero when a new bound state just emerges, then grows with M_Q, reaches local maximum, and drops discontinuously to zero when the next new bound state appears. For near-threshold binding energy $B \sim \frac{\Lambda^{2-\epsilon}}{M_Q^{1-\epsilon}}$, it requires $B_{min}(M_Q)$ go to zero as M_Q goes to infinity, at least as fast as M_Q^{-1}.

We illustrate this scenario in a toy model with a potential given as:

$$V(r) = \frac{-10 m_Y e^{-\sqrt{4m_Y^2 r^2+1}/2}}{\sqrt{4m_Y^2 r^2+1}}, \tag{3.8}$$

which is a Yukawa function (mimicking $\tilde{V}_{\text{long}}(r)$) at long distances while being non-singular at short distances. The behavior of $B_{min}(M_Q)$ (in units of the Yukawa mass) is shown in Fig. 3.4 as a function of the heavy meson mass (in units of the Yukawa mass). The dots correspond to values of M_Q just prior to the entrance of a new bound state, which are local maximum of $B_{min}(M_Q)$ during the process of increasing M_Q. The solid line with a slope of -1 on this log-log plot represents $B = \frac{\Lambda^2}{M_Q}$ with Λ fit to the lowest mass point on the plot, which apparently shows that the binding energies of the least binding states fall off with M_Q slightly faster than M_Q^{-1}. This is consistent with the expected scenario.

Though the plot is for this specific toy model, it seems apparent that paramet-

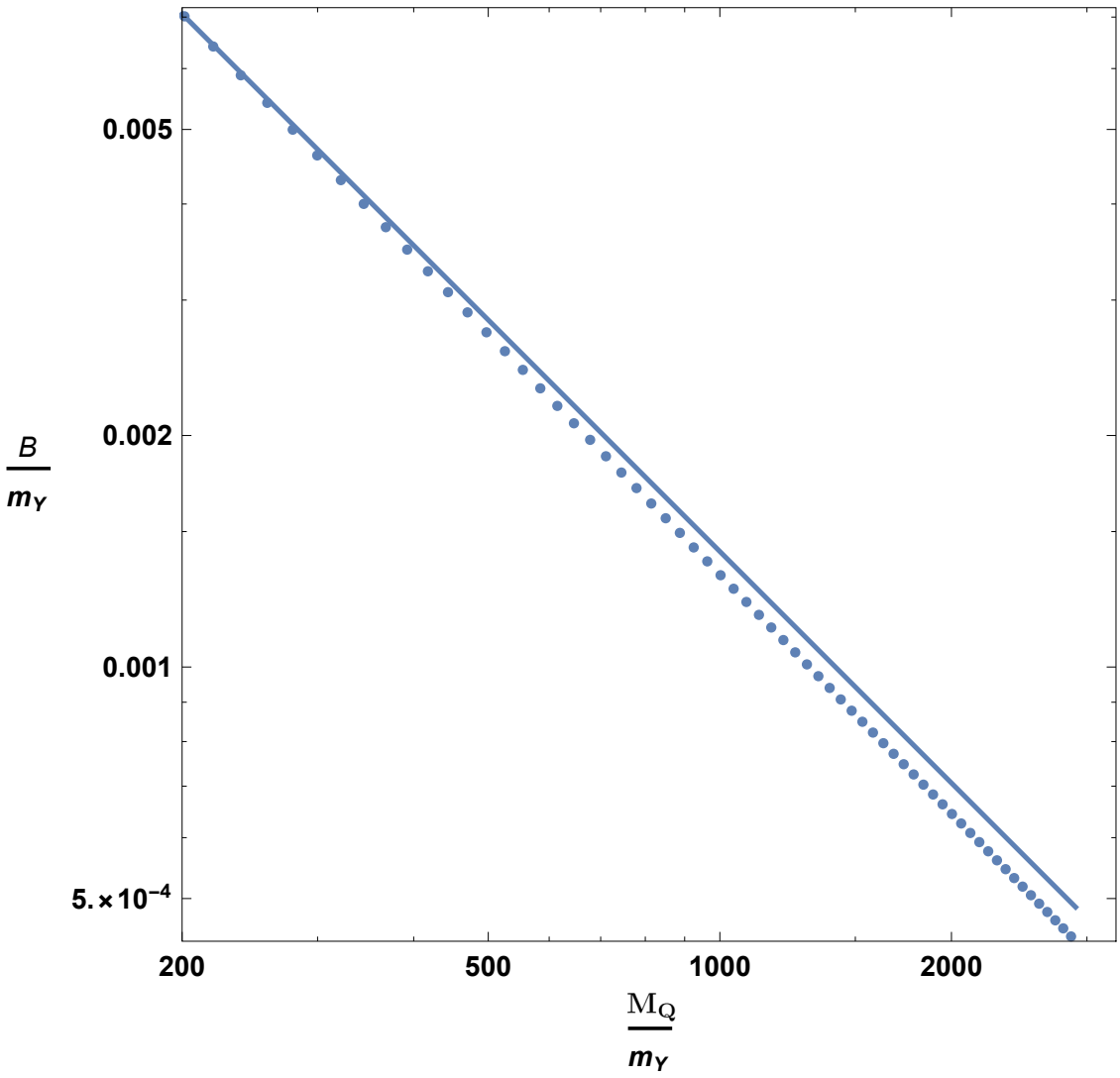

Figure 3.4: Binding energy of the least bound state for a toy model.

rically light bound tetraquark states at large mass M_Q exist for generic potential models that asymptote to a Yukawa form at long distance. Based on the previous analysis, there are a large number of these states exist, even for parametrically near-threshold region provided that M_Q is large enough.

Note that here we consider a toy description: a Schrödinger equation description. In real QCD, the system can emit pions, which renders the potential model description invalid. Thus, the conclusion that a large number of bound states exist

in Schrödinger equation description for large M_Q does not directly apply to QCD. This issue will be tackled in Sec. 3.3. Before that, let us at first generalize the conclusion of this section to more generic quantum numbers.

3.2.2 Other quantum numbers

The purpose of this section is to show the discussion in the previous section can be generated to attractive channels with quantum numbers other than $I = 1$, $J = 0$, positive parity states. For these general states, the one-pion-exchange interaction is complicated. The effect of the tensor force mixes channels with different L quantum numbers, causes a coupled-channel problem.

The solution is to choose a basis in which the channels decouple up to corrections that vanishes in the heavy quark mass limit so that the problem is effectively reduced to one kinetic degree of freedom. The argument is based on the Born-Oppenheimer approximation[219]. The Born–Oppenheimer approximation assumes that the dynamics of fast degree-of-freedom and slow degree-of-freedom can be treated separately because of their distinct time scales. It has been used in the context of other heavy quark exotic states such as heavy-quark hybrids[220, 221, 222].

Because of the potential between the two heavy mesons couples different channels, it can be expressed in a matrix form. In a Schrödinger equation description, the equation and potential can be generally written as:

$$
\begin{aligned}
&\left(-\frac{\overleftrightarrow{1}}{2\mu}\partial_r^2+\overleftrightarrow{V}\right)\vec{\psi}=E\vec{\psi}\\
&\text{with}\ \ \vec{\psi}(r)\equiv\begin{pmatrix}\psi_1(r)\\ \psi_2(r)\\ \vdots\\ \psi_k(r)\end{pmatrix}\\
&\text{and}\quad \overleftrightarrow{V}(r)\equiv\begin{pmatrix}V_{11}(r) & V_{12}(r) & ... & V_{1k}(r)\\ V_{21}(r) & V_{22}(r) & ... & V_{2k}(r)\\ \vdots & \vdots & \vdots & \vdots\\ V_{k1}(r) & V_{k2}(r) & ... & V_{kk}(r)\end{pmatrix},
\end{aligned}
\tag{3.9}
$$

where μ is the reduced mass. $\overleftrightarrow{V}(r)$ has a magnitude of order Λ and varies over a distance of order $\frac{1}{\Lambda}$; while the kinetic term is controlled by $\mu\sim M_Q$.

The diagonal terms are interactions that within a channel, and off-diagonal terms are cross-channel coupling. According to finite-dimensional spectral theorem, since $\overleftrightarrow{V}(r)$ is Hermitian, it is guaranteed to be diagonalizable by a unitary matrix $\overleftrightarrow{U}(r)$ for any fixed r, and the resulting diagonal matrix $\overleftrightarrow{\tilde{V}}(r)\equiv\overleftrightarrow{U}(r)\overleftrightarrow{V}(r)\overleftrightarrow{U}^{\dagger}(r)$ has only real entries.

Physically, the eigenvalues are the potential for the new channels expressed in the form of $\overleftrightarrow{\tilde{V}}(r)$, and the eigenvectors give the new channels, which are not coupled to each other, in terms of the old ones.

However, for a physical dynamic system, r is not a fixed value, thus $\overleftrightarrow{U}(r)$ and $\overleftrightarrow{V}(r)$ are changing with r, so there is no fixed diagonal $\overleftrightarrow{V}(r)$ for all r, which

naively would render the analysis complicated.

The key point is to notice that since we are considering the heavy quark mass limit, the two mesons move slowly so that the process is adiabatic. According to Born-Oppenheimer approximation, if the adiabatic system is in the lowest eigenstate for one value of r, it will remain in the lowest eigenstate for all value of r. This approximation will become perfect as $M_Q \to \infty$. In this case, the system will effectively act as a single channel with the potential given by the lowest eigenvalue.

Define $\vec{\tilde{\psi}}(r) \equiv \overleftrightarrow{U}(r)\vec{\psi}(r)$. One can decompose the Hamiltonian as:

$$\begin{aligned} &(H_0 + H_1 + H_2)\,\vec{\tilde{\psi}} = E\vec{\tilde{\psi}} \ \text{ with} \\ &H_0 = \frac{-\overleftrightarrow{1}}{2\mu}\partial_r^2 + \overleftrightarrow{\tilde{V}}(r) \ \ , \\ &H_1 = \frac{1}{\mu}\overleftrightarrow{U}'(r)\overleftrightarrow{U}^{\dagger}(r)\partial_r \\ &\text{and} \ \ H_2 = -\frac{1}{2\mu}\overleftrightarrow{U}''(r)\overleftrightarrow{U}^{\dagger}(r) \ . \end{aligned} \tag{3.10}$$

H_0 is diagonal. We are going to show that H_0 is dominant over H_1 and H_2 in the heavy quark mass limit. Notice that we are considering semi-classical bound states, so the spatial derivatives of ψ are of order $\sqrt{M_Q\Lambda}$. Thus, the scaling of H_0, H_1 and H_2 with M_Q are:

$$H_0 \sim \Lambda, \tag{3.11}$$

$$H_1 \sim \sqrt{\frac{\Lambda^3}{M_Q}}, \tag{3.12}$$

$$H_2 \sim \frac{\Lambda^2}{M_Q} \tag{3.13}$$

From the scaling, it clear that the diagonal H_0 is dominant, while H_1 and H_2 can be treated as perturbations. Since H_1 is entirely off-diagonal, it only contributes to the energy in the second order. Therefore, the contributions from H_1 and H_2 are of order $\frac{\Lambda^2}{M_Q}$, which can be neglected in the heavy quark mass limit.

Since in the heavy quark mass limit, only the contribution from diagonal H_0 survives, finding the bound state in terms of the lowest eigenvalue of $\overleftrightarrow{V}(r)$ becomes a problem with a single radial degree of freedom. Then all the discussions in the previous section can also be applied here. The conclusion is that, in the heavy quark mass limit, for all quantum numbers with attractive interaction at long distance, there are a large number of tetraquark states.

3.3 A more complete description

In infinite volume limit, the $\bar{q}\bar{q}'QQ$ tetraquark states of interest are loosely bounded states with a long distance between heavy quarks, while it is known in the literature that deeply bounded $\bar{q}\bar{q}'QQ$ tetraquark states with binding energy of order $\alpha_s^2 M_Q$ relative to the threshold exist. The energy level of the deeply bounded

tetraquark states are lower than the loosely bounded tetraquark states by more than m_π, Given that there is no symmetry prevents the loosely bounded one decaying to deeply bounded one by emission of pions, the loosely bounded tetraquark will decay via pion emission, which renders the discussion under Schrödinger equation description in previous section incomplete.

The potential model in the previous discussion is actually not valid because of the pion emission, so stable bound states with binding energy of order Λ presumably not exist. However, it will be shown in this section, that unstable but long-lived tetraquark resonances with binding energy of order Λ and narrow width do exist in the heavy quark mass limit.

The treatment is similar to the hydrogen spectrum. A Schrödinger equation description with coulomb potential gives rise to many bound states; while in QED, these states can decay through emission of photons, so none of the excited states are stable. However, these states are so long-lived that their decay widths are much smaller than the energy level spacing between two nearby states in the energy spectrum. Our goal in this section is to show that a similar scenario happens for these loosely bounded tetraquark states: their decay widths are parametrically smaller than their level spacing so that they exist as narrow resonances in the heavy quark mass limit.

As we are considering the heavy quark mass limit, the effects of relative order $\frac{\Lambda}{M_Q}$ will be dropped in the rest of the discussion in this chapter.

In the heavy quark mass limit, there is a separation between the fast and slow degree-of-freedoms. The light quarks and gluons are the fast degree-of-freedoms with

a characteristic scale Λ. The nonrelativistic heavy quarks are the slow degree-of-freedoms. At the leading order of NRQCD (Non-relativistic QCD)[62], the number of heavy quarks is fixed since pair creation is suppressed. The characteristic velocity of the heavy quarks is of order $\sqrt{\frac{\Lambda}{m_Q}}$, so the three momentum scale is of order $\sqrt{m_Q \Lambda}$.

For illustrative purposes, in the following analysis, we will focus on attractive positive parity $I = 1$, $J = 0$ channel. However, the conclusion holds for the mixed channel cases as explained in the previous section, with correction up to relative order $\frac{\Lambda}{M_Q}$ (which can be neglected in the heavy quark mass limit).

We are going to show that, in the heavy quark mass limit, for tetraquark states of order Λ below threshold, the scaling of widths Γ and level spacing ΔE with m_Q are:

$$\Gamma \sim \frac{\Lambda^2}{m_Q} \ , \tag{3.14}$$

$$\Delta E \sim \sqrt{\frac{\Lambda^3}{m_Q}} \ . \tag{3.15}$$

Then the ratio of widths to level spacing is:

$$\frac{\Gamma}{\Delta E} \sim \sqrt{\frac{\Lambda}{m_Q}} \ . \tag{3.16}$$

Thus, $\frac{\Gamma}{\Delta E}$ is vanishing in the heavy quark mass limit, which means the decay width is much smaller than level spacing so that these tetraquark states exist as narrow resonances.

The scaling of level spacing Eq. (3.15) comes from semi-classical analysis. The size of level spacing in the semi-classical region with long distance between heavy quarks can be characterized by binding energy B, which is of order Λ, divided the number of total states n_B in this region:

$$\Delta E \sim \frac{B}{n_B}, \tag{3.17}$$

where n_B is given in Eq. (3.6) as

$$n_B > \frac{\sqrt{M_Q B}}{\Lambda}, \tag{3.18}$$

from which it is easy to derive Eq. (3.15).

The rest of this section will be devoted to the scaling of decay width Eq. (3.14).

We will work in a Hamiltonian description of QCD. The full Hamiltonian includes unphysical states that do not respect Gauss's law. To proceed we introduce a projection operator $\hat{\mathcal{P}}^{\text{phys}}$ to project states from the full Hilbert space onto physical state with $\vec{P}_{\text{cm}} = 0$ and with the quantum number of interest. Then we can define a physical Hamiltonian $\hat{H}^{\text{phys}} = \hat{\mathcal{P}}^{\text{phys}} \hat{H} \hat{\mathcal{P}}^{\text{phys}}$, which acts in the Hilbert space of physical states with fixed quantum number of interest. The time-independent eigenstates $|\Phi\rangle$ can be solved by:

$$\hat{H}^{\text{phys}} |\Phi\rangle = E_\Phi |\Phi\rangle. \tag{3.19}$$

Here $|\Phi\rangle$ is state of the whole system, so encoded information of both slow and fast

degree of freedom.

Let us assume there exist a projection operator $\hat{\mathcal{P}}^{\rm r}$, which projects the physical Hamiltonian to a description of nonrelativistic quantum mechanics with a single spatial degree of freedom r, which corresponding to the distance between two heavy quarks, and a Yukawa-like potential that dependent on r as in Eq. (3.3). This space is the space of tetraquark states with no additional pions as in the previous section. The complement of $\hat{\mathcal{P}}^{\rm r}$ is defined as $\hat{\mathcal{Q}}^{\rm r} = (1 - \hat{\mathcal{P}}^{\rm r})$, which projects tetraquark states with no pions out of its space and implies the decay of tetraquark. Later we will see that the operator $\hat{\mathcal{P}}^{\rm r}$ indeed exists.

The energy eigenvalue equation can be rewritten in the form of a two-by-two matrix of operators

$$\begin{pmatrix} \hat{\mathcal{P}}^{\rm r}\hat{H}^{\rm phys}\hat{\mathcal{P}}^{\rm r} & \mathcal{P}^{\rm r}\hat{H}^{\rm phys}\hat{\mathcal{Q}}^{\rm r} \\ \hat{\mathcal{Q}}^{\rm r}\hat{H}^{\rm phys}\hat{\mathcal{P}}^{\rm r} & \hat{\mathcal{Q}}^{\rm r}\hat{H}^{\rm phys}\hat{\mathcal{Q}}^{\rm r} \end{pmatrix} \begin{pmatrix} |\Phi;\vec{P}\rangle_{\rm r} \\ |\Phi;\vec{P}\rangle_{\rm nr} \end{pmatrix} = E_\Phi \begin{pmatrix} |\Phi;\vec{P}\rangle_{\rm r} \\ |\Phi;\vec{P}\rangle_{\rm nr} \end{pmatrix}$$
$$\text{with } |\Phi;\vec{P}\rangle_{\rm r} \equiv \hat{\mathcal{P}}^{\rm r}|\Phi;\vec{P}\rangle \ , \ |\Phi;\vec{P}\rangle_{\rm nr} \equiv \hat{\mathcal{Q}}^{\rm r}|\Phi;\vec{P}\rangle \tag{3.20}$$

and by construction the states are eigenstates of the total momentum.

The full Hamiltonian can be decomposed as:

$$\begin{aligned} &\hat{H}^{\rm phys} = \hat{H}_0 + \hat{H}_I \ \text{ with} \\ &\hat{H}_0 \equiv \hat{\mathcal{P}}^{\rm r}\hat{H}^{\rm phys}\hat{\mathcal{P}}^{\rm r} + \hat{\mathcal{Q}}^{\rm r}\hat{H}^{\rm phys}\hat{\mathcal{Q}}^{\rm r} \\ &H_I \equiv \hat{\mathcal{P}}^{\rm r}\hat{H}^{\rm phys}\hat{\mathcal{Q}}^{\rm r} + \hat{\mathcal{Q}}^{\rm r}\hat{H}^{\rm phys}\hat{\mathcal{P}}^{\rm r} \ ; \end{aligned} \tag{3.21}$$

Let us denote a typical tetraquark state as $|\Phi\rangle_r$ which satisfies

$$\hat{H}_0|\Phi\rangle_r = \left(E + 2M_Q + \mathcal{O}\left(\frac{\Lambda^2}{M_Q}\right)\right)|\Phi\rangle_r\,, \tag{3.22}$$

where E is the energy relative to the threshold for breaking into two heavy mesons. The $\mathcal{O}\left(\frac{\Lambda^2}{M_Q}\right)$ correction can be neglected since we are considering the heavy quark mass limit. It is useful to define an effective two-body Hamiltonian $\hat{H}_0^{2\,\mathrm{body}} \equiv \hat{H}_0 - 2M_Q$ to get rid of the rest mass $2M_Q$. Then the Schrödinger equation becomes $\hat{H}_0^{2\,\mathrm{body}}|\Phi_j\rangle_r = E_j|\Phi_j\rangle_r$. One can rewrite the Schrödinger equation in positional space, depends on single kinetic degree of freedom r, so the semiclassical analysis in previous section can be applied here.

From Fermi's Golden rule, the decay width Γ is:

$$\begin{aligned}\Gamma_j &= 2\pi|_r\langle\Phi_j|\hat{H}_I|\Phi'\rangle_{nr}|^2\rho(E_{nr}) \\ &= 2_r\langle\Phi_j|\hat{H}_I\hat{G}(E_j)\hat{H}_I|\Phi_j\rangle_r\,, \\ \text{with } \hat{G}(E) &\equiv \lim_{\epsilon\to 0^+}\mathrm{Im}\left(\frac{1}{E-\hat{H}_0^{2\,\mathrm{body}}+i\epsilon}\right)\,.\end{aligned} \tag{3.23}$$

where $|\Phi\rangle_r$ is an initial tetraquark state in the space with no additional pions, and $|\Phi\rangle_{nr}$ is a final state outside this space. ρ is the density of states, and is also called spectrum function. It comes from integrating over all final state energies with energy conservation taken into account explicitly by delta function as $\rho(E_f) = |\frac{dn}{dE}|_{E_f} = \int \frac{dn}{dE}\delta(E - E_i)dE$. The second equation comes from the fact that (the spectral representation of) imaginary part of Green's function provides

the local density of states of the system[223]. In other words, $\hat{G}(E)$ comes from the decomposition in terms of continuum eigenstates of $\hat{H}_0$ that are outside the space r, and is only nonzero for states with energies that overlap E. These eigenstates in $\hat{G}(E)$ are tetraquark states with separation r plus one or more mesons.

In order to derive the scaling of Γ with m_Q. It is useful to define an gauge invariant operator $\hat{R}$, which measures the distance between the two heavy quarks, as:

$$\hat{R} \equiv \frac{\int \mathrm{d}^3x\, \mathrm{d}^3y\, |y|\, \hat{Q}^\dagger(\vec{x})\hat{Q}^\dagger(\vec{x}+\vec{y})\hat{Q}(\vec{x}+\vec{y})\hat{Q}(\vec{x})}{2} , \tag{3.24}$$

Denote a typical eigenstate of $\hat{R}$ as $|r, \psi_{\mathrm{fast,r}}\rangle$, where a fixed value r is the separation between two heavy quarks and $\psi_{\mathrm{fast,r}}$ describes the state of the fast degrees of freedom. $\psi_{\mathrm{fast,r}}$ depend implicitly on r. For each fixed separation r between heavy quarks, the light quarks and gluons have a corresponding distribution $\psi_{\mathrm{fast,r}}$ over space. For different heavy quarks separation r, the wave function of fast degree-of-freedom $\psi_{\mathrm{fast,r}}$ is different.

The wave function of the whole tetraquark system $|\Phi(r)\rangle_r$ can be written as:

$$|\Phi(r)\rangle_{\mathrm{r}} = \phi_{\mathrm{slow}}(r)|r, \psi^{\mathrm{opt}}_{\mathrm{fast,r}}\rangle \ . \tag{3.25}$$

The $\phi_{\mathrm{slow}}(r)$ is the distribution of different r, and therefore captures the information about the motion of the heavy quarks. In other words, it is the wave function related to the slow degree of freedom. $\phi_{\mathrm{slow}}(r)$ depends explicitly on r; while $\psi_{\mathrm{fast,r}}$,the wave function of the fast degree of freedom, depends implicitly on heavy quarks separation

r.

In other words, $|\Phi(r)\rangle_{\rm r}$ can also be doneted by:

$$\begin{aligned} |\Phi(r)\rangle_{\rm r} &= \phi_{\rm slow}(r)|r\rangle \otimes |\psi^{\rm opt}_{\rm fast,r}\rangle \ . \\ &= |\phi_{\rm slow}\rangle \otimes |\psi^{\rm opt}_{\rm fast,r}\rangle \\ &= |\phi_{\rm slow}, \psi^{\rm opt}_{\rm fast,r}\rangle \end{aligned} \tag{3.26}$$

One can decompose $\hat{\mathcal{P}}^{\rm r}$, assume it exists, as:

$$\begin{aligned} &\hat{\mathcal{P}}^{\rm r} = \int_0^\infty {\rm d}r \, |r, \psi^{\rm opt}_{\rm fast,r}\rangle\langle r, \psi^{\rm opt}_{\rm fast,r}| \ \text{ with} \\ &\hat{R}|r, \psi^{\rm opt}_{\rm fast,r}\rangle = r|r, \psi^{\rm opt}_{\rm fast,r}\rangle \\ &\langle r', \psi^{\rm opt}_{\rm fast,r}|r, \psi^{\rm opt}_{\rm fast,r'}\rangle = \delta(r-r') \end{aligned} \tag{3.27}$$

where "opt" means the optimal state among degenerate eigenstates of $\hat{R}$.

The next step is using energy considerations to determine the optimal state $\psi^{\rm opt}_{\rm fast,r}$. Once the optimal state is determined for every r, the projection operator $\hat{\mathcal{P}}^{\rm r}$ is fixed by Eq. (3.27).

One can define the potential operator by:

$$\hat{V} \equiv \hat{H} - \hat{T}^{\rm heavy}, \tag{3.28}$$

where $\hat{H}$ is the leading order NRQCD Hamiltonian, and $\hat{T}^{\rm heavy} \equiv \int d^3x Q^\dagger(\vec{x}) \left(-\frac{\vec{D}^2}{2m_Q}\right) Q(\vec{x})$ is the gauge invariant kinetic energy of the heavy quarks. $\hat{V}$ commutes with $\hat{R}$ be-

cause it does not contain a derivative with respect to r.

Then the potential can be defined by:

$$V_{\psi_{\text{fast,r}}}(r)\delta(r-r') = \langle r', \psi_{\text{fast,r}}|\hat{V}|r, \psi_{\text{fast,r}}\rangle \ . \tag{3.29}$$

Now finding the optimal states among eigenstates of $\hat{R}$ is just finding the ground state of the fast degree of freedom $\psi^{\text{opt}}_{\text{fast,r}}$ that minimizes $V_{\psi_{\text{fast,r}}}(r)$.

Recall the Born-Oppenheimer considerations, in which the slow and fast degree of freedom decouple. The heavy quark positions are the slow degree of freedom associated with characteristic momentum scale $\sqrt{m_Q\Lambda}$, while the light quarks and gluons are the fast degree of freedom with a characteristic scale Λ. Heavy quarks move slowly, so the change in r is slow and the system is adiabatic. Thus, the system will remain in the fast degree of freedom's ground state $\psi^{\text{opt}}_{\text{fast,r}}$.

Since we have the optimal states and projection operator, the next step is to use Fermi's Golden rule to derive the scaling of decay rate Γ using Eq. (3.23) based on $\hat{H}_1$'s effect on $|\Phi\rangle_{\text{r}} = \phi_{\text{slow}}(r)|r\rangle \otimes |\psi^{\text{opt}}_{\text{fast,r}}\rangle = |\phi_{\text{slow}}, \psi^{\text{opt}}_{\text{fast,r}}\rangle$.

Notice that in the incomplete Schrödinger equation description of previous section, we used the kinetic energy of the heavy quarks rather than the full kinetic energy of the total system including both slow and fast degree of freedom. The difference between these two is the previous missing part, $\hat{H}_I$. Thus, $\hat{H}_I$ can be obtained by subtracting the kinetic energy of heavy quarks $\hat{T}^{\text{heavy}}$ from the total kinetic energy of the tetraquark system:

$$\hat{H}_I|r,\psi^{\rm opt}_{\rm fast,r}(r)\rangle = \left(-\frac{D_r^2}{M_Q} - \hat{T}^{\rm heavy})\right)|r,\psi^{\rm opt}_{\rm fast,r}(r)\rangle, \tag{3.30}$$

where D_r is covariant derivative acting on the single degree of freedom r.

The covariant derivatives implies the inclusion of gluonic corrections. However since the fast degrees of freedom vary with characteristic scales of Λ, the contribution to covariant derivative is at order $\frac{\Lambda^2}{m_Q}$, so it can be neglected to the order at which we work. Thus, One can replace $-\frac{D_r^2}{M_Q}$ by $-\frac{\partial_r^2}{M_Q}$:

$$\hat{H}_I|\phi_{\rm slow},\psi^{\rm opt}_{\rm fast,r}\rangle = -\left(\hat{T}^{\rm heavy} + \frac{\partial_r^2}{M_Q}\right)|\phi_{\rm slow},\psi^{\rm opt}_{\rm fast,r}\rangle, \tag{3.31}$$

where the derivatives in the second term $\frac{\partial_r^2}{M_Q}$ act both explicitly on $\phi_{\rm slow}(r)$ and implicitly on $\psi^{\rm opt}_{\rm fast,r}$.

Consider the first piece in Eq. (3.31), the matrix element of the kinetic energy is:

$$\begin{aligned}&\langle\phi_{\rm slow},\psi^{\rm opt}_{\rm fast,r}|\hat{T}^{\rm heavy}(\vec{x})|\phi_{\rm slow},\psi^{\rm opt}_{\rm fast,r}\rangle \\ &= \langle\phi_{\rm slow},\psi^{\rm opt}_{\rm fast,r} - \frac{1}{M_Q}(\partial_r^2|\phi_{\rm slow}\rangle)\otimes|\psi^{\rm opt}_{\rm fast,r}\rangle + \mathcal{O}\left(\frac{\Lambda^2}{m_Q}\right)\end{aligned} \tag{3.32}$$

where the derivative in heavy quark kinetic energy operator $\hat{T}^{\rm heavy}$ only acts on the heavy quark part of $|r,\psi^{\rm opt}_{\rm fast,r}(r)\rangle$, but not on the fast degree of freedom part.

Then consider the second piece in Eq. (3.31). Recall that the derivative in the second piece acting both explicitly on $\phi_{\rm slow}$ and implicitly on $\psi^{\rm opt}_{\rm fast,r}$. To make it

clear, we write it in the tensor product form as:

$$\begin{aligned}\partial_r^2|\phi_{\rm slow},\psi^{\rm opt}_{\rm fast,r}\rangle &= \left(\partial_r^2|\phi_{\rm slow}\rangle\right)\otimes|\psi^{\rm opt}_{\rm fast,r}\rangle+\\ &2\left(\partial_r|\phi_{\rm slow}\rangle\right)\otimes\left(\partial_r|\psi^{\rm opt}_{\rm fast,r}\rangle\right)+|\phi_{\rm slow}\rangle\otimes\left(\partial_r^2|\psi^{\rm opt}_{\rm fast,r}\rangle\right)\ .\end{aligned} \tag{3.33}$$

In the first term, the derivative only acts on heavy quarks' state $|\phi_{\rm slow}\rangle$, which is the same as Eq. (3.32) of $\hat{T}^{\rm heavy}$ but with a different sign. Thus, this first term cancels with $\hat{T}^{\rm heavy}$.

In the third term of Eq. (3.33), the derivative only acts on $|\psi^{\rm opt}_{\rm fast,r}\rangle$. Recall that the characteristic scale of the fast degree-of-freedom is of order Λ. The contribution of this term to Eq. (3.31) of H is of order $\mathcal{O}\left(\frac{\Lambda^2}{m_Q}\right)$, which in the heavy quark mass limit should be neglected in our discussion as mentioned before.

Thus, only the contribution from the second term in Eq. (3.33) survives in Eq. (3.31):

$$\begin{aligned}\hat{H}_I|\phi_{\rm slow},\psi^{\rm opt}_{\rm fast,r}\rangle &= -\left(\hat{T}^{\rm heavy}+\frac{\partial_r^2}{M_Q}\right)|\phi_{\rm slow},\psi^{\rm opt}_{\rm fast,r}\rangle\\ &= -\frac{1}{m_Q}\left(\partial_r|\phi_{\rm slow}\rangle\right)\otimes\left(\partial_r|\psi^{\rm opt}_{\rm fast,r}\rangle\right)\ ,\end{aligned} \tag{3.34}$$

up to corrections of order $\left(\frac{\Lambda^2}{m_Q}\right)$.

Now we can evaluate the formula of decay width Eq. (3.23).

$$\Gamma_j = \frac{2}{m_Q^2} \int dr_1 dr_2 \left(\partial_{r_1} \langle \phi_{\rm slow,j}|\right) \otimes \left(\partial_{r_1} \langle \psi^{\rm opt}_{\rm fast,r}|\right) \hat{G}(E) \left(\partial_{r_2} |\phi_{\rm slow,j}\rangle\right) \otimes \left(\partial_{r_2} |\psi^{\rm opt}_{\rm fast,r}\rangle\right)$$

(3.35)

Introduce $X = (r_1 + r_2)/2$, $x = r_1 - r_2$. Note that, both r_1 and r_2 are dummy variable stand for separation between heavy quarks. Then,

$$\Gamma_j = \frac{1}{m_Q^2} \int_0^{X_m(B)} dX \int_{-2X}^{2X} dx\, \phi'_{\rm slow,j}(X - x/2)^* K(X, x; -B) \phi'_{\rm slow,j}(X + x/2) \times \left(1 + \mathcal{O}\left(\frac{\Lambda}{m_Q}\right)\right) ,$$

$$K(X, x; -B) \equiv \left(\langle X - x/2| \otimes \partial_X \langle \psi^{\rm opt}_{\rm fast,r}(X - x/2)|\right) \hat{G}(E) \left(|X + x/2\rangle \otimes \partial_X |\psi^{\rm opt}_{\rm fast,r}(X + x/2)\rangle\rangle\right) ,$$

(3.36)

where the prime indicates differentiation. The upper bound of the X integral, $X_m(B)$, is defined implicitly through:

$$V(X_m(B)) = -(B + m_\pi). \tag{3.37}$$

$X_m(B)$ is of order Λ^{-1} even if B is arbitrarily small because of the m_π in this equation.

The scaling of $K(X, x; E)$ is

$$K(X,x;E) = \sqrt{m_Q\Lambda^3}\ \kappa\left(X\Lambda, x\sqrt{m_Q\Lambda}, \frac{E}{\Lambda}\right) \tag{3.38}$$

$$K(X,x;E) \sim \mathcal{O}\left(\sqrt{m_Q\Lambda^3}\ E^{-a\sqrt{m_Q\Lambda}}\right) \ \text{ with } \ a>0$$

$$\text{when } \ V(X \pm x/2) + m_\pi > E \tag{3.39}$$

where κ is a dimensionless function of dimensionless variables.

$K(X,x;E)$ characterizes the response of the fast degrees of freedom for given values of the slow degrees of freedom; hence the dependence on E, will go as E/Λ (rather than E/m_Q). The dependence on x can be seen from the fact that $\hat{G}(E)$ has the heavy quark kinetic energy in the denominator. In the absence of that term in the denominator or when $m_Q \to \infty$, the dependence on x would necessarily be a δ-function (because of energy conservation factor $\delta(E_i - E_f)$ in Fermi's Golden rule). Moreover, the only place that m_Q enters in $K(X,x;E)$ is in the kinetic energy term. The presence of that term spreads out the dependence on $x = r_1 - r_2$, because the kinetic energy can take a continuous range of values. Since the conjugate space of x is momentum space, the dependence must scale as $x\sqrt{m_Q\Lambda}$ (where $\sqrt{m_Q\Lambda}$ is the characteristic momentum scaling in semiclassical regime). The dependence on X can be seen by integrating K with respect to X and x, yielding a result independent of m_Q. This is because when there is no m_Q-dependence or when $m_Q \to \infty$, the result is independent of m_Q. Since now we are working in expansions around $m_Q \to \infty$, the leading order result after integration should be independent of m_Q. Finally, the overall factor of $\sqrt{m_Q\Lambda^3}$ is obtainable from dimensional analysis

and the disappearance of m_Q once one integrates over X and x. Note that Eq. (3.38) implies that there are only substantial contributions to Γ_j from regions in which $x \sim \mathcal{O}\left((m_Q\Lambda)^{-1/2}\right)$, *i.e.* x is parametrically small.

In order to know the scaling of Γ, one also needs to know the scaling of $\phi_{\text{slow,j}}$. The system is in semiclassical regime. The classically allowed region, where $\phi_{\text{slow,j}}$ is away from the turning points, is the region of dominant contributions. In this region, according to the WKB approximation,ϕ can be approximated by:

$$\begin{aligned} \frac{\phi_{\text{slow,j}}(r)}{\mathcal{N}} &= \frac{\Lambda^{\frac{3}{4}}\sin\left(\delta_j(r)\right)}{\left(E_j - V(r)\right)^{\frac{1}{4}}}\,, \\ \delta_j(r) &\equiv \int_0^r dr' \sqrt{M_Q(E_j - V(r'))} \end{aligned} \tag{3.40}$$

where $\mathcal{N}$ is a dimensionless normalization constant:

$$\mathcal{N} = \left(\frac{\Lambda^{\frac{3}{2}}}{2}\int_0^{r_B} \frac{dr'}{\sqrt{E_j - V(r')}}\right)^{-\frac{1}{2}} \tag{3.41}$$

r_B is the turning point: $V(r_B) = E_j$.

$V(r)$ is of order $\mathcal{O}(\Lambda)$, and in general independent of m_Q. Thus,

$$\delta_j(r) = \sqrt{\frac{m_Q}{\Lambda}}\tilde{\delta}_j(r\Lambda) \tag{3.42}$$

where $\tilde{\delta}$ is dimensionless.

For tetraquark state with binding energy of order Λ below threshold, $\mathcal{N}$ is independent of m_Q, and of order unity.

Then let us look at the derivative of $\phi_{\text{slow,j}}$:

$$\phi'_{\text{slow,j}}(X \pm \frac{x}{2}) = -\mathcal{N}\left(\Lambda^3 m_Q^2 (E_j - \Lambda v(\Lambda X))\right)^{\frac{1}{4}} \cos\left(\sqrt{\frac{m_Q}{\Lambda}}\tilde{\delta}_j\left((X \pm \frac{x}{2})\Lambda\right)\right) \tag{3.43}$$

Insert ϕ' back to Γ's expression Eq. (3.36), one gets:

$$\Gamma_j = \frac{|\mathcal{N}|^2 \Lambda^{\frac{3}{2}}}{m_Q} \int_0^{X_m(B)} dX \left(E_j - \Lambda v(\Lambda X)\right)^{\frac{1}{2}} k_j(X, B) \times \left(1 + \mathcal{O}\left(\frac{\Lambda}{m_Q}\right)\right), \tag{3.44}$$

where $k_j(X, B)$ is defined as:

$$\begin{aligned} k_j(X, B) \equiv \sqrt{m_Q \Lambda^3} \int_{-\frac{X}{2}}^{\frac{X}{2}} dx\, \kappa\left(X\Lambda, x\sqrt{m_Q \Lambda}, -\frac{B}{\Lambda}\right) \\ \times \cos\left(\sqrt{\frac{m_Q}{\Lambda}}\tilde{\delta}_j\left((X - \frac{x}{2})\Lambda\right)\right) \cos\left(\sqrt{\frac{m_Q}{\Lambda}}\tilde{\delta}_j\left((X + \frac{x}{2})\Lambda\right)\right) \end{aligned} \tag{3.45}$$

In the expression of $k_j(X, B)$, the cosines are bounded by unity, and the integral over x yields a factor of $\frac{1}{\sqrt{m_Q \Lambda}}$, which cancels with the m_Q dependence in the factor $\sqrt{m_Q \Lambda^2}$ before integral. Thus, $k_j(X, B)$ is of order unity or less in a $\frac{\Lambda}{m_Q}$ expansion.

Since $\mathcal{N}$ is of order unity given that the tetraquark under consideration is order $\mathcal{O}(\Lambda)$ below threshold, it is easy to see that $\Gamma_j \sim \frac{\Lambda^2}{m_Q}$. Thus, the scaling in Eq. (3.14) is proved.

Therefore, we have shown model-independently that, in the heavy quark mass limit, there exist many barometrically narrow tetraquark resonances. Though the demonstration is for specific quantum numbers, the same argument is true for any

attractive channel as discussed in Section 3.2.2.

3.4 Near-threshold tetraquarks

The discussion in the previous section is for tetraquarks with binding energy of order $\mathcal{O}(\Lambda)$. The purpose of the current section is to extend the discussion to near-threshold tetraquarks with binding energy B that is parametrically decreasing with m_Q.

As discussed in Section 3.2.1, for near-threshold scenario, let us consider binding energy scales as:

$$B \lesssim \frac{\Lambda^{2-\epsilon}}{M_Q^{1-\epsilon}} \quad \text{for any } \epsilon \text{ with } 0 < \epsilon < 1 \,, \tag{3.46}$$

where b is a dimensionless numerical constant of order unity and $0 < \epsilon \leq 1$. The number of tetraquarks with binding energy smaller than B is $n_b > b\,(M_Q/m_\pi)^{\epsilon/2}$, which grows as m_Q increases. This means there are still a large number of tetraquarks, and the system is also in semi-classical limit.

Thus, most parts of the semi-classical analysis in the previous section are still valid here except for the scaling of some quantities discussed below.

The energy level spacing ΔE is changed since the density of states in near threshold region is higher than the density of states in region that is order $\mathcal{O}(\Lambda)$ below threshold.

$$\Delta E \sim \frac{B}{n_b} \sim \frac{\Lambda^{2-\frac{\epsilon}{2}}}{m_Q^{1-\frac{\epsilon}{2}}} \tag{3.47}$$

The derivation of the scaling of $\mathcal{N} = \left(\frac{\Lambda^{\frac{3}{2}}}{2}\int_0^{r_B}\frac{dr'}{\sqrt{E_j - V(r')}}\right)^{-\frac{1}{2}}$ with $V(r_B) = E_j$ is complicated. The integral region can be divided to three parts, which have different characteristic behaviors. We then write the full integral as the sum of these three parts: $I \equiv \int_0^{r_B}\frac{dr'}{\sqrt{E_j - V(r')}} = I_I + I_{II} + I_{III}$.

These three regions are separated by the behaviors of the potential $V(r)$, so that we need to approximate it in three different ways. For the near threshold states we are interested in, $B \lesssim \frac{\Lambda^{2-\epsilon}}{M_Q^{1-\epsilon}}$. Recall that in the discussion below Eq. (3.22), we have said that E is defined relative to the threshold. Let us focuses on $B \sim \frac{\Lambda^{2-\epsilon}}{M_Q^{1-\epsilon}}$, then the eigenenergy $E_j \sim \frac{\Lambda^{2-\epsilon}}{M_Q^{1-\epsilon}}$.

In denominator, whether E_j is comparable to $V(r)$ would greatly influence the scaling of the integrand, so we define Region I as from $r = 0$ to $r = r_1$, where r_1 is defined as the the lower end of the region where $V(r)$ is of order $\frac{\Lambda^{2-\epsilon}}{M_Q^{1-\epsilon}}$. From the long range Yukawa-like form potential such as Eq. (3.3), it is clear that $r_1 \sim 1/\Lambda$. In most of the region, the denominator is dominated by $V(r) \sim \Lambda$, so the integrand is of order $\frac{1}{\Lambda^{1/2}}$; while near r_1, the integrand is of order $\frac{m_Q^{1/2-\epsilon/2}}{\Lambda^{1-\epsilon/2}}$. Thus, $\frac{1}{\Lambda^{3/2}} \lesssim I_I \lesssim \frac{m_Q^{1/2-\epsilon/2}}{\Lambda^{2-\epsilon/2}}$.

Next, define r_2 as the lower end of the Region III, which is close to the turning point at r_B that $V(r)$ is well-approximated by $V(r_B) + V'(r_B)(r - r_B)$. It is easy to see from the form of $V(r)$ that $r_B \sim 1/\Lambda$, $r_2 \sim 1/\Lambda$, $r_B - r_2 \sim 1/\Lambda$, $\tilde{V}'(r_B) \sim \frac{\Lambda^{3-\epsilon}}{m_Q^{1-\epsilon}}$. Then $I_{III} \sim (r_B - r_2)\sqrt{\frac{1}{V'(r_B)(r_B - r_2)}} \sim \frac{m_Q^{1/2-\epsilon/2}}{\Lambda^{2-\epsilon/2}}$.

Then, region II is the region between r_1 and r_2. The length of this region is still $r_2 - r_1 \sim 1/\Lambda$, and the integrand is of order $\frac{1}{\Lambda^{1-\epsilon/2}}$, so $I_{II} \sim \frac{m_Q^{1/2-\epsilon/2}}{\Lambda^{2-\epsilon/2}}$.

Combine the three results: $I = I_I + I_{II} + I_{III} \sim \frac{m_Q^{1/2-\epsilon/2}}{\Lambda^{2-\epsilon/2}}$, which in turn gives

$\mathcal{N} = (\frac{\Lambda^{\frac{3}{2}}}{2} I)^{-\frac{1}{2}} \sim \frac{\Lambda^{1/4-\epsilon/4}}{m_Q^{1/4-\epsilon/4}}$.

Finally, $\Gamma \sim \frac{|\mathcal{N}|^2 \Lambda^2}{m_Q} \sim \frac{\Lambda^{\frac{5}{2}-\frac{\epsilon}{2}}}{m_Q^{\frac{3}{2}-\frac{\epsilon}{2}}}$. Then, for near threshold tetraquark with binding energy $B \sim \frac{\Lambda^{2-\epsilon}}{M_Q^{1-\epsilon}}$, we have $\frac{\Gamma}{\Delta E} \sim \sqrt{\frac{\Lambda}{m_Q}}$ which is the same as the generic case with $B \sim \Lambda$ in Eq. (3.16) of previous section.

3.5 Summary

This chapter has been focused on doubly heavy tetraquark with $q\bar{q}'Q\bar{Q}$ configuration. While there already exists arguments on the existence of $q\bar{q}'Q\bar{Q}$ tetraquark in the heavy quark mass limit[217, 218], the work in this chapter showed in a model-independent way that, in the heavy quark mass limit, many parametrically narrow $q\bar{q}'Q\bar{Q}$ tetraquark states exist, and many of them are parametrically close to threshold.

This work is not directly related to experiments, since $q\bar{q}'Q\bar{Q}$ near-threshold tetraquark has not been observed. Moreover, the charm quark mass and bottom quark mass are too small for the extreme heavy quark mass limit regime used in here to be valid. However, this work is still of theoretical interest, since it offers insight into near-threshold doubly heavy tetraquark systems, and the regime set up in this section can be extended to $q\bar{q}'Q\bar{Q}$ tetraquark system, which is of more phenomenological relevance and will be discussed in next chapter.

Chapter 4: Tetraquarks in the heavy quark mass limit: $q\bar{q}'Q\bar{Q}$

In the previous chapter, we have shown that in the heavy quark mass limit, there exist $\bar{q}\bar{q}'QQ$ tetraquark narrow resonances, with binding energy of order $\mathcal{O}(\Lambda)$ and $\frac{\Lambda^{2-\epsilon}}{M_Q^{1-\epsilon}}$ $(0 < \epsilon < 1)$, given that at a long distance the interaction between the two heavy quarks is attractive Yukawa-like interaction.

The purpose of this section is to use similar formalism to show the existence of large angular momentum $q\bar{q}'Q\bar{Q}$ tetraquark narrow resonance in the heavy quark limit.

4.1 Logic of this work

The analysis in the previous chapter for $\bar{q}\bar{q}'QQ$ type tetraquark cannot be directly used to proof the existence of $q\bar{q}'Q\bar{Q}$ type tetraquark. A $q\bar{q}'Q\bar{Q}$ tetraquark can decay to a more deeply bounded $q\bar{q}'Q\bar{Q}$ tetraquark through emission of pions, which is similar to the $\bar{q}\bar{q}'QQ$ tetraquark, so the same analysis can be used to deal with this decay channel. However, $q\bar{q}'Q\bar{Q}$ has an extra difficulty caused by a rearrange effect, which was not an issue in the previous $\bar{q}\bar{q}'QQ$ case. In this case, the $q\bar{q}'Q\bar{Q}$ can decay into heavy quarkonium plus one or more light meson, which renders the regime in the previous chapter invalid.

If one can show that this decay to heavy quarkonium channel is suppressed by heavy quark mass under certain regimes, then $q\bar{q}'Q\bar{Q}$ will exist as narrow resonance in the heavy quark mass limit.

It is useful to take a look at the spectrum of the $q\bar{q}'Q\bar{Q}$ tetraquark system. Consider the separation r between heavy quark Q and heavy anti-quark $\bar{Q}$. When r is very large, it is easy to see that the $q\bar{q}'Q\bar{Q}$ system will look like a bound state of heavy meson and heavy anti-meson. This is similar to the case in the previous chapter since there are many narrow tetraquark resonances, the spectrum of the light degrees of freedom is gapped. However, at a very short distance, Q and $\bar{Q}$ are close to each other and forms a heavy quarkonium, and the whole system may decay to heavy quarkonium plus one or more light mesons. Since the light meson can carry a continuous range of energy, the spectrum of the light degrees of freedom in this region is gapless.

The logic of this chapter is: at first we make some assumptions so that the potential description is valid, then we will prove the tetraquarks states exist, and the assumptions are indeed valid. Thus, the analysis is self-consistent.

In the heavy quark mass limit, we make the following assumptions:

- The system stays in the gapped region and away from the gapless region. Thus, the system will not decay into heavy quarkonium plus one or more light mesons.

- There exist many tetraquarks in this region, so that semi-classical analysis can be used.

- These tetraquarks' decay width is parametrically narrower than the energy level spacing. Thus, in the heavy quark mass limit, the potential description is valid, and one can use Schrödinger equation description.

- The separation r of Q and $\bar{Q}$ in these states are large enough so that Yukawa-like potential dominants, which will be used to prove the existence of many tetraquark narrow resonances.

It is easy to see that the most important part is to show the wave function of the system stays away from the gapless region and with r large enough so that Yukawa-like potential is valid. Then one can use an analysis the same as the previous chapter to prove our arguments.

Denote the potential as $V(r)$, which depends on a single degree-of-freedom r that is the distance between heavy quark and heavy anti-quark. The key point is to notice that $V(r)$ may have a potential well for a system with certain angular momentum L. Bounds states must exist inside this potential well in the heavy quark mass limit. If the location of the potential well r_{well} is at the gapped domain, the tunneling rate of wave function centered at this well to gapped region will be parametrically suppressed by m_Q. If at r_{well}, the potential is indeed Yukawa-like, then all the previous assumptions are indeed true, and the proof is self-consistent.

In the next section, we will use these assumptions to show that in the heavy quark mass limit, with large but not too large angular momentum L, many tetraquark states exists at r_{well} as large as $\frac{\phi}{m_\pi} \approx 2.28\,\text{fm}$, where ϕ stands for the golden ratio $\phi \approx 1.618$. With such a long separation between heavy quark and heavy anti-

quark, the Yukawa potential is expected to be dominant because of phenomenological knowledge of nucleon-nucleon potential[224], and the system is expected to be in a gapped domain. Thus, as in the previous chapter, the analysis is self-consistent and many tetraquark states exist as resonances parametrically narrow in m_Q.

4.2 Existence of the potential well

The goal of this section is to show that in the heavy quark mass limit, based on the assumptions in the previous section, a potential well with a minimum in the gapped region exists for channels with large but not too large angular momentum. This in turns leads to the existence of many tetraquark states in this potential well at a proper location.

As mentioned in the assumption, the potential $V(r)$ is Yukawa-like at large distances. Notice that when angular momentum L is large, the centrifugal term $\frac{1}{\mu}\frac{l(l+1)}{r^2}$ matters, which creates a centrifugal barrier. For large angular momentum, there may be a tensor force and mixing channel effects, but as discussed in the previous chapter, one can still reduce the problem to a single degree-of-freedom up to corrections that can be neglected in the heavy quark mass limit.

Generally, at long distance r, the potential is written as:

$$V(r) = -a\frac{e^{-m_\pi r}}{r} + \frac{l(l+1)}{2M_Q r^2}, \tag{4.1}$$

where a is a constant coefficient, and M_Q is the mass of heavy meson. M_Q is equal to the heavy quark mass m_Q with whose relative size corrections vanishes in the

heavy quark limit.

Let us think about the two terms in this potential. Denote

$$V(r) = -V_Y(r) + V_L(r) \tag{4.2}$$
$$V_Y(r) = a\frac{e^{-m_\pi r}}{r}$$
$$V_L(r) = \frac{l(l+1)}{2M_Q r^2}$$

Since V_L should be comparable to V_Y in the area we are interested in, it is clear that the angular momentum should scale as $L \sim \sqrt{m_Q}$. Otherwise, V_L is negligible in the heavy quark mass limit.

Generally, the functions look like Fig. 4.1, where the region for small r is not plotted, since the Yukawa form is only dominant when r is large enough, and the potential description is not valid when r is too small.

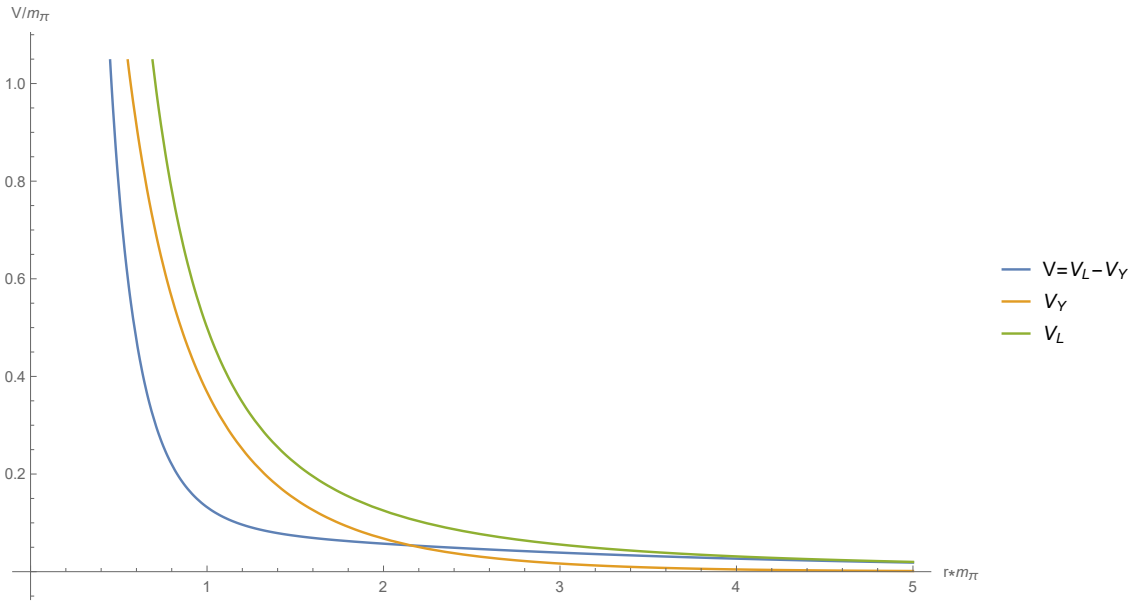

Figure 4.1: A potential without a minimum.

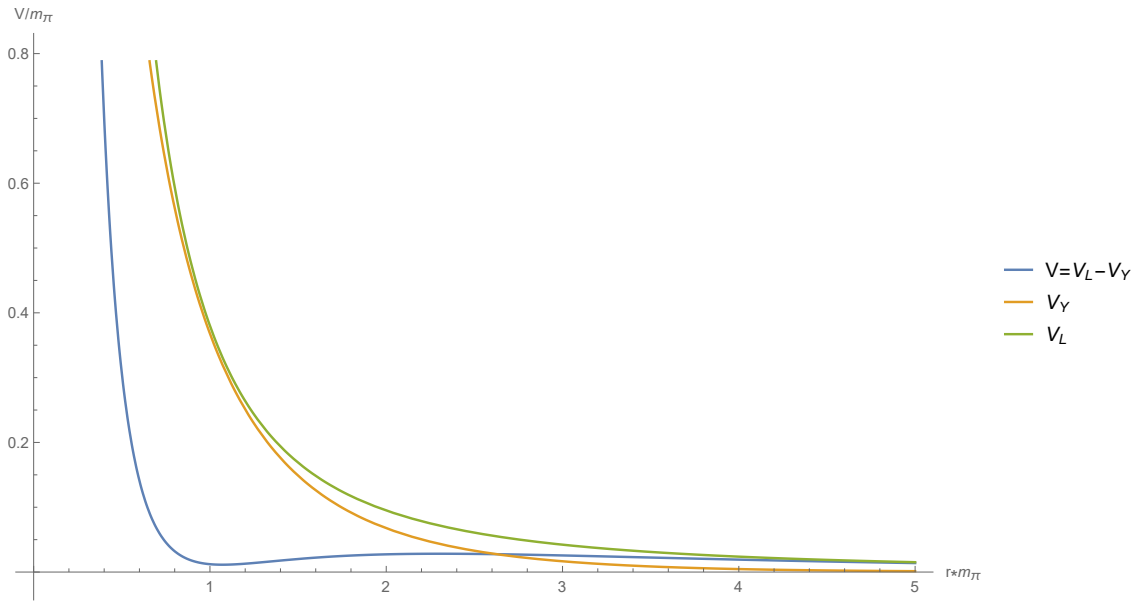

Figure 4.2: A potential with a potential well.

V_Y decreases exponentially in r, while V_L decreases polynomially in r. Potential well is a local minimum, so we should consider the derivative of the potential $V'(r) = V'_L(r) - V'_Y(r)$, and find where it equals 0, as shown in the Fig.4.2. Both $V'_L(r)$ and $V'_Y(r)$ are negative. When r is extremely large, $|V'_Y(r)| < |V'_L(r)|$ so $V'(r) < 0$. When r is not very large, it is possible that, $|V'_Y(r)| < |V'_L(r)|$ is always true as in Fig.4.3, such that there is no local minimum in the domain we are interested in. However, it is also possible that, $|V'_Y(r)| > |V'_L(r)|$ for not very large r, then one can find a potential well with a minimum centered at location r_{well} such that $V'(r_{\text{well}}) = 0$ and $V''(r_{\text{well}}) < 0$.

Whether the local minimum exists is determined by the relative size of the coefficients of these two potential terms, which can be arbitrarily tuned by fixing the angular momentum L. Although L is discrete in the heavy quark mass limit, the coefficient $\frac{l(l+1)}{2M_Q}$ can be arbitrarily close to any positive value when proper angular

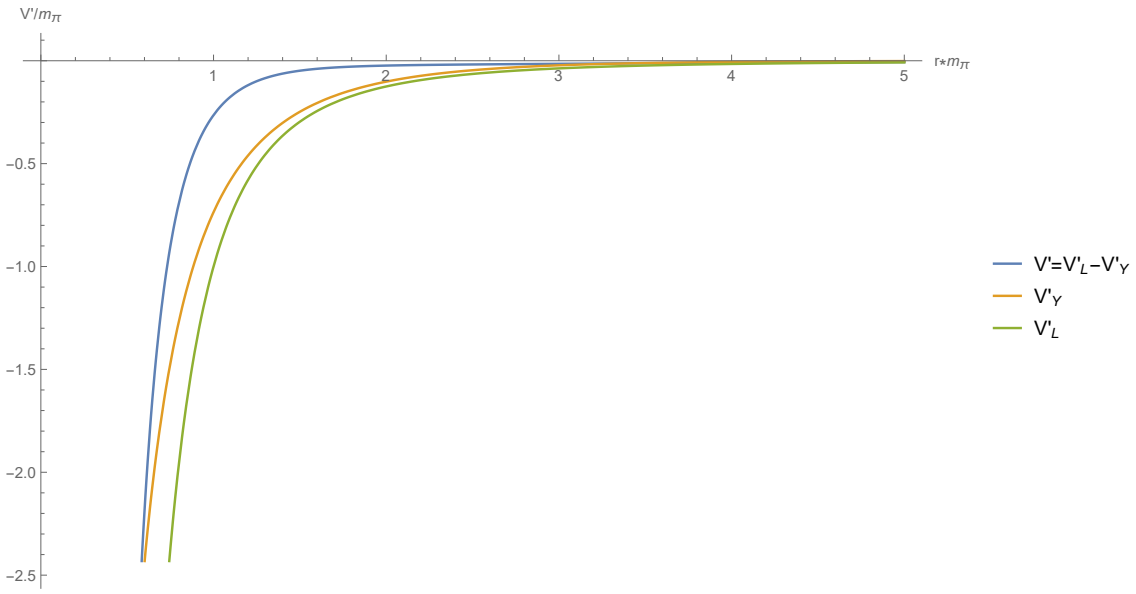

Figure 4.3: The derivative of potential terms when there is no potential well.

momentum $l \sim \sqrt{m_Q}$ is taken.

As the basic feature of the Schrödinger equation, when the mass approaches infinity, if a potential well exists, no matter how shallow the potential well is, there must exist a large number of bound states. This means, in the heavy quark limit, the semi-classical analysis can be used.

If we can show there exist r_{well} that is far away from the gapless region of the energy spectrum, then the system is exponentially hard to tunnel to the gapless domain because of simple quantum mechanics argument. Moreover, there is another reason we want r_{well} to be large: the Yukawa-like potential is not dominant when Q is too close to $\bar{Q}$.

Therefore, the question now becomes finding the local minimum point $r_{\text{well}}(a, l)$ of Eq.4.1, and tuning l to obtain the maximum value of $r_{\text{well}}(a, l)$.

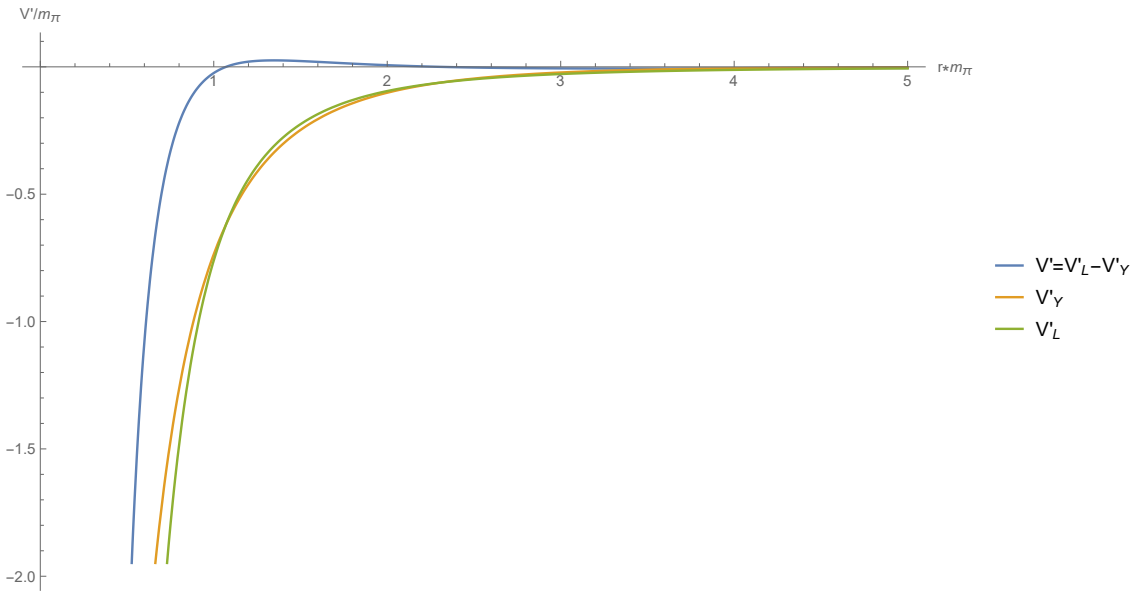

Figure 4.4: The derivative of potential terms when there is a potential well.

We rewrite Eq.4.1 in dimensionless form as:

$$f(t) \equiv \frac{V(\frac{t}{m_\pi})}{am_\pi} = -\frac{e^{-t}}{t} + \frac{k}{t^2}, \tag{4.3}$$

where $t \equiv m_\pi r$ and $k \equiv \frac{l(l+1)m_\pi}{2am_Q}$. When m_Q is large enough, by varying l, k can be arbitrarily close to any positive value.

Denote $t_{\min}(k) \equiv m_\pi r_{\text{well}}$ as the position of minimum point of $f(t)$, and denote the largest value of $t_{\min}(k)$ as t_{optimal},

$$t_{\text{optimal}} \equiv \max_{k\in(0,\infty)} \{t_{\min}(k)\} = \max_{k\in(0,\infty)} \{\arg\min_{t\in(0,\infty)} f(t)\} \tag{4.4}$$

After solving this optimization problem, one can find $t_{\text{optimal}} = \phi \equiv \frac{1+\sqrt{5}}{2}$, which happens to be the famous golden ratio, with corresponding $k \approx 0.42$. Thus, the largest r_{well} is $r_{\text{optimal}} \equiv \frac{t_{\text{optimal}}}{m_\pi} \approx 2.28\,\text{fm}$.

At $r_{\text{optimal}} > 2\,\text{fm}$, Q is far away from $\bar{Q}$, such that the system looks like a hadronic molecular of heavy meson and heavy anti-meson. Thus the system is in the gapped domain, whose upper end is around $r_{\text{gapless}} \sim 1/\Lambda$, where Λ is the typical hadronic scale. Also, the previous assumption that the Yukawa potential is dominant over the short distance interaction is expected to be valid because of phenomenological knowledge of nucleon-nucleon potential[224]. This will hold except in unnatural models where the short distance interaction is exceptionally large at such long distance.

Even if the one-pion-exchange Yukawa-like interaction is not dominant because of exceptionally strong short-distance interaction, the final argument about the existence of tetraquark still holds, provided the correction to the potential is small so that the exact location of the potential well r_{well} is still inside the gapped regime.

Since the possibility that the system tunnels to gapless domain can be neglected in the heavy quark mass limit, the system will not decay into heavy quarkonium plus one or more light mesons.

The tetraquark can still decay to a more deeply bounded tetraquark in the same potential well by emission of pions. This may render the Schrödinger equation description invalid. However, one can follow the same analysis as in the previous section, to show that, though these tetraquarks are not stable due to pion emission, their width is parametrically narrower than the energy level spacing. Thus, a large number of $q\bar{q}'Q\bar{Q}$ narrow resonances exist in the potential well.

4.3 Summary

This chapter has been focused on tetraquark with one heavy quark and one heavy anti-quark. It is shown that $q\bar{q}'Q\bar{Q}$ narrow resonances with appropriate large angular momentum exist in the extreme heavy quark mass limit. While there has been much experimental evidence of $q\bar{q}'Q\bar{Q}$ states, these observed states haven't known with large momentum configuration. The deviation between this theoretical work and the reality may well be a consequence of that the heavy quark mass in the real world is not sufficiently heavy for the arguments in this chapter to hold. However, this work may still shed light on the understanding of tetraquarks' structure of this type.

Chapter 5: Overall summary

Lattice QCD method and finding new systematic expansion regimes are two important approaches to handle non-perturbative QCD problems. The main body of this dissertation consists of three works related to these approaches.

In Chapter 2, we explored a subtle relationship between the infinite volume limit and the sign problem in the context of gauge theories with a θ-term. When the energy density function $\varepsilon(\theta)$ has a point of inflection between $-\pi$ and π, in certain regions one cannot obtain the correct $\varepsilon(\theta)$ from $\tilde{\varepsilon}(q)$, which is the infinite volume limit of $\tilde{\varepsilon}(q, V)$, via direct summation. This shows the severity of the sign problem. As a result, high accuracy of $\tilde{\varepsilon}(q, V)$ is required in order to not spoil the cancellation among different topological sectors. However, there exist regions where $\tilde{\varepsilon}(q)$ is sufficient to obtain $\varepsilon(\theta)$ by direct summation. This is remarkable because there are power-law differences in the volume between $\tilde{\varepsilon}(q, V)$ and $\tilde{\varepsilon}(q)$, which could have spoiled the summation. The reason why $\tilde{\varepsilon}(q)$ turns out to be sufficient in these regions can be explained using the saddle point approximation method. When V is large, the sum over topological sectors can be written as a sum of integrals, which is dominated by a single integral. This single integral may be approximated by a saddle point or a branch point. While this analysis has focused on a theoretical

issue, it may be helpful to extracting information about $\varepsilon(\theta)$ from practical lattice calculations.

In Chapter 3, we focused on tetraquarks containing two heavy quarks. While it has long been known that deeply bound tetraquarks must exist in the heavy quark limit of QCD[217, 218], this work showed that many parametrically narrow tetraquarks that are parametrically close to the threshold also must exist in this limit. A framework based on systematic expansions in terms of $1/m_Q$ is developed to analyze heavy tetraquarks. The full QCD Hamiltonian in the sector of the exotic quantum numbers can be decomposed into a piece describable via the Schrödinger equation and a remainder. The former can be used to deduce the existence of near-threshold tetraquarks in this circumstance. The remainder turns the exotic bound states into parametrically narrow resonances. While the result obtained here may be of theoretical interest, it is of limited direct phenomenological relevance because tetraquarks with two heavy quarks have yet to be observed experimentally. This may be because they are much less likely to form than tetraquarks containing a heavy quark and a heavy antiquark in particle experiments. It is also possible that charm or even bottom quarks are not sufficiently heavy for the bound states to form. However, the result here minimally shows that near-threshold narrow exotic hadron resonances can arise naturally in QCD when quarks are heavy enough.

In Chapter 4, we focused on tetraquarks containing a heavy quark and a heavy antiquark. Unlike the problem in the previous chapter where the strong interaction width of the tetraquarks arises solely due to channels in which the decay is into light mesons plus more deeply bound tetraquarks, the tetraquarks considered in Chapter

4 can also decay into light mesons plus heavy quarkoniums. This new decay channel is shown to be suppressed in the extreme heavy quark mass limit if there exists a potential well in the appropriate region. As an example, $q\bar{q}'Q\bar{Q}$ narrow resonances with a proper large angular momentum must exist in the extreme heavy quark mass limit. However, so far, none of $q\bar{q}'Q\bar{Q}$ candidates seen in experiments has a large angular momentum. It may be because the heavy quark mass is not large enough in the real world for this scenario to be valid. Nevertheless, this work provides insight into the relationship between the existence of tetraquarks in QCD and the heavy quark mass limit.

Bibliography

[1] Feng-Kun Guo, Christoph Hanhart, Ulf-G Meißner, Qian Wang, Qiang Zhao, and Bing-Song Zou. Hadronic molecules. *Reviews of Modern Physics*, 90(1):015004, 2018.

[2] Stephen Lars Olsen. Qcd exotics. *Hyperfine Interactions*, 229(1-3):7–20, 2014.

[3] Masaharu Tanabashi, K Hagiwara, K Hikasa, K Nakamura, Y Sumino, F Takahashi, J Tanaka, K Agashe, G Aielli, C Amsler, et al. Review of particle physics. *Physical Review D*, 98(3):030001, 2018.

[4] David Griffiths. *Introduction to elementary particles*. John Wiley & Sons, 2008.

[5] Arthur Jaffe and Edward Witten. Quantum yang-mills theory. *The millennium prize problems*, 1, 2006.

[6] David J Gross and Frank Wilczek. Ultraviolet behavior of non-abelian gauge theories. *Physical Review Letters*, 30(26):1343, 1973.

[7] Kenneth G Wilson. Confinement of quarks. *Physical review D*, 10(8):2445, 1974.

[8] G Peter Lepage. Lattice qcd for novices. *Strong Interactions at Low and Intermediate Energies*, pages 49–90, 1998.

[9] Holger Bech Nielsen and Masao Ninomiya. No-go theorum for regularizing chiral fermions. Technical report, Science Research Council, 1981.

[10] Roberto Frezzotti, Pietro Antonio Grassi, Stefan Sint, Peter Weisz, Alpha Collaboration, et al. Lattice qcd with a chirally twisted mass term. *Journal of High Energy Physics*, 2001(08):058, 2001.

[11] Leonard Susskind. Lattice fermions. *Physical Review D*, 16(10):3031, 1977.

[12] Paul H Ginsparg and Kenneth G Wilson. A remnant of chiral symmetry on the lattice. *Physical Review D*, 25(10):2649, 1982.

[13] Peter Hasenfratz, Victor Laliena, and Ferenc Niedermayer. The index theorem in qcd with a finite cut-off. *Physics Letters B*, 427(1-2):125–131, 1998.

[14] Martin Lüscher. Exact chiral symmetry on the lattice and the ginsparg-wilson relation. *Physics Letters B*, 428(3-4):342–345, 1998.

[15] David B Kaplan. A method for simulating chiral fermions on the lattice. *arXiv preprint hep-lat/9206013*, 1992.

[16] Yigal Shamir. Chiral fermions from lattice boundaries. *Nuclear Physics B*, 406(1-2):90–106, 1993.

[17] Yigal Shamir. Anomalies and chiral defect fermions. *Nuclear Physics B*, 417(1-2):167–180, 1994.

[18] W Keith Hastings. Monte carlo sampling methods using markov chains and their applications. 1970.

[19] Nicholas Metropolis, Arianna W Rosenbluth, Marshall N Rosenbluth, Augusta H Teller, and Edward Teller. Equation of state calculations by fast computing machines. *The journal of chemical physics*, 21(6):1087–1092, 1953.

[20] G Parisi. Common trends in particle and condensed matter physics. proceedings, winter advanced study institute. *Les Houches, France*, 1983.

[21] G Peter Lepage. The analysis of algorithms for lattice field theory. Technical report, 1989.

[22] William Detmold, Silas Beane, Konstantinos Orginos, and Martin Savage. Nuclear physics from lattice qcd. *Progress in Particle and Nuclear Physics*, 66(JLAB-THY-10-1166; DOE/OR/23177-1484; arXiv: 1004.2935), 2011.

[23] Gerard 't Hooft. A planar diagram theory for strong interactions. In *The Large N Expansion In Quantum Field Theory And Statistical Physics: From Spin Systems to 2-Dimensional Gravity*, pages 80–92. World Scientific, 1993.

[24] Gerard 't Hooft. A two-dimensional model for mesons. In *The Large N Expansion In Quantum Field Theory And Statistical Physics: From Spin Systems to 2-Dimensional Gravity*, pages 94–103. World Scientific, 1993.

[25] Edward Witten. Baryons in the 1n expansion. *Nuclear Physics B*, 160(1):57–115, 1979.

[26] Edward Witten. Large n chiral dynamics. *Annals of Physics*, 128(2):363–375, 1980.

[27] Edward Witten. Instatons, the quark model, and the 1/n expansion. *Nuclear Physics B*, 149(2):285–320, 1979.

[28] Gabriele Veneziano. U (1) without instantons. *Nuclear Physics B*, 159(1-2):213–224, 1979.

[29] Steven Weinberg. Tetraquark mesons in large-n quantum chromodynamics. *Physical review letters*, 110(26):261601, 2013.

[30] Marc Knecht and Santiago Peris. Narrow tetraquarks at large n. *Physical Review D*, 88(3):036016, 2013.

[31] GC Rossi and Gabriele Veneziano. The string-junction picture of multiquark states: an update. *Journal of High Energy Physics*, 2016(6):41, 2016.

[32] Thomas D Cohen. Quantum number exotic hybrid mesons and large nc qcd. *Physics Letters B*, 427(3-4):348–352, 1998.

[33] Thomas D Cohen and Richard F Lebed. Tetraquarks with exotic flavor quantum numbers at large n c in qcd (as). *Physical Review D*, 89(5):054018, 2014.

[34] Elizabeth Jenkins and Aneesh V Manohar. 1/n expansion for exotic baryons. *Journal of High Energy Physics*, 2004(06):039, 2004.

[35] Aneesh V Manohar. Large n qcd. *arXiv preprint hep-ph/9802419*, 1998.

[36] Sidney Coleman. *Aspects of symmetry: selected Erice lectures*. Cambridge University Press, 1988.

[37] Biagio Lucini and Marco Panero. Introductory lectures to large-n qcd phenomenology and lattice results. *Progress in Particle and Nuclear Physics*, 75:1–40, 2014.

[38] Richard F Lebed. Phenomenology of large n c qcd. *Czechoslovak Journal of Physics*, 49(9):1273–1306, 1999.

[39] Howard Georgi. Effective field theory. *Annual review of nuclear and particle science*, 43(1):209–252, 1993.

[40] Aneesh V Manohar. Effective field theories. In *Perturbative and nonperturbative aspects of quantum field theory*, pages 311–362. Springer, 1977.

[41] Antonio Pich. Effective field theory. *arXiv preprint hep-ph/9806303*, 1998.

[42] Cliff P Burgess. An introduction to effective field theory. *Annu. Rev. Nucl. Part. Sci.*, 57:329–362, 2007.

[43] Ira Z Rothstein. Tasi lectures on effective field theories. *arXiv preprint hep-ph/0308266*, 2003.

[44] Antonio Pich. Chiral perturbation theory. *Reports on Progress in Physics*, 58(6):563, 1995.

[45] Stefan Scherer. Introduction to chiral perturbation theory. In *Advances in Nuclear Physics, Volume 27*, pages 277–538. Springer, 2003.

[46] Veronique Bernard. Chiral perturbation theory and baryon properties. *Progress in Particle and Nuclear Physics*, 60(1):82–160, 2008.

[47] Véronique Bernard and Ulf-G Meißner. Chiral perturbation theory. *Annu. Rev. Nucl. Part. Sci.*, 57:33–60, 2007.

[48] Estia Eichten and Brian Russell Hill. An effective field theory for the calculation of matrix elements involving heavy quarks. *Phys. Lett.*, 234(FERMILAB-PUB-89-184-T):511–516, 1989.

[49] Howard Georgi. An effective field theory for heavy quarks at low energies. *Physics Letters B*, 240(3-4):447–450, 1990.

[50] Benjamin Grinstein. The static quark effective theory. *Nuclear Physics B*, 339(2):253–268, 1990.

[51] Thomas Mannel, Winston Roberts, and Zbigniew Ryzak. A derivation of the heavy quark effective lagrangian from qcd. *Nuclear Physics B*, 368(1):204–217, 1992.

[52] Matthias Neubert. Heavy quark symmetry. *arXiv preprint hep-ph/9306320*, 1993.

[53] Aneesh V Manohar and Mark B Wise. *Heavy quark physics*, volume 10. Cambridge university press, 2000.

[54] Nathan Isgur and Mark B Wise. Weak decays of heavy mesons in the static quark approximation. *Physics Letters B*, 232(1):113–117, 1989.

[55] Nathan Isgur and Mark B Wise. Weak transition form factors between heavy mesons. *Physics Letters B*, 237(3-4):527–530, 1990.

[56] Peter Cho. Heavy hadron chiral perturbation theory. *Nuclear Physics B*, 396(1):183–204, 1993.

[57] Tung-Mow Yan. Soft pions and heavy quark symmetry. *Chinese Journal of Physics*, 30(4):509–527, 1992.

[58] Mark B Wise. Chiral perturbation theory for hadrons containing a heavy quark. *Physical Review D*, 45(7):R2188, 1992.

[59] Gustavo Burdman and John F Donoghue. Union of chiral and heavy quark symmetries. *Physics Letters B*, 280(3-4):287–291, 1992.

[60] Tung-Mow Yan, Hai-Yang Cheng, Chi-Yee Cheung, Guey-Lin Lin, YC Lin, and Hoi-Lai Yu. Heavy-quark symmetry and chiral dynamics. *Physical Review D*, 46(3):1148, 1992.

[61] Peter Cho. Chiral perturbation theory for hadrons containing a heavy quark. the sequel. *Physics Letters B*, 285(1-2):145–152, 1992.

[62] Geoffrey T Bodwin, Eric Braaten, and G Peter Lepage. Rigorous qcd analysis of inclusive annihilation and production of heavy quarkonium. *Physical Review D*, 51(3):1125, 1995.

[63] Michael E Luke, Aneesh V Manohar, and Ira Z Rothstein. Renormalization group scaling in nonrelativistic qcd. *Physical Review D*, 61(7):074025, 2000.

[64] Benjamin Grinstein. A modern introduction to quarkonium theory. *International Journal of Modern Physics A*, 15(04):461–495, 2000.

[65] Nora Brambilla, Antonio Pineda, Joan Soto, and Antonio Vairo. Potential nrqcd: An effective theory for heavy quarkonium. *Nuclear Physics B*, 566(1-2):275–310, 2000.

[66] G Peter Lepage, Lorenzo Magnea, Charles Nakhleh, Ulrika Magnea, and Kent Hornbostel. Improved nonrelativistic qcd for heavy-quark physics. *Physical Review D*, 46(9):4052, 1992.

[67] Sean Fleming and Thomas Mehen. Doubly heavy baryons, heavy quark-diquark symmetry, and nonrelativistic qcd. *Physical Review D*, 73(3):034502, 2006.

[68] Ian M Barbour, Susan E Morrison, Elyakum G Klepfish, John B Kogut, Maria-Paola Lombardo, Ukqcd Collaboration, et al. Results on finite density qcd. *Nuclear Physics B-Proceedings Supplements*, 60(1-2):220–233, 1998.

[69] Mark Alford, Anton Kapustin, and Frank Wilczek. Imaginary chemical potential and finite fermion density on the lattice. *Physical Review D*, 59(5):054502, 1999.

[70] Gert Aarts. Complex langevin dynamics and other approaches at finite chemical potential. *arXiv preprint arXiv:1302.3028*, 2013.

[71] E Vicari and H Panagopoulos. Theta dependence of su (n) gauge theories in the presence of a topological term, phys, 2009.

[72] J Berges, Sz Borsanyi, D Sexty, and I-O Stamatescu. Lattice simulations of real-time quantum fields. *Physical Review D*, 75(4):045007, 2007.

[73] EY Loh Jr, JE Gubernatis, RT Scalettar, SR White, DJ Scalapino, and RL Sugar. Sign problem in the numerical simulation of many-electron systems. *Physical Review B*, 41(13):9301, 1990.

[74] Steven R White, Douglas J Scalapino, Robert L Sugar, EY Loh, James E Gubernatis, and Richard T Scalettar. Numerical study of the two-dimensional hubbard model. *Physical Review B*, 40(1):506, 1989.

[75] E Dagotto, A Moreo, RL Sugar, and D Toussaint. Binding of holes in the hubbard model. *Physical Review B*, 41(1):811, 1990.

[76] Pier Luigi Silvestrelli, Stefano Baroni, and Roberto Car. Auxiliary-field quantum monte carlo calculations for systems with long-range repulsive interactions. *Physical review letters*, 71(8):1148, 1993.

[77] DM Charutz and Daniel Neuhauser. Electronic structure via the auxiliary-field monte carlo algorithm. *The Journal of chemical physics*, 102(11):4495–4504, 1995.

[78] Roi Baer, Martin Head-Gordon, and Daniel Neuhauser. Shifted-contour auxiliary field monte carlo for ab initio electronic structure: Straddling the sign problem. *The Journal of chemical physics*, 109(15):6219–6226, 1998.

[79] Thomas A Vilgis. Polymer theory: path integrals and scaling. *Physics Reports*, 336(3):167–254, 2000.

[80] DC Handscomb. A monte carlo method applied to the heisenberg ferromagnet. In *Mathematical Proceedings of the Cambridge Philosophical Society*, volume 60, pages 115–122. Cambridge University Press, 1964.

[81] Masuo Suzuki. Relationship between d-dimensional quantal spin systems and (d+ 1)-dimensional ising systems: Equivalence, critical exponents and systematic approximants of the partition function and spin correlations. *Progress of theoretical physics*, 56(5):1454–1469, 1976.

[82] Masuo Suzuki, Seiji Miyashita, and Akira Kuroda. Monte carlo simulation of quantum spin systems. i. *Progress of Theoretical Physics*, 58(5):1377–1387, 1977.

[83] Kim Splittorff and JJM Verbaarschot. Phase of the fermion determinant at nonzero chemical potential. *Physical review letters*, 98(3):031601, 2007.

[84] Kim Splittorff and JJM Verbaarschot. Qcd sign problem for small chemical potential. *Physical Review D*, 75(11):116003, 2007.

[85] Dorota Grabowska, David B Kaplan, and Amy N Nicholson. Sign problems, noise, and chiral symmetry breaking in a qcd-like theory. *Physical Review D*, 87(1):014504, 2013.

[86] Tota Nakamura. Vanishing of the negative-sign problem of quantum monte carlo simulations in one-dimensional frustrated spin systems. *Physical Review B*, 57(6):R3197, 1998.

[87] S Choe, Ph de Forcrand, M Garcia Perez, S Hioki, Y Liu, H Matsufuru, O Miyamura, A Nakamura, I-O Stamatescu, T Takaishi, et al. Responses of hadrons to the chemical potential at finite temperature. *Physical Review D*, 65(5):054501, 2002.

[88] QCD-TARO Collaboration, Irina Pushkina, Philippe de Forcrand, Margarita Garcia Perez, Seyong Kim, Hideo Matsufuru, Atsushi Nakamura, Ion-Olimpiu Stamatescu, Tetsuya Takaishi, and Takashi Umeda. Properties of hadron screening masses at small baryonic density. *Publication speed*, 609:265–270, 2005.

[89] CR Allton, S Ejiri, SJ Hands, Olaf Kaczmarek, Frithjof Karsch, Edwin Laermann, Ch Schmidt, and L Scorzato. Qcd thermal phase transition in the presence of a small chemical potential. *Physical Review D*, 66(7):074507, 2002.

[90] CR Allton, M Döring, S Ejiri, SJ Hands, Olaf Kaczmarek, Frithjof Karsch, Edwin Laermann, and K Redlich. Thermodynamics of two flavor qcd to sixth order in quark chemical potential. *Physical Review D*, 71(5):054508, 2005.

[91] Rajiv V Gavai and Sourendu Gupta. Pressure and nonlinear susceptibilities in qcd at finite chemical potentials. *Physical Review D*, 68(3):034506, 2003.

[92] Rajiv V Gavai and Sourendu Gupta. On the critical end point of qcd. *Physical Review D*, 71(11):114014, 2005.

[93] Massimo D'Elia and Maria-Paola Lombardo. Finite density qcd via an imaginary chemical potential. *Physical Review D*, 67(1):014505, 2003.

[94] Massimo D'Elia and Maria-Paola Lombardo. Qcd thermodynamics from an imaginary mu b: results on the four flavor lattice model. *Physical Review D*, 70(7):074509, 2004.

[95] Philippe De Forcrand and Owe Philipsen. The qcd phase diagram for small densities from imaginary chemical potential. *Nuclear Physics B*, 642(1-2):290–306, 2002.

[96] Philippe De Forcrand and Owe Philipsen. The qcd phase diagram for three degenerate flavors and small baryon density. *Nuclear Physics B*, 673(1-2):170–186, 2003.

[97] Philippe De Forcrand and Owe Philipsen. The chiral critical line of nf= 2+ 1 qcd at zero and non-zero baryon density. *Journal of High Energy Physics*, 2007(01):077, 2007.

[98] Vicente Azcoiti, Víctor Laliena, Giuseppe Di Carlo, and Angelo Galante. Finite density qcd: a new approach. *Journal of High Energy Physics*, 2004(12):010, 2005.

[99] Vicente Azcoiti, Giuseppe Di Carlo, Angelo Galante, and Victor Laliena. Phase diagram of qcd with four quark flavors at finite temperature and baryon density. *Nuclear Physics B*, 723(1-2):77–90, 2005.

[100] Andre Roberge and Nathan Weiss. Gauge theories with imaginary chemical potential and the phases of qcd. *Nuclear Physics B*, 275(4):734–745, 1986.

[101] Ian M Barbour, Susan E Morrison, Elyakum G Klepfish, John B Kogut, and Maria-Paola Lombardo. The critical points of strongly coupled lattice qcd at nonzero chemical potential. *Physical Review D*, 56(11):7063, 1997.

[102] Zoltan Fodor and Sandor D Katz. A new method to study lattice qcd at finite temperature and chemical potential. *Physics Letters B*, 534(1-4):87–92, 2002.

[103] Zoltan Fodor and Sandor D Katz. Lattice determination of the critical point of qcd at finite t and mu. *Journal of High Energy Physics*, 2002(03):014, 2002.

[104] Zoltan Fodor and Sandor D Katz. Critical point of qcd at finite t and mu, lattice results for physical quark masses. *Journal of High Energy Physics*, 2004(04):050, 2004.

[105] Zoltan Fodor, Sandor D Katz, and Christian Schmidt. The density of states method at non-zero chemical potential. *Journal of High Energy Physics*, 2007(03):121, 2007.

[106] V Azcoiti, G Di Carlo, and AF Grillo. New proposal for including dynamical fermions in lattice gauge theories: The compact-qed case. *Physical review letters*, 65(18):2239, 1990.

[107] Jan Ambjørn, Konstantinos N Anagnostopoulos, Jun Nishimura, and Jacobus JM Verbaarschot. The factorization method for systems with a complex action. a test in random matrix theory for finite density qcd. *Journal of High Energy Physics*, 2002(10):062, 2002.

[108] Christian Schmidt, Zoltan Fodor, and Sandor Katz. The density of states method at finite chemical potential. *arXiv preprint hep-lat/0512032*, 2005.

[109] Georgio Parisi, Yong Shi Wu, et al. Perturbation theory without gauge fixing. *Sci. Sin*, 24(4):483–496, 1981.

[110] G Parisi, JR Klauder, WP Petersen, J Ambjorn, SK Yang, F Karsch, and HW Wyld. On complex probabilities. *Stochastic Quantization*, 131:381, 1988.

[111] Gert Aarts, Erhard Seiler, and Ion-Olimpiu Stamatescu. Complex langevin method: When can it be trusted? *Physical Review D*, 81(5):054508, 2010.

[112] Edward Witten. Analytic continuation of chern-simons theory. *AMS/IP Stud. Adv. Math*, 50:347, 2011.

[113] Marco Cristoforetti, Francesco Di Renzo, Luigi Scorzato, AuroraScience Collaboration, et al. New approach to the sign problem in quantum field theories: High density qcd on a lefschetz thimble. *Physical Review D*, 86(7):074506, 2012.

[114] H Fujii, D Honda, M Kato, Y Kikukawa, S Komatsu, and T Sano. Hybrid monte carlo on lefschetz thimbles—a study of the residual sign problem. *Journal of High Energy Physics*, 2013(10):147, 2013.

[115] Andrei Alexandru, Gökçe Başar, Paulo F Bedaque, Henry Lamm, and Scott Lawrence. Finite density qed 1+ 1 near lefschetz thimbles. *Physical Review D*, 98(3):034506, 2018.

[116] Andrei Alexandru, Paulo F Bedaque, Henry Lamm, Scott Lawrence, and Neill C Warrington. Fermions at finite density in 2+ 1 dimensions with sign-optimized manifolds. *Physical review letters*, 121(19):191602, 2018.

[117] Yuto Mori, Kouji Kashiwa, and Akira Ohnishi. Toward solving the sign problem with path optimization method. *Physical Review D*, 96(11):111501, 2017.

[118] Wolfgang Bietenholz, A Pochinsky, and U-J Wiese. Meron-cluster simulation of the theta vacuum in the 2d o (3) model. *Physical review letters*, 75(24):4524, 1995.

[119] Shailesh Chandrasekharan and Uwe-Jens Wiese. Meron-cluster solution of fermion sign problems. *Physical Review Letters*, 83(16):3116, 1999.

[120] Shailesh Chandrasekharan. Fermion bag approach to lattice field theories. *Physical Review D*, 82(2):025007, 2010.

[121] Atsushi Nakamura, Shotaro Oka, and Yusuke Taniguchi. Qcd phase transition at real chemical potential with canonical approach. *Journal of High Energy Physics*, 2016(2):54, 2016.

[122] Anyi Li, Andrei Alexandru, Keh-Fei Liu, et al. Critical point of n f= 3 qcd from lattice simulations in the canonical ensemble. *Physical Review D*, 84(7):071503, 2011.

[123] Slavo Kratochvila and Philippe De Forcrand. The canonical approach to finite density qcd. *arXiv preprint hep-lat/0509143*, 2005.

[124] Keh-Fei Liu. Finite density algorithm in lattice qcd—a canonical ensemble approach. *International Journal of Modern Physics B*, 16(14n15):2017–2032, 2002.

[125] Anyi Li, Andrei Alexandru, Keh-Fei Liu, Xiangfei Meng, chi QCD Collaboration, et al. Finite density phase transition of qcd with n f= 4 and n f= 2 using canonical ensemble method. *Physical Review D*, 82(5):054502, 2010.

[126] Philippe De Forcrand. Simulating qcd at finite density. *arXiv preprint arXiv:1005.0539*, 2010.

[127] Matthias Troyer and Uwe-Jens Wiese. Computational complexity and fundamental limitations to fermionic quantum monte carlo simulations. *Physical review letters*, 94(17):170201, 2005.

[128] Gdt Hooft. Computation of the quantum effects due to a four-dimensional pseudo-particle. *Physical review: D*, 14(12):3432–3450, 1976.

[129] Gerard't Hooft. How instantons solve the u (1) problem. *Physics Reports*, 142(6):357–387, 1986.

[130] Steven Weinberg. The u (1) problem. *Physical Review D*, 11(12):3583, 1975.

[131] JM Pendlebury, S Afach, NJ Ayres, CA Baker, G Ban, Georg Bison, Kazimierz Bodek, Martin Burghoff, Peter Geltenbort, Katie Green, et al. Revised experimental upper limit on the electric dipole moment of the neutron. *Physical Review D*, 92(9):092003, 2015.

[132] Jihn E Kim and Gianpaolo Carosi. Axions and the strong c p problem. *Reviews of Modern Physics*, 82(1):557, 2010.

[133] Murray Gell-Mann. The interpretation of the new particles as displaced charge multiplets. *Il Nuovo Cimento (1955-1965)*, 4(2):848–866, 1956.

[134] Roberto D Peccei and Helen R Quinn. Cp conservation in the presence of instantons. *Phys. Rev. Lett.*, 38(ITP-568-STANFORD):1440–1443, 1977.

[135] Roberto D Peccei and Helen R Quinn. Constraints imposed by cp conservation in the presence of pseudoparticles. *Physical Review D*, 16(6):1791, 1977.

[136] Steven Weinberg. A new light boson? *Physical Review Letters*, 40(4):223, 1978.

[137] Frank Wilczek. Problem of strong p and t invariance in the presence of instantons. *Physical Review Letters*, 40(5):279, 1978.

[138] Richard Bradley, John Clarke, Darin Kinion, Leslie J Rosenberg, Karl van Bibber, Seishi Matsuki, Michael Mück, and Pierre Sikivie. Microwave cavity searches for dark-matter axions. *Reviews of Modern Physics*, 75(3):777, 2003.

[139] Gianfranco Bertone and Dan Hooper. History of dark matter. *Reviews of Modern Physics*, 90(4):045002, 2018.

[140] Roger F. Dashen. Some features of chiral symmetry breaking. *Phys. Rev.*, D3:1879–1889, 1971.

[141] Edward Witten. Large N Chiral Dynamics. *Annals Phys.*, 128:363, 1980.

[142] Edward Witten. Baryons in the 1/n Expansion. *Nucl. Phys.*, B160:57, 1979.

[143] R. Brower, S. Chandrasekharan, John W. Negele, and U. J. Wiese. QCD at fixed topology. *Phys. Lett.*, B560:64–74, 2003.

[144] Douglas A. Smith and Michael J. Teper. Topological structure of the SU(3) vacuum. *Phys. Rev.*, D58:014505, 1998.

[145] M. Gockeler, M. L. Laursen, G. Schierholz, and U. J. Wiese. Topological Charge of (Lattice) Gauge Fields. *Commun. Math. Phys.*, 107:467, 1986.

[146] M. Luscher. Topology of Lattice Gauge Fields. *Commun. Math. Phys.*, 85:39, 1982.

[147] Peter Woit. Topological Charge in Lattice Gauge Theory. *Phys. Rev. Lett.*, 51:638, 1983.

[148] Edward Witten. Theta dependence in the large N limit of four-dimensional gauge theories. *Phys. Rev. Lett.*, 81:2862–2865, 1998.

[149] Michael F Atiyah and Isadore M Singer. The index of elliptic operators on compact manifolds. *Bulletin of the American Mathematical Society*, 69(3):422–433, 1963.

[150] H. Leutwyler and Andrei V. Smilga. Spectrum of Dirac operator and role of winding number in QCD. *Phys. Rev.*, D46:5607–5632, 1992.

[151] Massimo D'Elia and Francesco Negro. theta dependence of the deconfinement temperature in Yang-Mills theories. *Phys. Rev. Lett.*, 109:072001, 2012.

[152] B. Alles and A. Papa. Mass gap in the 2D O(3) non-linear sigma model with a theta=pi term. *Phys. Rev.*, D77:056008, 2008.

[153] B. Alles, M. Giordano, and A. Papa. Behavior near theta=pi of the mass gap in the two-dimensional O(3) non-linear sigma model. *Phys. Rev.*, B90(18):184421, 2014.

[154] S. Aoki, R. Horsley, T. Izubuchi, Y. Nakamura, D. Pleiter, P. E. L. Rakow, G. Schierholz, and J. Zanotti. The Electric dipole moment of the nucleon from simulations at imaginary vacuum angle theta. 2008.

[155] Haralambos Panagopoulos and Ettore Vicari. The 4D SU(3) gauge theory with an imaginary theta term. *JHEP*, 11:119, 2011.

[156] Vicente Azcoiti, Giuseppe Di Carlo, Angelo Galante, and Victor Laliena. New proposal for numerical simulations of theta vacuum - like systems. *Phys. Rev. Lett.*, 89:141601, 2002.

[157] A. I. Vainshtein, Valentin I. Zakharov, V. A. Novikov, and Mikhail A. Shifman. ABC's of Instantons. *Sov. Phys. Usp.*, 25:195, 1982. [Usp. Fiz. Nauk136,553(1982)].

[158] Stefan Vandoren and Peter van Nieuwenhuizen. Lectures on instantons. *arXiv preprint arXiv:0802.1862*, 2008.

[159] G't Hooft. Symmetry breaking through bell-jackiw anomalies. In *Instantons In Gauge Theories*, pages 226–229. World Scientific, 1994.

[160] Curtis G Callan Jr, RF Dashen, and David J Gross. The structure of the gauge theory vacuum. In *Instantons In Gauge Theories*, pages 29–35. World Scientific, 1994.

[161] Curtis G Callan Jr, Roger Dashen, and David J Gross. Toward a theory of the strong interactions. *Physical Review D*, 17(10):2717, 1978.

[162] R Jackiw and Claudio Rebbi. Vacuum periodicity in a yang-mills quantum theory. In *Instantons In Gauge Theories*, pages 25–28. World Scientific, 1994.

[163] Sidney Coleman. *Aspects of symmetry: selected Erice lectures*. Cambridge University Press, 1988.

[164] F. W. J. Olver. On Bessel functions of large order. *Phil. Trans. Roy. Soc. Lond.*, A247:328–368, 1954.

[165] George B Arfken, Hans J Weber, and Frank E Harris. *Mathematical methods for physicists: A comprehensive guide*. Academic press, 2011.

[166] M Gell-Mann. Gell-mann 1964. *Phys. Lett*, 8:214, 1964.

[167] Claude Amsler and Nils A Törnqvist. Mesons beyond the naive quark model. *Physics reports*, 389(2):61–117, 2004.

[168] Claude Amsler. Proton-antiproton annihilation and meson spectroscopy with the crystal barrel. *Reviews of Modern Physics*, 70(4):1293, 1998.

[169] GS Adams, T Adams, Z Bar-Yam, JM Bishop, VA Bodyagin, BB Brabson, DS Brown, NM Cason, SU Chung, RR Crittenden, et al. Observation of a new j pc= 1-+ exotic state in the reaction pi- p pi+ pi- pi- p at 18 gev/c. *Physical Review Letters*, 81(26):5760, 1998.

[170] SU Chung, K Danyo, RW Hackenburg, C Olchanski, JS Suh, HJ Willutzki, SP Denisov, V Dorofeev, VV Lipaev, AV Popov, et al. Exotic and q q resonances in the pi+ pi- pi- system produced in pi- p collisions at 18 gev/c. *Physical Review D*, 65(7):072001, 2002.

[171] RJ Jaffe. Multiquark hadrons. i. phenomenology of q 2 q 2 mesons. *Physical Review D*, 15(1):267, 1977.

[172] Mark Alford and RL Jaffe. Insight into the scalar mesons from a lattice calculation. *Nuclear Physics B*, 578(1-2):367–382, 2000.

[173] Gt Hooft, G Isidori, L Maiani, AD Polosa, and V Riquer. A theory of scalar mesons. *arXiv preprint arXiv:0801.2288*, 2008.

[174] John Weinstein and Nathan Isgur. K k^{-} molecules. *Physical Review D*, 41(7):2236, 1990.

[175] G Janssen, BC Pearce, K Holinde, and J Speth. Structure of the scalar mesons f 0 (980) and a 0 (980). *Physical Review D*, 52(5):2690, 1995.

[176] Milan P Locher, Valeri E Markushin, and Han Q Zheng. Structure of f0(980) from a coupled channel analysis of s wave pi pi scattering. *The European Physical Journal C-Particles and Fields*, 4(2):317–326, 1998.

[177] Stephen Godfrey and Stephen L Olsen. The exotic xyz charmonium-like mesons. *Annual Review of Nuclear and Particle Science*, 58:51–73, 2008.

[178] S-K Choi, SL Olsen, I Adachi, H Aihara, V Aulchenko, T Aushev, T Aziz, AM Bakich, V Balagura, I Bedny, et al. Observation of a resonancelike structure in the pi+- psi mass distribution in exclusive b k pi+- psi decays. *Physical review letters*, 100(14):142001, 2008.

[179] Bernard Aubert, R Barate, D Boutigny, F Couderc, J-M Gaillard, A Hicheur, Y Karyotakis, JP Lees, V Tisserand, A Zghiche, et al. Study of the b- j/psi k- pi+ pi- decay and measurement of the b- x (3872) k- branching fraction. *Physical Review D*, 71(7):071103, 2005.

[180] Bernard Aubert, M Bona, Y Karyotakis, JP Lees, V Poireau, E Prencipe, X Prudent, V Tisserand, J Garra Tico, E Grauges, et al. Study of b x (3872) k, with x (3872) j/psi pi+ pi-. *Physical Review D*, 77(11):111101, 2008.

[181] Darin Acosta, T Affolder, MH Ahn, T Akimoto, MG Albrow, D Ambrose, S Amerio, D Amidei, A Anastassov, K Anikeev, et al. Observation of the narrow state x (3872) j/psi pi+ pi- in p^- p collisions at s= 1.96 t e v. *Physical review letters*, 93(7):072001, 2004.

[182] A Abulencia, D Acosta, J Adelman, T Affolder, T Akimoto, MG Albrow, D Ambrose, S Amerio, D Amidei, A Anastassov, et al. Measurement of the dipion mass spectrum in x (3872) j/psi pi+ pi- decays. *Physical review letters*, 96(10):102002, 2006.

[183] Timo Aaltonen, J Adelman, T Akimoto, B Álvarez González, S Amerio, D Amidei, A Anastassov, A Annovi, J Antos, G Apollinari, et al. Precision measurement of the x (3872) mass in j/psi pi+ pi- decays. *Physical review letters*, 103(15):152001, 2009.

[184] G Gokhroo, G Majumder, K Abe, I Adachi, H Aihara, D Anipko, T Aushev, T Aziz, AM Bakich, V Balagura, et al. Observation of a near-threshold d 0 d^- 0 pi 0 enhancement in b d 0 d^- 0 pi 0 k decay. *Physical review letters*, 97(16):162002, 2006.

[185] R Aaij, C Abellan Beteta, B Adeva, M Adinolfi, C Adrover, A Affolder, Z Ajaltouni, J Albrecht, F Alessio, M Alexander, et al. Observation of x (3872) production in pp collisions at sqrt(s)= 7 tev. *The European Physical Journal C*, 72(5):1972, 2012.

[186] Serguei Chatrchyan, Vardan Khachatryan, AM Sirunyan, A Tumasyan, W Adam, E Aguilo, T Bergauer, M Dragicevic, J Erö, C Fabjan, et al. Measurement of the x (3872) production cross section via decays to j/psi pi+ pi- in pp collisions at sqrt(s)= 7 tev. *Journal of High Energy Physics*, 2013(4):154, 2013.

[187] Bernard Aubert, R Barate, D Boutigny, F Couderc, Y Karyotakis, JP Lees, V Poireau, V Tisserand, A Zghiche, E Grauges, et al. Observation of a broad structure in the pi+ pi- j/psi mass spectrum around 4.26 gev/c 2. *Physical review letters*, 95(14):142001, 2005.

[188] M Ablikim, MN Achasov, XC Ai, O Albayrak, DJ Ambrose, FF An, Q An, JZ Bai, R Baldini Ferroli, Y Ban, et al. Observation of a charged charmoniumlike structure in e+ e- pi+ pi- j/psi at s= 4.26 gev. *Physical review letters*, 110(25):252001, 2013.

[189] A Bondar, A Garmash, R Mizuk, D Santel, K Kinoshita, I Adachi, H Aihara, K Arinstein, DM Asner, T Aushev, et al. Observation of two charged bottomoniumlike resonances in y (5 s) decays. *Physical review letters*, 108(12):122001, 2012.

[190] Roel Aaij, B Adeva, M Adinolfi, A Affolder, Z Ajaltouni, S Akar, J Albrecht, F Alessio, M Alexander, S Ali, et al. Observation of j/psi p resonances consistent with pentaquark states in lambda b 0 j/psi k- p decays. *Physical review letters*, 115(7):072001, 2015.

[191] Roel Aaij, C Abellan Beteta, Bernardo Adeva, Marco Adinolfi, Christine Angela Aidala, Ziad Ajaltouni, Simon Akar, Pietro Albicocco, Johannes Albrecht, Federico Alessio, et al. Observation of a narrow pentaquark state, p c (4312)+, and of the two-peak structure of the p c (4450)+. *Physical review letters*, 122(22):222001, 2019.

[192] CPDG Patrignani, DH Weinberg, CL Woody, RS Chivukula, O Buchmueller, Yu V Kuyanov, E Blucher, S Willocq, A Höcker, C Lippmann, et al. Review of particle physics. *Chin. Phys.*, 40:100001, 2016.

[193] ES Swanson. The new heavy mesons: a status report, phys, 2006.

[194] Mikhail B Voloshin. Charmonium. *Progress in Particle and Nuclear Physics*, 61(2):455–511, 2008.

[195] Hua-Xing Chen, Wei Chen, Xiang Liu, and Shi-Lin Zhu. The hidden-charm pentaquark and tetraquark states. *Physics Reports*, 639:1–121, 2016.

[196] Richard F Lebed, Ryan E Mitchell, and Eric S Swanson. Heavy-quark qcd exotica. *Progress in Particle and Nuclear Physics*, 93:143–194, 2017.

[197] A Esposito, A Pilloni, and Antonio D Polosa. Multiquark resonances. *Physics Reports*, 668:1–97, 2017.

[198] Ahmed Ali, Jens Sören Lange, and Sheldon Stone. Exotics: heavy pentaquarks and tetraquarks. *Progress in Particle and Nuclear Physics*, 97:123–198, 2017.

[199] Stephen Lars Olsen, Tomasz Skwarnicki, and Daria Zieminska. Nonstandard heavy mesons and baryons: Experimental evidence. *Reviews of Modern Physics*, 90(1):015003, 2018.

[200] Marek Karliner, Jonathan L Rosner, and Tomasz Skwarnicki. Multiquark states. *Annual Review of Nuclear and Particle Science*, 68:17–44, 2018.

[201] Chang-Zheng Yuan. The xyz states revisited. *International Journal of Modern Physics A*, 33(21):1830018, 2018.

[202] Emi Kou, Phillip Urquijo, W Altmannshofer, F Beaujean, G Bell, M Beneke, II Bigi, F Bishara, M Blanke, C Bobeth, et al. The belle ii physics book. *Progress of Theoretical and Experimental Physics*, 2019(12):123C01, 2019.

[203] A Cerri, VV Gligorov, S Malvezzi, J Martin Camalich, J Zupan, S Akar, J Alimena, BC Allanach, W Altmannshofer, L Anderlini, et al. Opportunities in flavour physics at the hl-lhc and he-lhc. *arXiv preprint arXiv:1812.07638*, 2018.

[204] Mikhail B Voloshin. Molecular quarkonium. *arXiv preprint hep-ph/0605063*, 2006.

[205] J-M Richard. Exotic hadrons: review and perspectives. *Few-Body Systems*, 57(12):1185–1212, 2016.

[206] Yan-Rui Liu, Hua-Xing Chen, Wei Chen, Xiang Liu, and Shi-Lin Zhu. Pentaquark and tetraquark states. *Progress in Particle and Nuclear Physics*, 2019.

[207] Sasa Prelovsek and Luka Leskovec. Evidence for x(3872) from d d* scattering on the lattice. *Physical review letters*, 111(19):192001, 2013.

[208] Song-Haeng Lee, Carleton DeTar, Daniel Mohler, Heechang Na, MILC Collaborations, et al. Searching for the x(3872) and zc(3900) on hisq lattices. *arXiv preprint arXiv:1411.1389*, 2014.

[209] M Padmanath, CB Lang, and Sasa Prelovsek. X (3872) and y (4140) using diquark-antidiquark operators with lattice qcd. *Physical Review D*, 92(3):034501, 2015.

[210] Nils A Törnqvist. From the deuteron to deusons, an analysis of deuteronlike meson-meson bound states. *Zeitschrift für Physik C Particles and Fields*, 61(3):525–537, 1994.

[211] Eric Braaten and Masaoki Kusunoki. Low-energy universality and the new charmonium resonance at 3870 mev. *Physical Review D*, 69(7):074005, 2004.

[212] Martin Cleven, F-K Guo, Christoph Hanhart, and U-G Meißner. Bound state nature of the exotic z b states. *The European Physical Journal A*, 47(10):120, 2011.

[213] Marek Karliner and Jonathan L Rosner. New exotic meson and baryon resonances from doubly heavy hadronic molecules. *Physical review letters*, 115(12):122001, 2015.

[214] S Dubynskiy and Mikhail B Voloshin. Hadro-charmonium. *Physics Letters B*, 666(4):344–346, 2008.

[215] Eric Braaten. How the z c (3900) reveals the spectra of charmonium hybrids and tetraquarks. *Physical review letters*, 111(16):162003, 2013.

[216] Raul A Briceno, Thomas D Cohen, S Coito, Jozef J Dudek, E Eichten, CS Fischer, M Fritsch, W Gradl, A Jackura, M Kornicer, et al. Issues and opportunities in exotic hadrons. *Chinese Physics C*, 40(4):042001, 2016.

[217] Thomas D Cohen and Paul M Hohler. Doubly heavy hadrons and the domain of validity of doubly heavy diquark-antiquark symmetry. *Physical Review D*, 74(9):094003, 2006.

[218] Aneesh V Manohar and Mark B Wise. Exotic qqqq states in qcd. *Nuclear Physics B*, 399(1):17–33, 1993.

[219] Max Born and Robert Oppenheimer. Zur quantentheorie der molekeln. *Annalen der Physik*, 389(20):457–484, 1927.

[220] Matthias Berwein, Nora Brambilla, Jaume Tarrús Castellà, and Antonio Vairo. Quarkonium hybrids with nonrelativistic effective field theories. *Physical Review D*, 92(11):114019, 2015.

[221] Nora Brambilla, Wai Kin Lai, Jorge Segovia, Jaume Tarrús Castellà, and Antonio Vairo. Spin structure of heavy-quark hybrids. *Physical Review D*, 99(1):014017, 2019.

[222] Nora Brambilla, Gastão Krein, Jaume Tarrús Castellà, and Antonio Vairo. Born-oppenheimer approximation in an effective field theory language. *Physical Review D*, 97(1):016016, 2018.

[223] Mariana M Odashima, Beatriz G Prado, and E Vernek. Pedagogical introduction to equilibrium green's functions: condensed-matter examples with numerical implementations. *Revista Brasileira de Ensino de Física*, 39(1), 2017.

[224] Noriyoshi Ishii, Sinya Aoki, and Tetsuo Hatsuda. Nuclear force from lattice qcd. *Physical review letters*, 99(2):022001, 2007.